Ph.D. Thesis

MONITORING AND GEOMORPHOLOGIC CHARACTERIZATION OF DEBRIS FLOWS AT CATCHMENT SCALE

Contributions to debris-flow hazard assessment

by:
Clàudia Abancó Martínez de Arenzana

director:
Marcel Hürlimann

co-director:
José Moya Sánchez

Barcelona, June 2013

Department of Geotechnical Engineering and Geosciences
Technical University of Catalonia (UPC-BarcelonaTech)

Acta de qualificació de tesi doctoral	**Curs acadèmic:**

Nom i cognoms
CLÀUDIA ABANCÓ MARTÍNEZ DE ARENZANA

Programa de doctorat
DOCTORAT EN ENGINYERIA DEL TERRENY

Unitat estructural responsable del programa
DEPARTAMENT D'ENGINYERIA DEL TERRENY, CARTOGRÀFICA I GEOFÍSICA (ETCG)

Resolució del Tribunal

Reunit el Tribunal designat a l'efecte, el doctorand / la doctoranda exposa el tema de la seva tesi doctoral titulada MONITORING AND GEOMORPHOLOGIC CHARACTERIZATION OF DEBRIS FLOWS AT CATCHMENT SCALE_____.

Acabada la lectura i després de donar resposta a les qüestions formulades pels membres titulars del tribunal, aquest atorga la qualificació:

☐ APTA/E   ☐ NO APTA/E

(Nom, cognoms i signatura)	(Nom, cognoms i signatura)
President/a	Secretari/ària

(Nom, cognoms i signatura)	(Nom, cognoms i signatura)	(Nom, cognoms i signatura)
Vocal	Vocal	Vocal

_____, _____ d'/de _____ de _____

El resultat de l'escrutini dels vots emesos pels membres titulars del tribunal, efectuat per l'Escola de Doctorat, a instància de la Comissió de Doctorat de la UPC, atorga la MENCIÓ CUM LAUDE:

☐ SÍ   ☐ NO

(Nom, cognoms i signatura)	(Nom, cognoms i signatura)
Presidenta de la Comissió de Doctorat	Secretària de la Comissió de Doctorat

Barcelona, _____ d'/de _____ de _____

Resum

Els corrents d'arrossegalls són moviments de massa molt ràpids i es consideren un dels fenòmens més perillosos que es produeixen a les regions de muntanya. La investigació en aquest camp ha incrementat de manera rellevant durant les últimes dècades. No obstant, encara queden moltes qüestions pendents de resoldre sobre els mecanismes de desencadenament d'aquest tipus de fenòmens i del seu comportament dinàmic; ambdós, punts claus en l'avaluació de la perillositat.

El propòsit global d'aquest treball és la millora d'alguns aspectes del procés d'avaluació de la perillositat dels corrents d'arrossegalls a escala de conca; concretament: l'estimació de la magnitud dels episodis, la determinació de la intensitat d'aquests i la caracterització dels factors desencadenants. Bona part dels objectius s'ha dut a terme mitjançant l'auscultació d'una conca en la qual els corrents d'arrossegalls són relativament freqüents. També s'han analitzat dades obtingudes mitjançant la caracterització geomorfolòfica d'altres conques. A més a més, aquest treball ha contribuït a augmentar el coneixement sobre els corrents d'arrossegalls al Pirineu.

En el context d'aquesta tesi, s'ha instal·lat un sistema de monitorització de corrents d'arrossegalls al Pirineu, al torrent del Rebaixader (Alta Ribagorça, Pirineu Central) concretament. Des del juliol de 2009 s'hi han registrat 6 corrents d'arrossegalls, amb volums d'entre 1000 i 21000 m^3, 11 fluxos hiperconcentrats (volums d'entre 350 i 2800 m^3) i 4 despreniments rocosos. La diferenciació entre tipus de processos i la identificació de les diverses fases dels fluxos s'ha basat principalment en la vibració del terreny. L'anàlisi detallat de la vibració del terreny generada pels processos torrencials ha revelat que hi ha diversos factors fortament influents en el senyal registrat pels geòfons. Concretament, s'ha identificat un decreixement significatiu del senyal als geòfons que no s'havien situat prop del canal actiu. La vibració del terreny generada per alguns corrents d'arrossegalls s'ha registrat, no només mitjançant la tècnica convencional del mostrejat digital del senyal sinó també mitjançant la transformació de la senyal en impulsos. Ambdues tècniques mostren resultats favorables per a la detecció i la caracterització dels corrents. Tot i així, la transformació en impulsos mostra alguns avantatges en qüestions de consum d'energia i simplicitat del mètode, aspectes que són crucials en els sistemes d'alerta primerenca i alarma (EWAS). D'altra banda, la caracterització de les pluges a la conca suggereix que habitualment, al torrent del Rebaixader, es desencadenen corrents d'arrossegalls amb pluges de durada del voltant de les 2 hores i d'intensitat horària crítica entorn els 15 mm/h. Malgrat tot, s'ha detectat que alguns episodis plujosos primaverals d'intensitat moderada, acompanyats d'una possible infiltració d'aigua provinent de la fusió de la neu, també poden provocar fluxos torrencials i despreniments rocosos. Concretament, es presenta un anàlisi detallat de tres despreniments rocosos desencadenats durant la primavera.

D'altra banda, en aquest estudi es presenta també una metodologia per preveure l'erosió que es pot produir en un torrent susceptible al desencadenament de corrents d'arrossegalls, durant un episodi. La metodologia s'ha basat en la creació d'un arbre de decisió (aplicant tècniques de mineria de dades) sobre una base de dades de paràmetres geomorfològics, recol·lectats al camp i a partir d'un model digital d'elevacions, que incorpora dades de 110 trams que corresponen a 17 torrents. Finalment s'ha proposat un arbre de decisió general, el qual caldria calibrar per tal de poder-lo aplicar a altres conques i zones climàtiques.

Abstract

Debris flows are very fast mass movements and are considered as one of the most hazardous phenomenain mountainous regions. Research on this field has strongly improved during the last decades. However,many open questions remain concerning the details of the triggering mechanisms of this type of phenomena and their dynamic behaviour; both of them key points in the hazard assessment.

The global purpose of this work is to improve some aspects of the debris-flow hazard assessment atcatchment scale; particularly the estimation of the events' magnitude, the determination of their intensity and the characterization of the triggering factors. Most of the objectives have been carried out by means of the auscultation of a catchment in wich the debris flows are frequent. Furthermore, data of geomorphological characterization of other catchments have been analysed. This work aims at increasing the knowledge on debris flows in the Pyrenees.

In the context of this thesis, a debris-flow monitoring system has been set up in the Pyrenees, in the Rebaixader torrent (Alta Ribagorça, Central Pyrenees). Since July 2009, six debris flows involving volumes ranging from 1000 to 21000 m3, eleven debris floods (volumes from 350 to 2800 m3) and four rockfalls have been registered. The distinction between processes and the identification of the different phases of the flow events have mainly been based on ground vibration data. The detailed analysis of the ground vibration generated by torrential processes has revealed that there are several on-site factors strongly influencing the signal registered by the geophones. In particular, a significant decrease of the signal has been recognized at the geophones that were not placed close to the active channel. The ground vibration signal generated by some debris-flow events has not only been registered using the conventional digital

sampling of the ground velocity signal, but also by means of transforming the ground velocity into impulses. Both techniques are suitable for the detection and characterization of the debris-flow events. However, the transformation into impulses shows interesting advantages, such as the low power consumption and the simplicity of the analysis of this type of signal in comparison to the conventional one.

Both aspects are crucial in early warning and alarm systems (EWAS). Besides, the characterization of the rainfalls in the catchment has revealed that the most common debris-flow triggering rainfalls in the Rebaixader torrent last around 2 hours and the critical hourly intensity value is around 15 mm/h. However, it has been detected that also spring episodes of moderate intensity, accompanied by the potential

infiltration from snowmelt can trigger torrential flows and rockfalls. In particular, a detailed analysis of three rockfalls that occurred in spring is presented.

Moreover, a methodology to estimate the entrainment of bed material in a debris-flow event is presented within this study. The methodology was based on the creation of a decision tree (applying data mining techniques) over a database of geomorphologic parameters, collected in the field and from a digital elevation model, which incorporates 110 reaches from 17 torrents. Finally, a general decision tree was proposed that should be calibrated and adapted, in order to widen its application to other catchments and climatic regions.

Resumen

Las corrientes de derrubios son movimientos de ladera muy rápidos y estan considerados como uno de los fenómenos más peligrosos que se producen en las regiones montañosas. La investigación en este campo ha aumentado de forma muy relevante durante las últimas décadas. No obstante, todavía quedan muchas cuestiones pendientes de resolver sobre los mecanismos de desencadenamiento de este tipo de fenómenos y el comportamiento dinámico, siendo ambos puntos clave en la evaluación de la peligrosidad.

El propósito global de este trabajo es la mejora de algunos aspectos de la evaluación de la peligrosidad de corrientes de derrubios a escala de cuenca. Algunos de estos aspectos son la estimación de la magnitud de los eventos, la determinación de la intensidad de estos o la caracterización de los factores desencadenantes. Buena parte de los trabajos de investigación se han llevado a cabo mediante la auscultación y de una cuenca en la que las corrientes de derrubios son relativamente frecuentes. También se analizado datos obtenidos mediante la caracterización geomorfológica de otras cuencas. Además, este trabajo ha contribuido a incrementar el conocimiento sobre las corrientes de derrubios en el Pirineo.

En el contexto de esta tesis se ha instalado un sistema de auscultación de corrientes de derrubios en el Pirineo, en el torrente del Rebaixader (Alta Ribagorça, Pirineo Central). Desde Julio de 2009 se han registrado seis corrientes de derrubios con volúmenes entre los 1000 y los 21000 m^3, once flujos hiperconcentrados (volúmenes entre los 350 y los 2800 m^3) y cuatro desprendimientos rocosos. La distinción entre tipos de procesos y la identificación de las distintas fases de los flujos, se ha basado principalmente en la vibración del terreno. El análisis detallado de la vibración del terreno generada por los procesos torrenciales ha revelado que existen distintos factores marcadamente influyentes en la señal registrada por los geófonos. En particular, se identificó un decrecimiento significativo de la señal en los geófonos que no se situaron cerca del canal activo. La vibración del terreno generada por algunas corrientes de derrubios se ha registrado no sólo mediante la técnica convencional de muestreo digital de la señal, sino también con una transformación de la señal en impulsos. Ambas técnicas han resultado favorables para la detección y caracterización de las corrientes. Sin embargo, la transformación en impulsos muestra algunas ventajas especialmente interesantes, como son el bajo consumo de energía y la simplicidad del análisis, aspectos son cruciales en los sistemas de alerta temprana y alarma (EWAS). Por otra parte, la caracterización de las lluvias en la cuenca sugiere que las corrientes de derrubios en el Rebaixader habitualmente son provocadas por lluvias de duración de unas 2 horas y con un valor de intensidad horaria crítica de unos 15 mm/h. Aún así, se ha detectado que algunos episodios de lluvias primaverales de intensidad moderada, acompañadas de una posible infiltración de agua procedente de la fusión de la nieve, podían también provocar flujos torrenciales y desprendimientos rocosos. Se presenta un análisis detallado de tres desprendimientos rocosos desencadenados durante la primavera.

En esta tesis doctoral también se presenta una metodología para prever el volumen de material que puede erosionar a lo largo de su recorrido una corriente de derrubios. La metodología se ha basado en la creación de un árbol de decisión (aplicando técnicas de minería de datos) a partir de una base de datos de parámetros geomorfológicos, recolectados en campo y a partir de un modelo digital de elevaciones, que incorpora dades de 110 tramos de 17 torrentes. Finalmente, se propone un árbol de decisión general, el cual debería ser calibrado para su posible aplicación a otras cuencas y regiones climáticas.

Acknowledgments

*del món! Also to my **flatmates:** Mercè, Anna, Ander, Aïda and Maria with who I shared infinite conversations and good times, they have always been there during the difficult days. And of course I want to thank my **friends** who have given me their unconditional support, it doesn't matter from where: Vic, Sant Hilari, Manlleu, Panama, Frankfurt, Argentina or wherever. Special thanks to Olga, for her help on the design of the thesis.*

*Last but not least, I want to give my most special thanks to **Roger**, for being there everyday, for helping me in the field, for all the support, for the discussions, for being my anchor to the life out of the debris flows, for, for, for…*

[x]

1. Introduction

1.1. Motivation

Debris flows are a type of mass movements consisting in a high density flowing mixture of solid material and water, which often occur in steep torrents (Costa, 1984; Johnson and Rodine, 1984). Debris flows are one of the most dangerous mass movements, as they travel at high velocities (several meters per second) and they can affect populated areas and infrastructures in mountainous regions, as well as other elements at risk, causing economic losses and even casualties (Jakob and Hungr, 2005).

In the Pyrenees, during the last decades, some important events have taken place, such as the event in Biescas that affected a camping site in 1996 (Figure 1a), causing almost one hundred casualties (Alcoverro et al., 1999). More recently (in 2008) an event affected the border between Catalonia and Andorra (Figure 1b), causing the destruction of part of the border, including the main buildings, but luckily without casualties. Moreover, two big events caused damages in the road to access to the Port Ainé ski resort (Luis-Fonseca et al., 2011; Portilla et al., 2010).

a)

b)
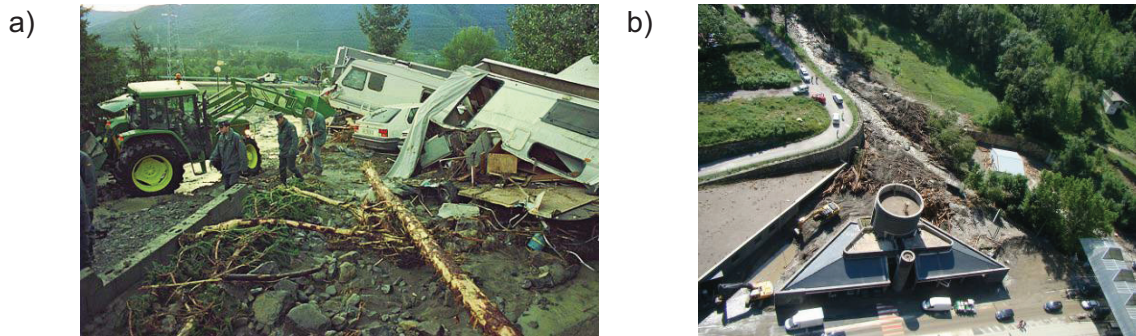
Figure 1: Disastrous debris-flow events in the Pyrenees: a) Biescas event (1996) (source: diariodenoticias.com) and b) Riu-Runer event (2008), affecting the border between Andorra and Catalonia (source: Euroconsult S.A.).

Debris flows are popular phenomena in mountainous areas worldwide, especially where the human settlements in the foothills are bigger. Even though, the difficulties to access the triggering areas of debris flows and the coexistence of this phenomena with other torrential processes, make the research challenging and it is not unexpected that they have been less understood than other mass movements.

Debris-flow hazard assessment consists on determine *where* and *when will debris flows occur* and *how big they can be* (Fell et al., 2008). After identifying the susceptible catchments where debris flow can occur (*where*), the following step towards the hazard assessment is the prediction of the magnitude (*how big*) and of the probability of occurrence of the events (*when*). The probability of occurrence is the likelihood of debris flow of a certain magnitude to occur in a specific location. The magnitude of debris flows is described as the volume or the peak discharge of the event. To identify the hazard intensity other data is used, such as the velocity of the event, the flow depth, etc. (Jakob and Weatherly, 2005).

Research on debris flow has strongly increased during the last decades. Thus, the understanding of this phenomenon, its mechanics and its related hazards have strongly been improved, but there are still many uncertainties (e.g. how can we predict their magnitude or temporal occurrence in a specific catchment? which is the potential area that can be affected? how can we reduce their damages?) regarding debris flows and associated processes (e.g.Davies et al., 2013; Jakob and Hungr, 2005; Takahashi, 2007). In order to develop new techniques to evaluate debris-flow hazard assessment or develop models to solve some steps of this process, data of real events are needed.

Data on debris-flow events are available in some areas worldwide (Badoux et al., 2009; Marchi et al., 2002; Suwa, 1989) and in some regions debris-flow hazard assessment guidelines have also been developed (Fiebiger, 1997; Heinimann et al., 1998; Hübl et al., 2011; Kienholz, 1978; Petrascheck and Kienholz, 2003). In contrast, there are other regions where knowledge on debris flow is scarce, such as the Pyrenees.

This thesis focuses on specific parts of the debris-flow hazard assessment at catchment scale, with the intention of developing techniques to solve some parts of the process or increasing knowledge in particular aspects of the debris-flow behaviour. The contributions of this thesis have been pursued through two main tools: monitoring of a torrent and geomorphologic characterization of torrents and catchments.

The procedure of the hazard assessment in a specific catchment consists on the determination of the potential magnitude of the events and their probability of occurrence (Figure 2). The parameters to evaluate the magnitude are the volume of the events, their peak discharge or the inundated area (Jakob, 2005). The probability of occurrence can be determined by the datation of past events or, in case of not being possible, by the frequency of the triggering factors. Finally, the debris-flow hazard assessment also includes parameters to quantify the intensity of the hazard. These parameters are normally the flow velocity, the flow depth or the runout distance.

This thesis specifically contributes on increasing the knowledge on the dynamic behaviour of this type of process and its triggering factors. The application of these results is not only scientific but it is also associated to the development of early warning and alarm systems (EWAS). Other contributions arise from the development of a simple methodology to estimate the entrainment than can occur when a debris flow takes place in the catchment. This is carried out by means of geomorphologic characterization.
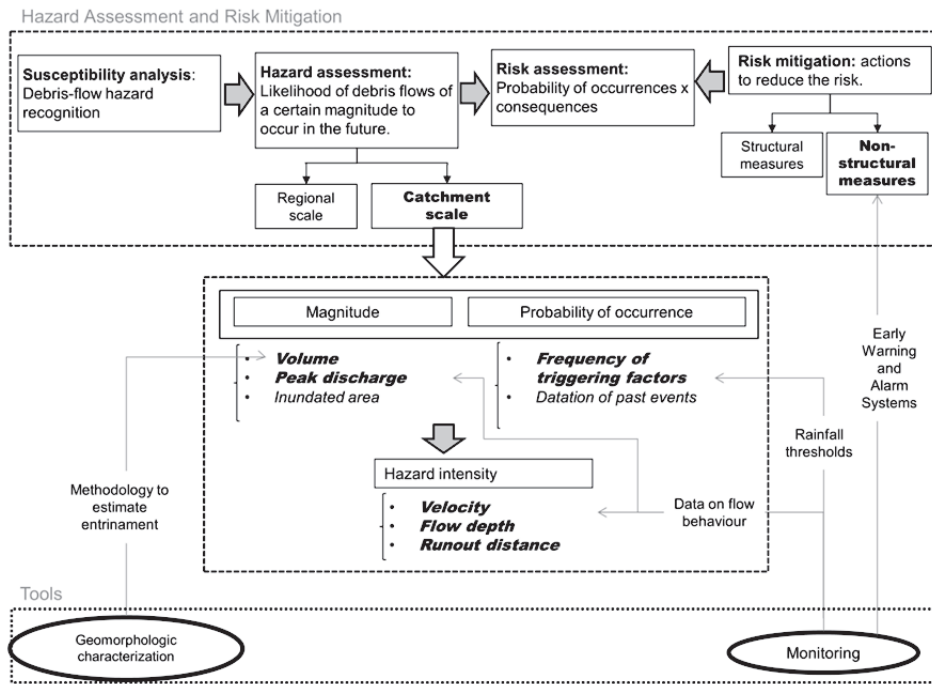
Figure 2: Scheme of the debris-flow hazard assessment and risk mitigation. The tools and contributions of this PhD are indicated.

1.2. General background

In the following a general background of the debris flow phenomena and related hazard is provided. Moreover, in each chapter, specific sections describing the state-of-the-art are provided.

1.2.1. Debris flow definition

Debris flows are fast movements formed by a mix of water and solids (sand, boulders, gravel, silt and sometimes a minor fraction of clay) with behaviour similar to liquid concrete, as described by Johnson and Rodine (1984). Varnes (1978) defined debris flows as a type of landslide belonging to the *flow* group, that also includes debris avalanches or mudflows among others. However, as discussed by Hungr, what some authors described movements classified as debris avalanches and mudflows by Varnes (1978) are considered as specific debris flow types in other classifications (e.g.Hungr et al., 2001).

The differences between debris flows and other types of flows such as debris floods or hyperconcentrated flows are smooth and only few comprehensive literature is available (Hungr et al., 2001). The difference between them, from the rheological point of view

lies in the sediment concentration, nevertheless different concentration thresholds have been defended by other authors (e.g. Costa, 1984; Vallance, 2000). Another distinction, easier to work with, considers the debris-flow peak discharge is up to 50 times the major flood discharge (Hungr, 2000; VanDine, 1985) (Figure 3). Moreover, morphological evidences, such as lateral levees, small-scale banks slides or collapses, bed erosion and solid transport may help us to recognise the typology of the event after it had taken place (Coussot and Meunier, 1996).

Two end-members of debris flows can be distinguished: muddy debris flows and granular debris flows. The muddy debris flows have a fine fraction (containing clay) more than 10%. The granular debris flows contain a low quantity of fine particles, and consequently the contact between the grains play a major role in the mass behaviour (Coussot and Meunier, 1996). This difference in behaviour is relevant for many steps of the hazard assessment, such as the monitoring (especially for the vibration sensors).

Figure 3: Triangular diagram of torrential and other mass movements, modified after Phillips and Davies (1991), (ONR-24-800, 2007).

1.2.2. Debris-flow Hazard and Risk

Generally, two types of debris-flow hazard assessments can be divided: studies at regional scale and studies at local or catchment scale. Regional studies usually apply GIS-techniques and incorporate some statistical analysis, simple runout models and aerial photographs or satellite images (Hürlimann and Lantada, 2005; Iverson et al., 1998; Liu and Lei, 2003; Pallas et al., 2004; Vallance et al., 2003). Detailed debris-flow

hazard assessment at local or catchment scale is not very common. Nevertheless, especially such local assessments are, in the end, necessary for the correct zonation of the territory in mountainous areas. Local analysis of debris-flow hazard because need the application of an extensive field surveying, and sophisticated runout modelling amongst others (among others Chau and Lo, 2004; Glade, 2005; Hürlimann et al., 2006; Pasuto and Soldati, 2004). Physical models of complex phenomena such as debris flows require monitoring of the flow events (i.e. velocity and peak discharge) to be properly calibrated.

The debris-flow hazard assessment is often followed by a risk analysis and evaluation (risk assessment). The debris-flow risk can be described as the product of the probability of debris-flow occurrence times the consequences of the event (Fell et al., 2008). For the management of the risk, it is usual to develop risk mitigation measures to reduce the hazard intensity or the vulnerability of the elements at risk. There exist many different kinds of mitigation measures, but they can roughly be categorized as structural or non-structural measures. The first type reduces the frequency and severity of the hazard, while the second one reduces the hazard consequences (Nadim and Lacasse, 2008).

One of the most efficient non-structural measures of risk mitigation for debris flows is the implementation of early warning and alarm systems (EWAS). The EWAS are based on the results obtained by monitoring systems. Generally, the EWAS can advise the responsible and affected persons hours or even days in advance of an approaching hazard (www.besafenet.org). Most of the recent publications on early warning systems include rainfall thresholds and are related to shallow landslides and debris flows (Aleotti, 2004; Baum and Godt, 2010; Brunetti et al., 2010; Jakob et al., 2006; Salameh et al., 2009; Tiranti and Rabuffetti, 2010). On the other side, an alarm system informs the responsible and affected persons immediately of the danger by optical or acoustic devices (e.g. lights or siren). Only very few alarm systems for torrential processes have been published in literature, and even fewer are operational (Arattano and Marchi, 2008; Badoux et al., 2009; Bessason et al., 2007; Kung et al., 2008; LaHusen, 2005a).

1.2.3. Debris flow initiation

1.2.3.1.   Debris-flow initiation mechanisms

Debris flows occur in many mountainous regions, if conditions are favourable. As inherent factors in the catchment, there may be steep slopes and a source of granular

unconsolidated sediment to be incorporated into the flowing mass. The material can belong to a colluvium, a residual soil, glacial deposits, pyroclastic material, etc. and normally consists of sand, fine material and gravel. Rainfall is the most common triggering factor for debris flows, but they can also be triggered by earthquakes or volcanic eruptions (Costa, 1984; Iverson, 1997; Takahashi, 1981).

From the point of view of the initiation mechanism, two types of debris flows can be distinguished: landslide triggered debris flows, and in-channel debris flows. The landslide triggered debris flows are events that start with a slope failure. Then, the sliding mass flows into the stream and becomes a flow like motion. Material from the channel is incorporated into the flowing mass by entrainment, as widely explained in the following section. In contrast, the in-channel debris flows start inside the torrent, when the extremely large water discharge starts to incorporate the loose materials in the channel bed, if the slope is sufficiently steep (Hungr et al., 2005).

1.2.3.2. Triggering rainfall

A threshold for the triggering of rainfall-induced landslides defines the rainfall conditions that, when reached or exceeded, are likely to provoke one or more events (Guzzetti et al., 2007). There are two classes of thresholds: the physical or process-based ones (e.g. Crosta and Frattini, 2003; Godt et al., 2008) and the empirical ones (e.g. Caine, 1980; Cepeda et al., 2010). In this research study, only empirical thresholds are treated.

Empirical rainfall thresholds are a widespread tool in the research of rainfall-triggered landslides and debris flows (see http://rainfallthresholds.irpi.cnr.it) and can be established applying statistical analysis of historic data. Guzzetti et al. (2007) proposed different types of empirical rainfall thresholds for landslide triggering, which can be divided into two major ones: 1) rainfall thresholds defined by precipitation data achieved by specific rainfall events; and 2) thresholds including the antecedent rainfall.

On the other side, the analysis of rainfall data has been used to establish critical rainfall thresholds for debris-flow triggering. A common way to define the debris-flow triggering rainfalls is combining the duration of the rainfall and the rainfall intensity. ID thresholds have the general form:

$$I = c + \alpha D^{\beta}$$ (Equation 1)

where: I is (mean) rainfall intensity, D is rainfall duration, and c≥0, α and β are parameters (Guzzetti et al., 2007).

An excellent review of most of the existing thresholds was published (Guzzetti et al., 2007). This review includes many different thresholds for debris flows, but only a preliminary general one focuses on the Pyrenees (Corominas et al., 2005) and not even one refers to other parts of Spain. Rainfall analysis of historic debris-flow events in the Eastern Pyrenees indicated that 180 to 200 mm total rainfall in 24 to 48 h is necessary to trigger debris flows (Corominas and Moya, 1999; Corominas et al., 2002; Hürlimann et al., 2003a). These results were obtained using daily rainfall amounts, which are the available record of most of the rain gauges existing in the region. However, rainfall data with higher resolution corresponding to recent events have shown, that a short, high intensity rainstorm can also trigger debris flows (Gironès, 2003; Hürlimann et al., submitted), as occurs in other mountain ranges. This latter result illustrates that the analysis of the critical rainfall for debris-flow formation using daily data is rather limited and rainfall records of better resolution are needed.

1.2.4. Post-failure behaviour

1.2.4.1. Runout

In a debris flow, different parts can be identified (Figure 4). They usually consist of one or various surges with steep fronts, charged with boulders, followed by a mass more and more diluted as the distance from the front increases. It usually ends with a muddy water tail (*afterflow*), typically turbulent (Arattano and Marchi, 2008; Hungr, 2000; Iverson, 1997).
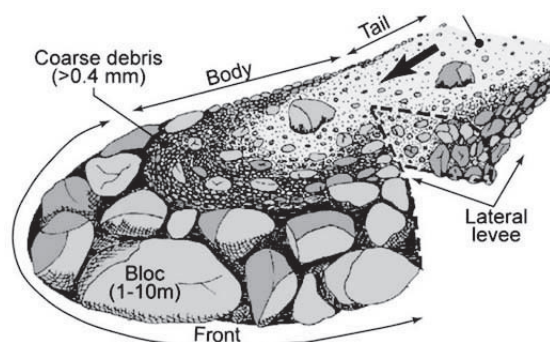

Figure 4: Scheme of a debris-flow mass running down the slope. The main features can be distinguished: steep front, main body and diluted tail (Bardou, 2002).

The velocities that debris flow can achieve are extremely high (up to 35 m/s), and the amount of material involved can be 10 or 100 times the volume of the initial landslide. For this reason, all over the world, debris flows claim hundreds of lives and big amounts of money and properties every year. A necessary information for debris-flow hazard assessment is the energy or intensity along the flow path (Hungr, 1997; Jakob, 2005). The intensity is generally determined by numerical modelling, or by monitoring data, but simple methods could be applied for a preliminary approximation (Hürlimann et al., 2008; Rickenmann, 2005).After the initiation of the debris flow (from a landslide or remobilization of the channel bed material), the moving mass acts as a rapid loading over the material of the flow path, and may entrain loose material from the bed and banks.

Debris-flow numerical models are necessary for engineering practice and are useful to understand the rheological post-failure behaviour of a debris flow event. The total runout distance, the area affected by the event and the energy along the flow path are often determined by a numerical model or other methods of runout prediction (empirical, analytical or simple flow routing). The different models can be classified concerning the dimension of the calculation (1D/2D) or the rheological laws that they use. In debris-flow literature it is used the hydraulic definition and the term one-dimensional (1D) for calculations along a previously selected topographic profile. In contrast, two-dimensional (2D) methods determine debris-flow dynamics over an area typically represented by a digital elevation model (DEM). Thus, 1D methods must be extrapolated into two dimensions to obtain a hazard map, while 2D techniques can be used to directly create a hazard map (Medina et al., 2008) .

1.2.4.2. Entrainment

The entrainment is a common characteristic of debris flows, and has a great influence on both the final volume of the event and the flow behaviour, since it causes variations in the bulk density. A basic step towards debris flow hazard assessment is the prediction of the magnitude (volume). In order to predict the volume of a possible event, the entrainment has to be considered, however there are very few quantitative approaches proposed (e.g. Hungr et al., 1984; Spreafico et al., 1999). On the other side, some authors have suggested that entrainment varies the mobility of the debris flows; therefore it is also relevant to delineate the possible runout lengths (Crosta et al., 2008; Hungr et al., 2005).

The entrainment is a process affected by many factors, but mainly conditioned by the presence of loose material deposited in the path of the debris flow. When the flow composed of water and solid material travels over these deposits (colluvium, glacial till, etc.), the entrainment of the material can occur.

The mechanism of the entrainment can be described by two approaches: the sliding mechanism and the hydrodynamic approach. The "sliding mechanism" is based on Mohr-Coulomb failure criterion (Hungr et al., 2005; Takahashi, 1978; Takahashi, 1991), while the hydrodynamic approach based on bedload transport formulas of fluvial hydraulics (Fraccarolo and Capart, 2002; Rickenmann et al., 2003). The way to introduce the effect of the entrainment in the numerical models differs from one to another. In some cases, an algorithm representing one of the two approaches mentioned is included in the code to decide how much material is entrained along the torrent, while in other cases simply a predefined erosion rate is considered for a specific reach of the torrent.

Further literature review on debris-flow entrainment is presented in Chapter 6 (Estimate of debris-flow entrainment using field and topographical information).

1.2.5. Debris flow monitoring systems

Before 1960, just eye witnesses had reported debris flows, and their behaviour was described in base of that. After 1960, first pictures were taken in Japan by engineers or incidental witnesses. Later in the 70's, systematic observation started in catchments where debris flow occur frequently, by means of debris flow monitoring stations (Suwa and Okuda, 1985; Zhang, 1993).

Field observations of moving debris flows in the monitoring stations are useful to improve knowledge about triggering, dynamic behaviour and accumulation of material generated by this type of phenomena. The data obtained by the monitoring systems can be used for the debris-flow hazard assessment: to back analyse events with runout numerical models and calibrate them, but also to make predictions of future events. Monitoring stations, can also be adapted for their use as a tool to protect against future debris flow events (that can be potentially destructive), working as early warning or alarm systems, EWAS (LaHusen, 2005a).

Upon the knowledge of the author, nowadays in Europe debris-flow monitoring stations are only situated in the Alps: Italy (Berti et al., 2000; Marchi et al., 2002), Austria (Hübl and Kaitna, 2010), Switzerland (Badoux et al., 2009; Hürlimann et al., 2003b) and

France (Navratil et al., 2011) or in the Icelandic fjords (Bessason et al., 2007) while other stations are located in China (Zhang, 1993), Japan (Lavigne et al., 2000; Suwa et al., 2009) , Taiwan (Yin et al., 2009) and USA (LaHusen, 2005a) among others. However, previously to this work there was no monitored site located in a catchment with a climate with a strong Mediterranean influence.

A wide review of types of sensors and use of them is included in Chapter 2 (Technical issues and general data gathered at the Rebaixader debris-flow monitoring site). More details on ground vibration sensors are included in Chapter 3 (Transformation of ground vibration signal for debris-flow monitoring and detection in alarm systems) and Chapter 4 (Analysis of the ground vibration produced by debris flows and other torrential processes at the Rebaixader monitoring site).

1.3. Objectives

The aim of this thesis is to increase data and knowledge on some aspects of the debris-flow hazard assessment at catchment scale. The objectives are raised from a multidisciplinary approach by using two main tools: monitoring and geomorphologic characterization (Figure 2).

Here only the main objectives are cited, however, specific objectives are indicated inside each chapter.

The three principal objectives of the thesis are:

- Developing and setting-up a complete debris-flow monitoring system in a selected catchment in the Pyrenees. The system must be able to detect and provide a detailed characterization of triggering conditions and dynamic behaviour of debris flows and other torrential processes. The objective concerns Part I of this work.
- Analysing the data gathered along the duration of this PhD (4-years) with the intention of:
  - Describing the processes occurred at the monitored catchment. This may contribute to the general characterization of the magnitude, the hazard intensity and the triggering factors of the torrential processes.
  - Interpreting the ground vibration signal produced by the events in order to identify detailed characteristics of them. Several features of the

[11]

seismic sensors make them reliable on their use on monitoring and alarm systems. Therefore, it is crucial to determine what type of information could they provide and how should the ground vibration be acquired and analysed. It is not expected to define a complete EWAS but to provide some key points on the installation and calibration.

- o Giving a detailed characterization of the triggering factors of the events.
- o Providing a magnitude-frequency relationship for debris flows in the monitored catchment.

This objective also concerns Part I of this thesis.

- Developing a simple methodology to estimate the entrainment that can be involved in a debris-flow event. This may contribute on the prediction of the magnitude of future debris-flow events, and this methodology should be applicable to debris-flow prone torrents not only in the Pyrenees but also in other regions. This objective belongs to Part II of this PhD thesis.

1.4. Thesis layout

The body of this document is structured in two main parts (Figure 5):

- *Part I: Monitoring* is based on the experiences gathered in the debris-flow monitoring system
- *Part II: Geomorphologic characterization* concerns the estimation of the entrainment produced by debris flows

Part I is structured as follows: Chapter 2 provides a general review on the pre-existing debris-flow monitoring systems and a comprehensive description of the self-developed monitoring system. It also includes a general description of the test site of Rebaixader torrent, where the monitoring system was implemented. Principal characteristics of the events recorded between 2009 and 2012 are also included in this chapter. A great part of the results presented in this chapter are summarized in Hürlimann et al. (submitted). Chapter 3 has been published in Abancó et al (2012) and describes in detail the method used to transform the complex ground vibration signal measured by the geophones in a monitoring system into a simpler signal. This chapter also introduces the influencing factors of the ground vibration signal, which are treated with more detail in Chapter 4. The main part of Chapter 4 is focused on the characterization and

distinction of torrential processes by means of ground vibration. Two different data acquisition systems are compared. This chapter also deals with the definition of thresholds for the detection of events, which is a key point for the development of alarm systems. A paper is being prepared based on the content of Chapter 4 (Abancó et al., in prep). Chapter 5 gives a detailed description of rockfall events detached from the debris-flow source area in the Rebaixader monitoring site, and is based on the content of the publication Hürlimann et al.(2012).

Part II is considerably shorter than Part I. It contains Chapter 6, which is based on geomorphologic data not gathered in monitoring systems but by field campaigns. This chapter presents a method to estimate the volume of entrained material that can be involved into a debris flow event based on field and topographic data. Chapter 6 is being prepared to be submitted as an article to Natural Hazards journal in Abancó&Hürlimann (in prep).

Chapter 7 provides the final general conclusions of the study (both Part I and Part II). It also contains an outlook for future research lines as an implication of this work. At last, as appendix, a list of publications is included.
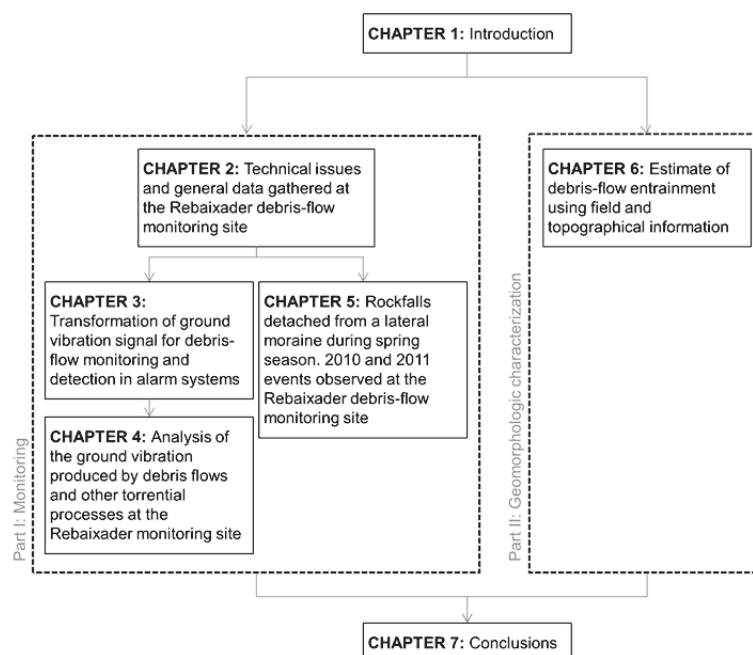
Figure 5: Scheme of the thesis layout

Part I: Monitoring

2. Technical issues and general data gathered at the Rebaixader debris-flow monitoring site

2.1. Introduction

2.1.1. Summary on debris-flow monitoring

Herein, a state of the art on debris-flow monitoring is presented distinguishing three major aspects: 1) initiation, 2) flow dynamics, and 3) accumulation. Whereas, most monitoring systems focus on the initiation and flow dynamics, the accumulation is mainly observed marginally by video camera or geospatial techniques. Thus, this review principally describes sensor and devices related to the first two aspects. No detailed analysis is performed on geomatic techniques, although in recent time, great advances have been achieved applying such techniques including terrestrial laser scan (e.g.Jaboyedoff et al., 2012) or other airborne and spaceborne methods (Pack, 2005).

One of the difficulties in debris-flow monitoring relates to the fact that the process is stochastic. In contrast to slow-moving mass movements, which are monitored by a constant sampling rate, debris flows occur in a random and temporally limited time span. Thus, most debris-flow monitoring systems are able to switch from a "non-event" mode with a low sampling rate to an "event" mode with a high frequency of measurements. The switch between the two modes is triggered by an indirect

[17]

measurement magnitude exceeding a pre-defined threshold, which can be related to ground vibration detected at geophones, to rainfall intensity or other parameters.

2.1.2. Initiation

In the following, the available sensors normally utilized for debris flow monitoring are divided in two classes regarding their location. On one side, the sensors are directly placed inside the active channel in order to measure for example discharge or pore water pressure. On the other side, the sensors can be installed somewhere in the catchment to measure meteorological parameters or soil conditions.

Sensors installed in the catchment, but outside the channel bed

The most common sensors measure meteorological variables. Regarding debris-flow initiation, primary and secondary climatic factors can be distinguished (Wieczorek and Glade, 2005). The primary factors are the ones that are directly related to the trigger of debris flows (normally intense rainstorms), while the secondary ones refer to the antecedent rainfall or snowmelt. Rain gauges are the most common sensors to record precipitation (Hürlimann et al., 2003b; Marchi et al., 2002; McCoy et al., 2010) , although weather radars have shown an increased importance, especially in debris-flow warning (Chiang and Chang, 2009; Winter et al., 2010). In areas with possible snowfall episodes, the effect of snowmelt can influence the primary and particularly the secondary factors mentioned above (Badoux et al., 2009; Hürlimann et al., 2010). Thus, a device measuring the snow height should be considered in such areas.

In addition, there are geotechnical sensors measuring the stress-strength soil conditions. Such sensors are commonly used in landslide monitoring (e.g.Reid et al., 2008). They include different physical magnitudes such as soil water content, suction, pore water pressure, among others (e.g.Godt et al., 2009). Studies based on these geotechnical information are not so common (e.g.Coe et al., 2008; Kean et al., 2011), but they may give relevant information for warning purposes (Greco et al., 2010).

Sensors installed inside the channel bed

Sensors directly placed in the active channel mostly focus on debris flows initiated by progressive entrainment of channel bed material or by firehose effect. Generally, pore

pressure sensors are installed to analyse flow dynamics (see following section) and rarely to record initiation conditions. An example of such monitoring site is located in the Italian Alps, where pore pressure and discharge is measured in the Fiames torrent (Gregoretti, 2012).

2.1.3. Flow dynamics

Ground vibration sensors

It is well known that the passing of a debris flow produces strong vibrations in the ground (Arattano and Moia, 1999; Johnson and Rodine, 1984; Suwa and Okuda, 1985). In general, these vibrations are rapidly damped with distance (LaHusen, 2005a) and affected by other factors like the lithology or the assembly of the sensor (Abancó et al., 2012).

There is a variety of types of sensors used to detect the ground vibration induced by the phenomena including seismometers, geophones or accelerometers. However, the geophones are the most common ground vibration sensors utilised in debris-flow monitoring systems (Arattano and Moia, 1999; Badoux et al., 2009; Berti et al., 1999; Hürlimann et al., 2011).

Additionally, geophones data can provide valuable information on the dynamics of the phenomena. Their measurements have been used to determine information on the mean velocity of the flow front between two adjacent devices or the energy dissipated into the ground (e.g.Arattano and Marchi, 2005; Suwa et al., 2000). Other relevant data such as the magnitude of the event or the type of flow could be obtained, but until now, no clear trends have been found due to the heterogeneous characteristics of the monitoring sites and the relatively low energy dissipated. Further information on geophones is widely explained in the following chapters of this work.

Sensors related to flow height

Flow height is generally registered by a device that measures distance. Ultrasonic devices, radars or lasers are frequently used (Badoux et al., 2009; Kean et al., 2011; McArdell et al., 2007). All these sensors measure the distance from a given and fixed point to the ground. When the flow passes underneath the sensor, this distance decreases due to the debris-flow height. The result is a measurement of the flow height as a function of time. Similarly as the geophones data, flow height sensors can be used

[19]

to determine mean flow velocity. Travel time among two adjacent measurements provides this value. The measurements from flow height sensors also offer information on channel erosion. If calibrated at the installation, variations on the original distance to the ground correlate well with channel erosion.

Pressure and load sensors

Pressure transducers, which are normally fixed in the channel bed, measure the pressure excerpted by the fluid passing over sensor. The later relates to the changing pore fluid pressure when a debris flow is passing above them (Berti et al., 1999; Kean et al., 2011; McArdell et al., 2007; McCoy et al., 2010).

Load cells are usually utilized for dynamic studies. They are normally installed in structures exposed into the flow to determine impact pressure of a debris flow on the structure (Hu et al., 2011; Hübl et al., 2009; Luis-Fonseca et al., 2011) and to measure normal or shear forces caused by the flow (McArdell et al., 2007; McCoy et al., 2010). These values are commonly used in land use planning and the design of active protection elements (Fuchs et al., 2007).

Additional devices

Video cameras are very valuable in debris-flows monitoring systems. They are included in most of the monitoring sites. They provide visual information on the occurrence and dynamic behaviour of a passing debris flow. The cost reduction of the IR cameras has recently increased their monitoring capabilities even under poor visual conditions. Video data are mainly studied to confirm an event and to distinguish between different processes (debris flow vs. debris flood), but they can also be used for detailed investigation by sophisticated image processing (e.g.Chang and Lin, 2007). The main drawbacks of video technologies include the rather elevated cost, the quite high power consumption and the large data volume.

In addition, acoustic sensors are sometimes also included in a monitoring system. They offer the possibility to register the sound induced by the phenomena. Microphones are used to register audible sound (20 Hz to 44 kHz), while infrasonic devices are applied to monitor the low end of the acoustic spectra. Acoustic sensors have shown to be an

excellent complement to seismic sensors, and in some cases even detect the phenomena earlier than the seismic sensors. (e.g.Kogelnig et al., 2011a).

Finally, artificial boulders" have measured the internal dynamics of debris flows (e.g. acceleration and pressure), while they were entrained and transported by the flow (e.g. Lee et al., 2010).

2.2. Description of the Rebaixader monitoring system

2.2.1. Settings

The Rebaixader catchment is located in the central part of the Pyrenean mountain range and drains an area of 0.53 km^2 into the Noguera Ribagorçana River (Figure 6). The basin is situated in the Axial Pyrenees, where bedrock consists of Paleozoic metamorphic rocks including Devonian slates and phyllites formed during the Hercynian orogeny (Muñoz, 1992). Colluvium and granular glacial deposits (tills) cover the bedrock. A large lateral moraine located between 1425 and 1710 m a.s.l. plays a major role on the debris-flow activity. A steep accurate scarp in this lateral moraine forms the initiation zone for the debris flows with almost unlimited sediment availability (Figure 6a). Slope angles in this initiation area are high and range from about 30 up to 70 degrees (Figure 6c). A strongly incised channel zone with an average bed slope of about 21 degrees is located downstream the scarp between 1350 and 1425 m a.s.l. . Finally, a debris fan with a mean slope angle of about 18 degrees drains the torrent into the Noguera Ribagorçana River.

The meteorological conditions of the site are affected by three factors: the vicinity of the Mediterranean Sea, the influence of the west winds from the North-Atlantic and the orographic effects of the Pyrenees. The annual precipitation in the area ranges from 800 to 1200 mm and is strongly influenced by the orographic effect (CAC, 2004).

Several major factors have supported the selection of the Rebaixader torrent for monitoring purposes: 1) an apparently high debris-flow frequency, 2) rather easy access to the torrent, 3) the initiation, transit and accumulation zone are within a small distance (about 1 km), and 4) no torrent control measures disturb the debris-flow dynamics.

[21]
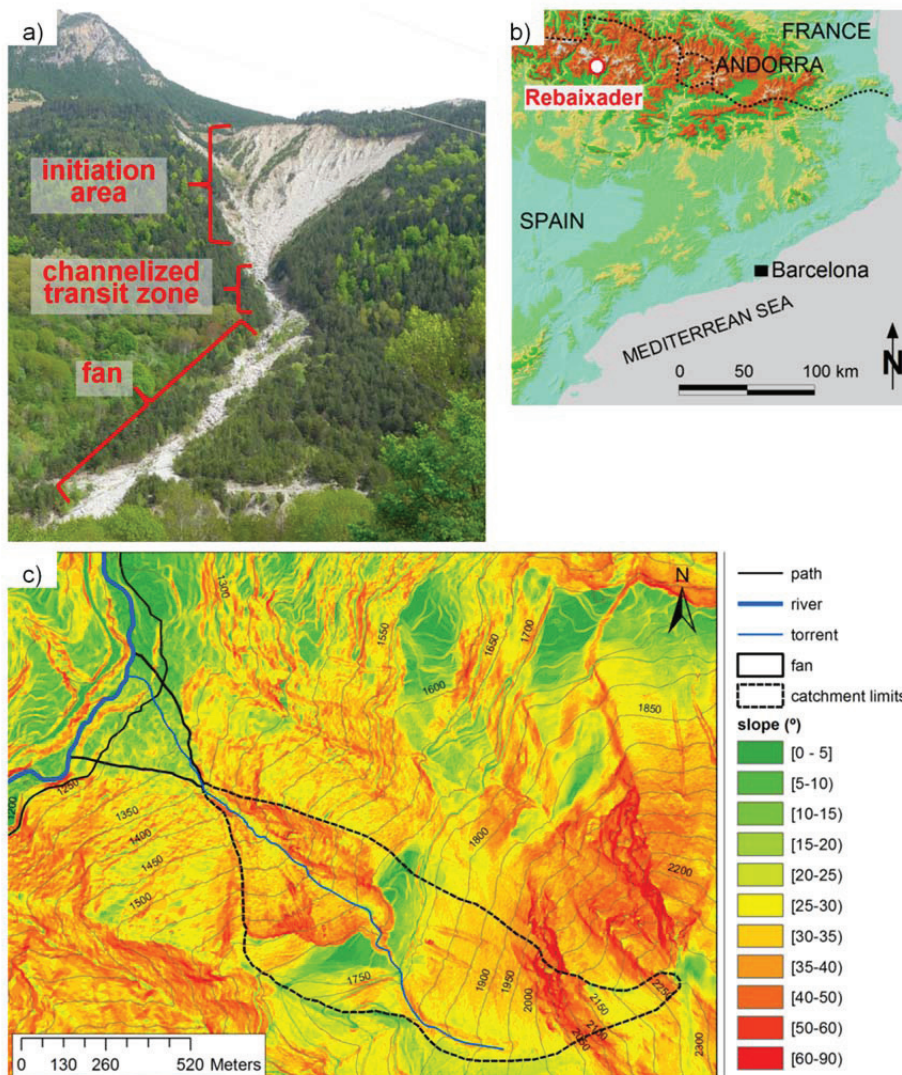
Figure 6: a) Overview of the Rebaixader. b) Situation of the Rebaixader test site. c) Classified slope map of the catchment area derived from the 2m cell-size digital elevation model.

2.2.2. Overview of the monitoring system

The Rebaixader monitoring system incorporates a total of 6 different stations (Figure 7a): four stations recording information on the initiation mechanisms (two meteorological stations and two infiltration stations), and two stations focussing on the debris flow detection and the dynamic behaviour of the flows.

Since summer 2009, when first sensors were installed, the monitoring system has continuously been improved (Table 1). In a first phase, a wired sensor network was

installed including geophones, an ultrasonic device and a meteorological station. This network was complemented in 2011 by a video camera. During 2012, a wireless network related to the initiation mechanisms was installed. Moreover, a new seismic acquisition system was added in June 2012 just before the main debris-flow season.
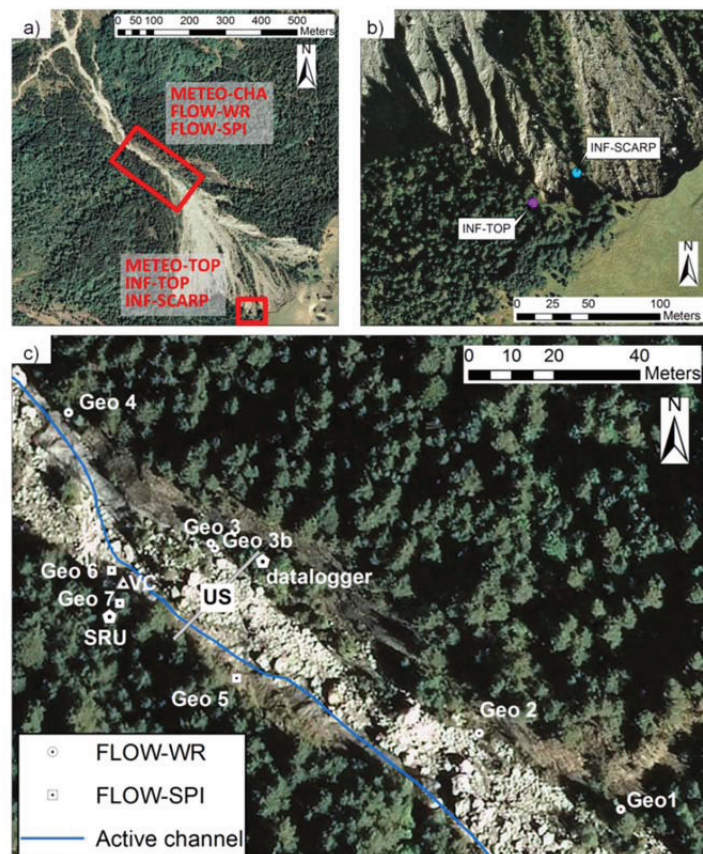
Figure 7: a) Situation of the six monitoring stations installed in the Rebaixader site (see Table 1 for abbreviations). b) Close up of the two infiltration stations located at the side moraine. c) Location of the measuring the flow behaviour at station FLOW-WR and FLOW-SPI. Geo stands for geophone, US for ultrasonic device, VC for video camera and SRU for seismic recording unit

While the wired sensor network has standard characteristics like many other wired monitoring systems (see following sections for detailed explanations), we developed a wireless monitoring system adapted to the specific needs of debris-flow monitoring. This new class of sensor network devices has been provided with wireless communication capabilities, showing ultra-low power consumption (up to 5 years battery life using AA standard cells) and long range communication (200-500 m). The wireless monitoring system is integrated by 7 nodes, which communicate in a multi-hop fashion to deliver the information into a gateway. The wireless communication is based

on the IEEE802.15.4 protocol at 2.4GHz. The gateway offers enhanced computational and storage capabilities as well as modem communication to the UPC server. Eventually, the data is transmitted periodically to a backend system in a database that provides metadata and has a safe backup strategy. A web-based user interface is also implemented to manage the network remotely.

Completing the monitoring, we started in 2012 with a periodic terrestrial laser scanning of the area affected by debris flow including the initiation area, the channelized transit zone and the accumulation zone on the fan. Thus, morphologic changes in all the three zones can be analysed in the future.

Table 1: Stations and sensors installed in the Rebaixader monitoring system.

	Abbreviation of station	Wired or wireless*	Sensors (number of sensors)	Model	Installation year
Initiation	METEO-CHA	wr	rain gauge (1)	RM YOUNG 52203	2009
			air temperature sensor (1)	Campbell Scientific CS215	2009
			relative air humidity sensor (1)		2012
	METEO-TOP	wl	rain gauge (1)	Decagon ECRN-100	2012
			air temperature sensor (1)	Decagon PASSECT	2012
			snow height sensor (1)	Campbell Scientific SR50A/AT	2012
	INF-TOP & INF-SCARP	wl	soil moisture sensor (3 & 3)	Decagon 10HS	2012
			water potential sensor (2 & 2)	Decagon MPS-2	2012
			soil temperature sensor (2 & 2)		
Flow dynamics	FLOW-WR	wr	geophones (5)	Geospace 20 DX	2009
			ultrasonic device (1)	Pepperl+Fuchs UC6000-30GM-IUR2-V15	2009
			video camera (1)	Mobotix MX-M12D-Sec-DNight-D43N43	2011
	FLOW-SPI	wr	geophones (3)	Geospace 20 DX	2012

* wr for wired network and wl for wireless network

2.2.3. Monitoring of debris-flow initiation

In 2009, the meteorological station called METEO-CHA was installed in the transit zone (Figure 7a). This station includes a rain gauge with a resolution of 0.1 mm and an air temperature sensor. In 2012, the temperature sensor was replaced with a device measuring both temperature and relative humidity of the air. The station also consists of a Campbell Scientific CR200 datalogger and a Wavecom Fastrack GSM modem for data transmission. As an important drawback, the effect of the snowmelt in spring cannot be correctly analysed by this type of sensors. Therefore, during 2012, a second meteorological station called METEO-TOP was installed at the top of the side moraine (Figure 7a). It includes an ultrasonic device for snow height measurements, a raingauge and a temperature sensor. This latter station forms part of the wireless network described above.

During 2012, two additional stations were installed to analyse the infiltration of water into the ground, the pore water pressure and the soil temperature (Figure 7b). One station (INF-TOP) is located at the top of the lateral moraine. The other station (INF-SCARP) was positioned inside the scarp in an area, where geomorphologic indicators (i.e. presence of shrubs and small trees) suggested a low activity. Both stations consist of three soil moisture sensors and two sensors registering both suction and soil temperature. These sensors are collocated at three different depths (between -15cm and -75cm) in order to measure saturation mechanisms and freezing-thawing effects. Both stations are integrated in the wireless network.

The meteorological and infiltration data are recorded at a constant sampling rate of 5 minutes.

2.2.4. Monitoring of flow dynamics

In the Rebaixader test site, three types of devices focus on the flow behaviour: 1) geophones measuring ground vibration of the passing debris flow, 2) an ultrasonic device recording the flow height; and, 3) a video camera for visual observations. All these devices are installed in the channelized transit zone of the torrent along a reach of about 175 m (Figure 7c).

Two approaches are used to monitor ground motion. On one side, the ground vibration is transformed into impulse per second (*IS*) time series. On the other side, the ground velocity signal is directly recorded at 250 samples per second. The transformation technique and its advantages are extensively explained in Chapter 3 and in Abancó et

al. (2012), while the procedure to analyse ground velocity signals can be found in other studies (Huang et al., 2007; Kogelnig, 2012; Marchi et al., 2002).

The first approach applying signal transformation is used in the station FLOW-WR and incorporates 5 geophones. Four geophones (Geo1, Geo2, Geo3 and Geo 4) are mounted inside a metal sheet box, which is fixed on bedrock, while the fifth geophone (Geo3b) is mounted directly on bedrock. All geophones are installed on the right bank of the torrent, about 8 – 25 m away from the currently active channel (Figure 7c). They are connected by electrical wires with a Campbell Scientific CR1000 datalogger. The datalogger counts the number of impulses at each geophone and checks the sum every second. If one of the geophones exceeds the detection threshold (Dth) (20 IMP/sec during three consecutive seconds), the station switches from the "no-event" mode to the "event" mode (Figure 8). During the "event" mode, the impulse per second time series of the five geophones are registered in the datalogger internal memory at 1 sample per second, while the sum of impulses is recorded every 60 minutes during the "no-event" mode.

The FLOW-WR station also incorporates an ultrasonic device. The raw measurements, which strongly depend on the air temperature, are automatically and internally corrected by means of a temperature sensor that is connected to the device. The ultrasonic device is mounted within a PVC box on a steel construction that is fixed at cables hanging over the torrent at about 6 m. The device is connected by a standard electrical cable with the datalogger. When the datalogger program switches to "event" mode, the ultrasonic device is measuring at 1 sample per second, while only one value every 60 minutes is recorded during the "no-event" mode (Figure 8).

An additional device of station FLOW-WR is the day/night camera, which provides images in visible and infrared light. The camera is configured to take a daily picture of the selected channel reach and to record a video during the "event" mode (Figure 8). A switch port of the datalogger starts the camera via a relay, while a second relay turns on two infrared spotlights for images during night. The daily pictures and event videos are saved in a memory card, which is downloaded manually every field survey.

The FLOW-WR station also involves a GSM modem for data transmission and a GPS receiver, which permits time synchronization with the other stations.

At the beginning of summer 2012, the new station FLOW-SPI was installed. This station consists of three geophones located on the left torrent bank about 3 to 5 m from the active channel (Figure 7c), one on bedrock (Geo5) and two in soil (Geo6 and Geo7). The geophones are connected to a 24 bits broadband seismic recording unit (Spider produced by Worldsensing), which allows digitizing the three channels at 250 samples per second and synchronises time by a GPS. Data can be visualized and downloaded by the gateway of the wireless network described in the previous section.
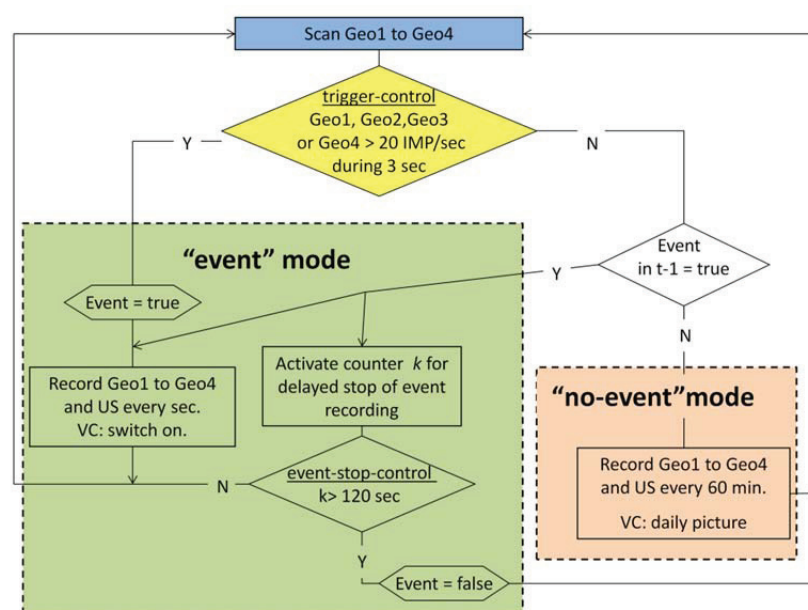
Figure 8: Flowchart of the datalogger program installed in the station FLOW-WR controlling the geophones (Geo1 to Geo4), the ultrasonic device (US) and the video camera (VC)

2.3.   Data recorded at the Rebaixader monitoring system

2.3.1. General aspects and temporal occurrence

Between July 2009 and December 2012, the station FLOW-WR has triggered 363 times the "event" mode. The available records of all these triggers were analysed and the resulting information was completed by more than 30 field visits.

The procedure of the data analysis included various steps. First, geophone and ultrasonic data were analysed and compared with debris-flow features observed at

other monitoring sites (e.g. Marchi et al., 2002) and described in the literature (e.g. Hungr et al., 2001). When evidences of an event were detected, a field survey was carried out. During this reconnaissance, morphologic changes in the scarp, channel and fan were described and photos were taken at eight control points (Figure 9). Finally, the video images were checked to verify the process classification. Unfortunately, the video camera was not running before summer 2011 and the ultrasonic sensor was not operational during many events because of rockfalls that destroyed twice this device.
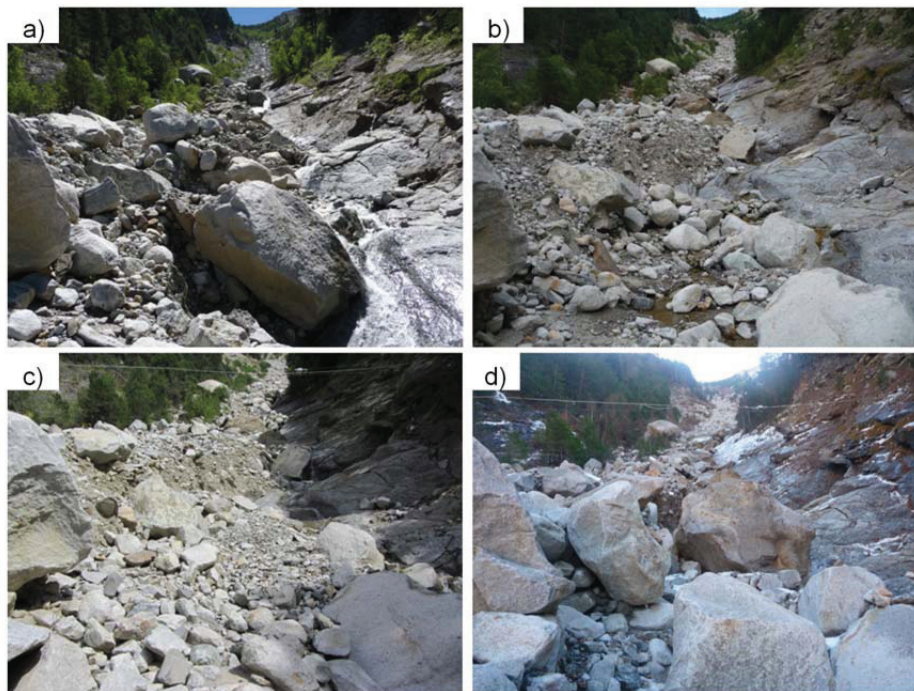
Figure 9: Example of morphologic changes at the control point situated at the fan apex. The photos are taken upstream covering the channel reach, where the two flow stations are installed. a) pre July 2010 debris flow, b) post July 2010 debris flow, c) pre July 2012 debris flow, d) post July 2012 debris flow.

The interpretation of the available data showed that most of the triggers were not associated with debris flows. Thus, a classification of different triggers was established distinguishing between: 1) debris flows, 2) debris floods, 3) rockfalls; and, 4) other triggers. Since the monitoring system and our data interpretation have continuously improved, the procedure of this process distinction was adapted over the years. In the following, the most important criteria of our classification will be described.

In this work, we are not only focusing on debris flows but also on debris floods, because both processes represent an important torrential hazard (Badoux et al., 2009). The classification between debris flows and debris floods is based on the terminology proposed by Hungr et al. (2001). The class "rockfall" was necessary, because various big boulder falls affected our monitoring system and activated the "event" mode (see Chapter 5 and Hürlimann et al., 2012). At last, the class "other triggers" principally includes events provoked by technical problems and other mass movements or erosional processes in the steep open scarp of the lateral moraine, which exceeded the ground vibration threshold of the highest geophones Geo1 or Geo2.

After the classification of the 363 triggers, a total of 6 debris flows and 11 debris floods were defined (Table 2). Surprisingly, also 4 major rock falls were recorded by the monitoring system. The analysis of the 342 "other triggers" showed that 216 were provoked by a short circuit in the 2-wired cable that connects geophone Geo1 and the datalogger. This short circuit was caused by the 13th May 2010 rockfall cutting the cable and producing the large amount of accidental triggers between May and July (Fig 5a).

Figure 10: a) Temporal occurrence of debris flows, debris floods, rockfalls and other triggers recorded at Rebaixader monitorin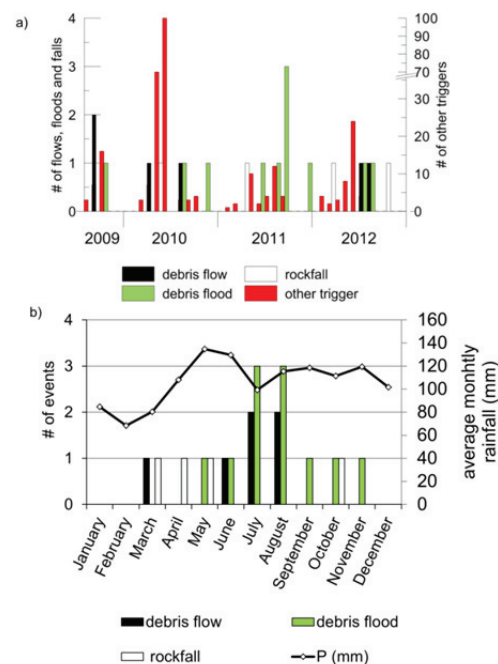g site. b) Monthly distribution of the debris flows, debris floods and rockfalls and comparison with average monthly rainfall values

[29]

The temporal evolution of the events shows that normally two debris flows were detected every year, except of 2011, when several debris floods occurred (Figure 10a). The monthly distribution of the 6 debris flows, 11 debris floods and 4 major rockfalls indicates that most of the events occurred during summer (57%) with a peak in July and August (Figure 10b). The other events took place in spring (24%) and in autumn (19%), while no event occurred during winter. The initiation of most of the spring events is related to snowmelt and freezing-thawing effects (Hürlimann et al., 2010; Hürlimann et al., 2012). The average monthly rainfall obtained from the Digital Climatic Atlas of Catalonia (CAC, 2004) is added as general information.

Table 2: Summary of recorded data for the 6 debris flows ("DFlow") and 11 debris floods ("DFlood") observed at Rebaixader torrent. See text for abbreviations.

Date and time of trigger (dd/mm/yyyy hh:mm)	Type	Volume (m^3)	Rainfall				Ground vibration		Ultrasonic device data	
			D_P (min)	P_{tot} (mm)	P_{h_max} (mm/h)	P_{a_3d} (mm)	IS_{max} (IMP/sec)	IS_{mean} (IMP/sec)	$dH_{pre-post}$ (cm)	dH_{max_10s} (cm)
01/08/2009 16:42	DFlow	6600	120	32.2	26.5	0	94	nd	nd	nd
07/08/2009 13:08	DFlow	9000	120	35	30	106.5	460	nd	nd	nd
01/09/2009 19:18	DFlood	1000	135	33.2	20.5	nd	nd	nd	nd	nd
25/03/2010 23:38	DFlow	2100	180	15.1	9	20.2	160	75	nd	nd
11/07/2010 12:43	DFlow	12500	200	97.3	49.3	3.1	244	118	nd	nd
21/07/2010 19:04	DFlood	1000	55	11	11	5.3	203	28.4	nd	nd
09/10/2010 20:59	DFlood	1600	50	12.1	12.1	0	99	28.2	-2	13
30/05/2011 10:18	DFlood	850	nd	nd	nd	nd	204	28.1	48	29
13/07/2011 0:32	Dflood	700	20	9.2	9.3	3	166	25.8	20	35
05/08/2011 10:58	DFlood	2800	30	13.8	13.8	2.4	118	26.1	33	19
05/08/2011 14:00	DFlood	2500	60	15.6	15.6	16.2	90	18.8	-46	22
07/08/2011 2:23	DFlood	350	35	10.5	10.7	39.5	80	24.4	0	6
03/11/2011 14:42	DFlood	600	90	14.4	13.4	58.6	134	20.4	-28	28
07/06/2012 16:53	DFlood	750	nd	nd	nd	nd	186	22.0	-2	10
27/06/2012 20:09	DFlow	4000	115	17.6	15.8	nd	128	80	-1.7	55
04/07/2012 20:27	DFlow	16200	100	16.6	15.6	0.1	204	119	3.2	225
05/07/2012 15:26	DFlood	1000	45	4.5	4.5	28.8	367	22.2	nd	15

2.3.2. Ground vibration records

In this work, we focussed on the data recorded at the station FLOW-WR, which includes measurements of all the events observed between 2009 and 2012 (Table 2). A specific analysis on the seismic data registered at FLOW-SPI can be found in Chapter 4.

The ground vibration produced by the passing of two selected debris flows is illustrated in Figure 11. As previously mentioned, the ground vibration signal is transformed and recorded by impulse per second (IS) at station FLOW-WR.

As widely explained in Chapter 4, the most typical feature in seismic recordings of a debris flow is the steep front (e.g. Arattano et al., 2012; Suwa et al., 2009). This maximum vibration is generally induced by the impacts of large boulders, which are transported at the head of the granular debris flow (Arattano and Moia, 1999). Other common features include a posterior gradual decrease after the front and the possibility of additional peaks corresponding to surges.

Most of these characteristics were observed in the *IS* time series registered during the debris-flow events at Rebaixader torrent, but clearest features were revealed by geophone Geo4, located in the distal part of the channel zone (Figure 11). The differences visible in the *IS* time series of the geophones can be attributed to their positions along the channel (Figure 7c). On one side, the ground vibration signal is affected by the distance between geophone and the active channel, the lithology and the sensor assembly (Abancó et al., 2012). On the other side, there are mechanisms related to the dynamic behaviour of the moving mass within the channel reach monitored by station FLOW-WR. The geophones are situated in the rather steep channel connecting the initiation zone with the fan (Figure 6c), and the ground vibration data seem to indicate that most events transform in this reach into mature debris flows. This transformation is particularly visible in the records of the July 4th 2012 debris flow (Figure 11b). The downstream geophones (principally Geo4) indicate the typical steep front, while the geophones installed at the highest elevation (especially Geo1) do not show debris-flow features. The rather high ground vibration at the beginning of the record at geophone Geo1 may be associated with small-scale mass movement (for example debris slides or flows) that travelled to the lower part of the scarp, where the flow is not yet channelized.
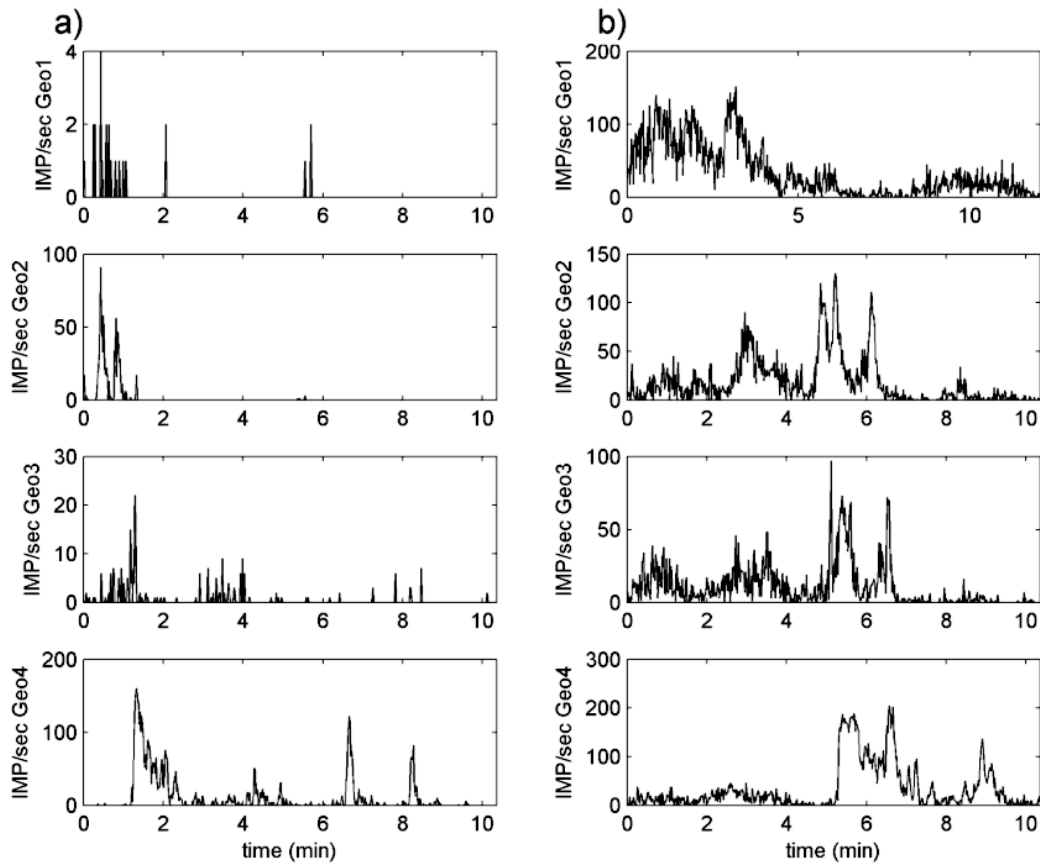
Figure 11: Ground vibration produced by the passing of two debris flows. The data measured at four geophones of station FLOW-WR is presented as impulse per second time series. a) 25th March 2010 debris flow and b) 4th July 2012 debris flow

2.3.3. Flow hydrographs

Stage measurements by the ultrasonic device data are very incomplete (Table 2). Initially, the sensor was installed at the higher part of the channel reach near geophone Geo2, where several rockfalls damaged and finally destroyed the device. In August 2010, a new sensor was installed about 65 m downstream, where the probability of rockfall damage is much smaller.

Nonetheless, the available stage data provided valuable information on the temporal evolution of flow height and on the erosion or accumulation potential of the events at the cross section monitored. A typical debris-flow front was registered by the ultrasonic device during the July 4th 2012 debris flow (Figure 12a). A sharp increase of the stage measurements (more than 2 m in 7 seconds) is clearly visible at the front of the event

(at 60 sec), while subsequently the device seems to be blocked at a constant value during more than one minute (between 75 sec and 150 sec) overlooking an important surge (at about 135 sec). This surge and other following surges were detected by the ground vibration signal recorded at geophone Geo5 of station FLOW-SPI (installed next to US device; see Figure 7c). In fact, the first half of the hydrograph includes several intervals of constant values, which seem to be related to a malfunction of the sensor during the most energetic phase of the flow. For comparison, the hydrograph of the August 5th 2011 debris flood (triggered at 10:58) is illustrated (Figure 12b). The differences with the debris-flow hydrograph are evident and no abrupt change is visible in the stage measurements. In contrast, the hydrograph is characterised by a continuous increase over several minutes. The first records in the "no-event" mode showed that the debris flood terminated with an accumulation of almost 0.5 m of sediment in the channel bed.
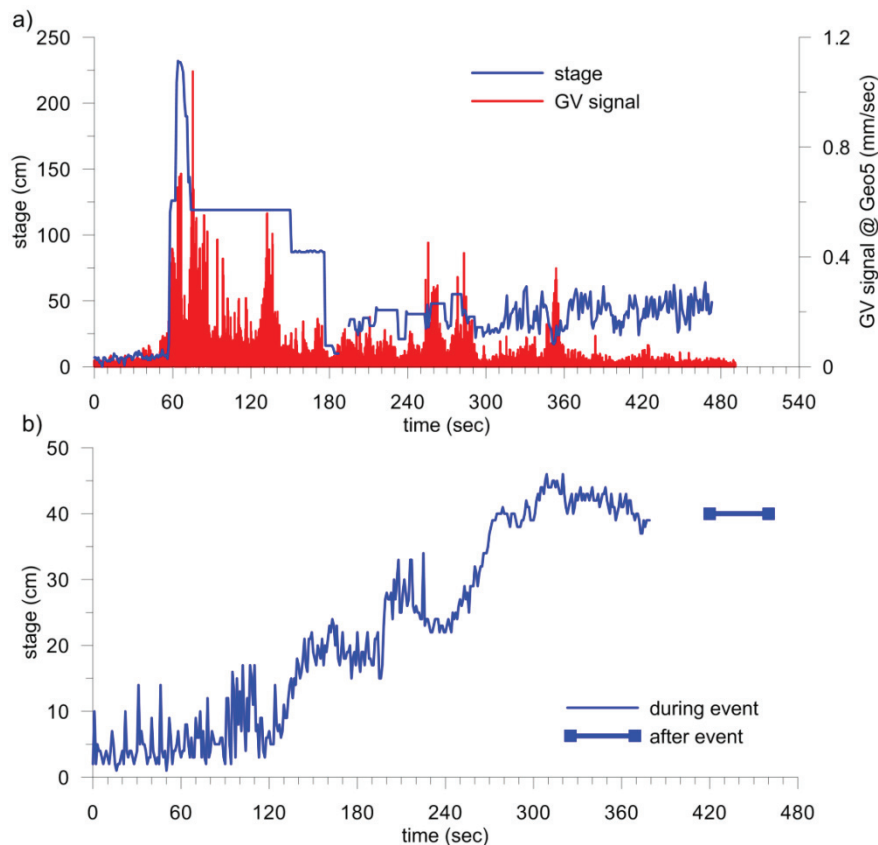

Figure 12: Debris flow versus debris flood hydrographs measured at the ultrasonic device. a) 4th July 2012 debris flow; the absolute ground vibration signal recorded at geophone Geo5 of station FLOW-SPI is added for comparison. b) 5th August 2011 debris flood (triggered at 10:58)

[33]

In addition, the maximum increase of flow height within different time intervals (5, 10 and 30 seconds) was calculated in order to quantify the characteristics at the front of the flows. The maximum increase within 10 seconds (dH_{max_10s}) is listed in Table 2 for all debris flows and debris floods. In spite of the incomplete dataset, dH_{max_10s} – values of 55 cm and even 225 cm were calculated for debris flows revealing a fast and large increase of flow height at the front. In contrast, smaller values between 6 and 35 cm were calculated for debris floods indicating a minor and smoother increase of flow height.

The potential of erosion or accumulation was analysed by comparing the level of the channel bed before and after an event ($dH_{pre-post}$). The resulting values were checked by the daily pictures taken by the video camera (see Fig. 2c for location), which cover the cross section of the ultrasonic device, and by the photos taken at the control point near the fan apex (Fig. 4). Absolute values of $dH_{pre-post}$ range from zero (no change of the channel bed elevation) to almost half a meter: 48 cm of accumulation during May 30th 2011 debris flood, or 46 cm of erosion during August 5th 2011 debris flood (Table 2). At the end of 2011, bedrock cropped out at the cross section indicating that the previous flows were able to remove all the available channel bed sediment. The irrelevant changes measured for the 2012 events indicate that no new material was accumulated by these events.

2.3.4. Characteristics of the triggering rainfalls

In this section, some aspects of the triggering rainfalls are presented and compared with data gathered at other monitoring sites. The hydrologic response of the soil is not commented, because only preliminary data are available from the infiltration stations, which were installed in 2012.

We focussed on the rainfalls that generated debris flows and debris floods, while additional rainfall episodes completed the dataset as "no events". The data recorded at station METEO-CHA show that the debris flows and debris floods were triggered by short and high-intensity rainstorms (Fig. 8a and 8b). The duration of the triggering rainfalls, D_P, was always smaller than 220 minutes for both process types and mostly around 2 hours for debris flows (Table 2). While the total rainfall amount, P_{tot}, does not permit a clear separation between rainfalls that caused debris flows, debris floods and no events (Figure 13a), the peak hourly rainfall, P_{h_max}, better allows defining

[34]

preliminary thresholds (Figure 13b). Critical hourly rainfall amounts, which cause debris flows in the Rebaixader torrent, might be around 15 mm/h for the summer season and even lower than 10 mm/h during spring. The triggering in spring seems to be affected by a combination of snowmelt and thawing-freezing (see values of 25th March 2010 debris flow in Table 2). Recently installed sensors, which measure soil moisture, water potential and temperature of the soil, will provide additional information on this aspect. Finally, the influence of antecedent rainfall was analysed, but neither 3-days nor 10-days antecedent rainfall played a significant role in the triggering of debris flows and debris floods (Figure 13c).
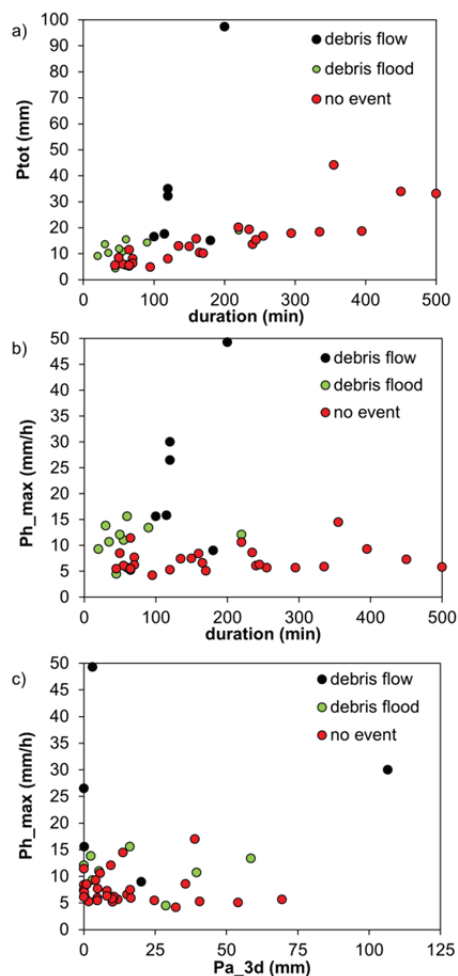
Figure 13: Rainfalls characteristics associated with the initiation of debris flows and debris floods (major rainstorms not triggering events are added for comparison). All the data were measured at the meteorological station METEO-CHA. Total rainfall, P_{tot} (a) and maximum hourly rainfall, P_{h_max} (b) versus rainfall duration. c) The effect of 3-days antecedent rainfall, P_{a_3d}

Figure 14 shows a plot of rainfall duration versus average rainfall intensity for the events observed at Rebaixader. The graph shows that short durations up to one hour

[35]

seem to be more useful for the distinction between flow events (debris flows and debris floods) and "no events". However, spring events associated with snowmelt generate some misinterpretation in this distinction (especially the 25th March 2010 debris flow). Therefore, we consider that additional events are necessary in order to define a reliable rainfall threshold for the Rebaixader torrent. Nevertheless, our dataset was compared with the thresholds established at three debris-flow monitoring sites: the Moscardo torrent in Italy (Deganutti et al., 2000), the Illgraben torrent in Switzerland (McArdell and Badoux, 2007) and the Chalk Cliffs basin in the United States (Coe et al., 2008). This comparison shows that the Rebaixader data fits rather well with the one established at Illgraben.
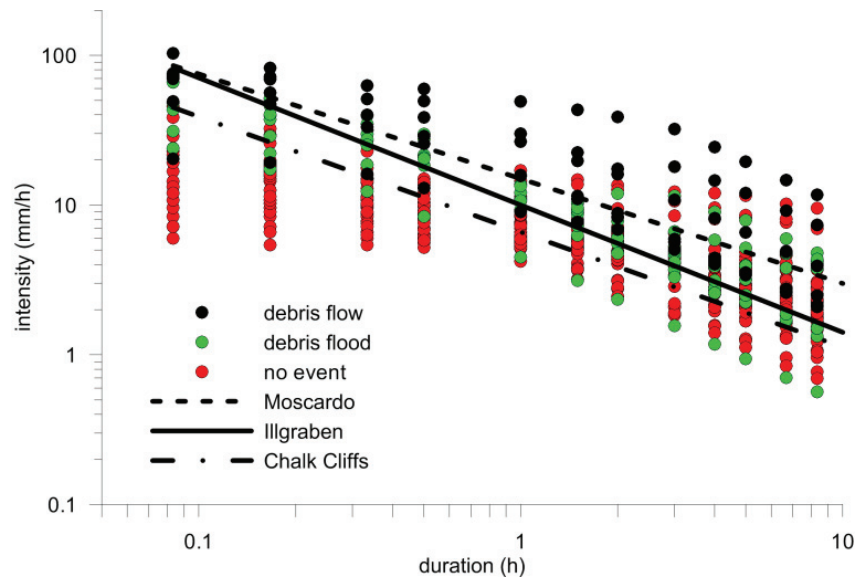
Figure 14: Rainfall intensity – duration relationship of the Rebaixader data compared with thresholds established at three other debris-flow monitoring sites (for references, see text)

2.3.5. *Volume estimates and associated relationships*

The volume represents essential information for the global interpretation of a monitored event. Ideally, the total volume, *V*, of debris flows and debris floods can be estimated by the following expression

$$V = \sum_{t=t_0}^{t_{end}} A(t)\, v(t)\Delta t \qquad\qquad \textbf{(Equation 2)}$$

, where t_0 and t_{end} are the start and end times of the event, $A(t)$ and $v(t)$ are the flow area and flow velocity at time *t* and Δt is the time between the sensor recordings.

[36]

Because the determination of *v(t)* was not possible at Rebaixader site, we calculated the mean front flow velocity, v_m, by geophone and ultrasonic sensor data (see Arattano and Marchi, 2005) and simplified Equation 1 into

$$V = v_m \sum_{t=t_0}^{t_{end}} A(t)\, \Delta t \qquad \text{(Equation 3)}$$

The flow area was generally approximated by the flow height measured at the ultrasonic device and the information of the cross section shape measured during the field campaigns. The video images were used to check the flow area of debris floods, because smaller debris floods did not directly pass below the ultrasonic device. There were also a few events that only included geophone recordings (no stage measurements neither video images). Then, Equation 2 was reduced into

$$V = v_m\, A_{peak}\, \beta\, D_{event} \qquad \text{(Equation 4)}$$

, where A_{peak} is the peak flow area measured in the field, β is a shape factor of the ground vibration signals (representing in a simple way the shape of the hydrograph) and D_{event} is the duration of the event (corresponding to the duration of important ground vibration recorded at geophone Geo4).

In spite of the lack of a complete dataset for many events, volume estimates of all the recorded debris flows and debris floods were carried out by one of the described methods (Table 2). The volumes of the debris flows ranged from 2100 m^3 to 16200 m^3, while debris floods normally included rather small volumes of some hundreds of cubic meters up to 1000 m^3. However, there were also two large debris floods involving about 2500 and 2800 cubic meters.

The volume estimates were first compared with the ground vibration data. The relationships between event volume and different parameters extracted from the IS time series are given in Figure 10. The sum (ISsum), the mean (ISmean) and the maximum (ISmax) of the IS time series registered at all the geophones were analysed. An increase of these three parameters with the volume was expected, since larger events produce larger peak discharges (e.g. Rickenmann, 1999), and consequently stronger ground vibration. However, no clear relationships were visible. Only a small positive correlation was recognised between event volume and ISsum , while no relation between ISmax and volume was observed. In contrast, the expected positive relationship between event volume and ISmax was detected at geophone Geo4 (Figure 15d). The ISmax – values recorded at Geo4 can also be used to distinguish between

[37]

debris flows and debris floods. These data support the hypothesis that there is a transformation of the flow in the steep channel reach and a mature debris flow can be best observed at the outlet of the channel.
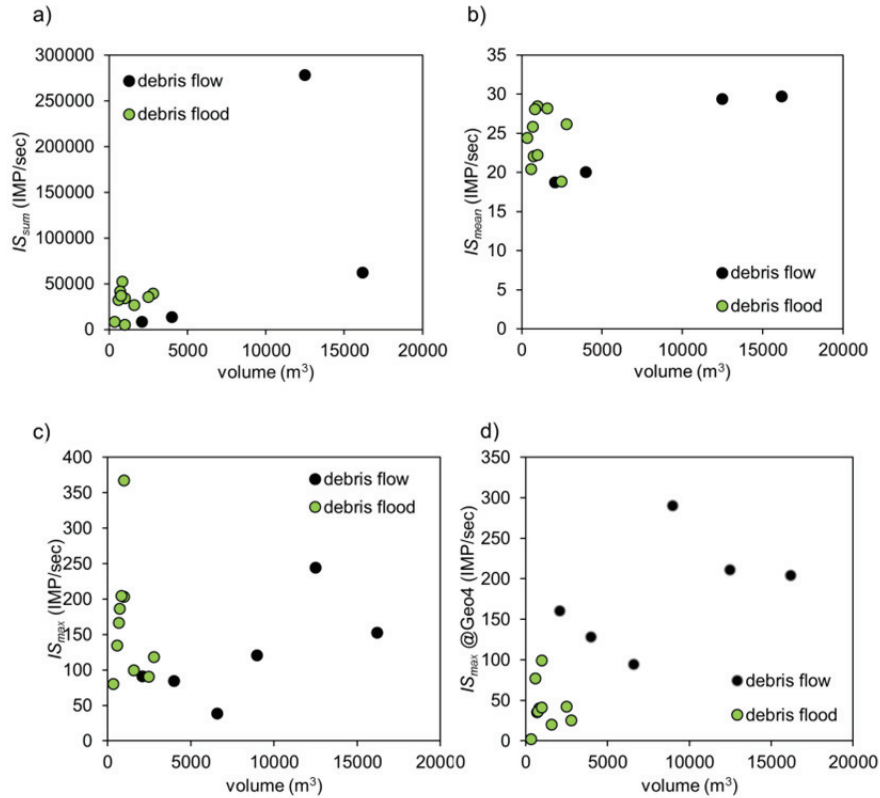
Figure 15: Relation between ground vibration signals measured at the geophones of station FLOW-WR as impulse per second (IS) time series and the event volumes distinguishing between debris flows and debris floods. a) Sum of IS time series, ISsum, b) mean of IS time series, ISmean, c) maximum of each IS time series measured at all geophones, ISmax, d) maximum of each IS time series measured at geophone Geo4

In addition, the volumes of debris flows and debris floods were compared with the total triggering rainfall, P_{tot}, and maximum hourly rainfall, P_{h_max} (Figure 16). The graphs show a general trend indicating that the event volume increases with both larger rainfall amounts and larger rainfall intensities. Only the largest debris flow, which occurred on 4th July 2012 and mobilized a total volume of about 16200 m^3, does not match this trend and rainfall values are smaller. This may be related with the absence of debris flows during 2011 and a large amount of material remained accumulated in the lower parts of the open scarp at the beginning of summer 2012. This hypothesis is supported

[38]

by observations gathered during the field reconnaissance. A similar relationship between sediment availability, debris flow occurrence and amount of triggering rainfall was proposed for the Moscardo torrent (Deganutti et al., 2000).
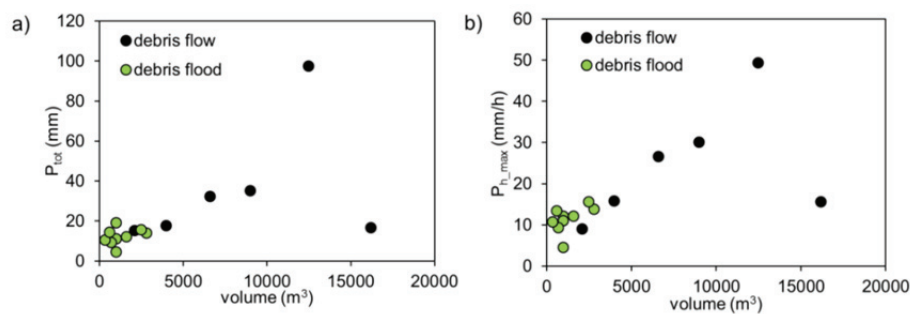
Figure 16: Relationships between the characteristics of the triggering rainfall and event volumes distinguishing between debris flows and debris floods. a) Total rainfall amount versus volume and b) maximum hourly rainfall versus volume

Finally, the volume estimates and the information on the temporal occurrence were used to plot a magnitude (*M*) – cumulative frequency (*CF*) relationship (Figure 17). Such relationships are fundamental information in hazard and risk analysis at catchment scale (Jakob, 2005). In the Rebaixader torrent, the resulting *MCF* relationship can be represented by a power law with the following expression:

$$CF = 326\ V^{-0.68}$$
Equation 5

A comparison with other catchment-scale *MCF* relationships is difficult, because most of them have been established by dendrochronology or other dating techniques only taking into account large exceptional events (Corominas and Moya, 2010; Jakob and Friele, 2010). The slope of the power law relation indicated in Eq. (4) is in good accordance with the one expressed by Corominas and Moya (2010) for the Tordó torrent, in the Pre-Pyrenees, although the frequency of debris flows is one order of magnitude higher in the Rebaixader torrent.
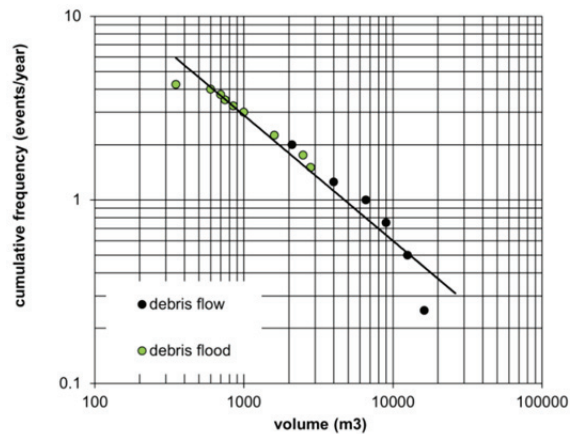
Figure 17: Magnitude versus cumulative frequency of debris flows and debris floods observed at the Rebaixader torrent. Straight line indicates the power law expression of Equation 5.

2.4. Discussion on debris-flow monitoring

Apart from the outcomes directly related to the processes, many lessons were learnt regarding technical issues of monitoring. In the following, we first discuss three overall problems in debris-flow monitoring, then we explain our experiences on sensor selection and finish with a remark on data interpretation.

First of all, debris flow is a stochastic process and thus the monitoring system should differentiate between a "no-event" mode with a low sample rate and an "event" mode with a fast sampling. A differentiation of monitoring modes strongly reduces the data amount as well as the power consumption, and it also facilitates the post-processing of the records. This switch should especially be operational in the stations measuring the flow dynamics, while the meteorological and the infiltration stations may record at constant frequency. At Rebaixader, the switch into the "event" mode is defined by a critical ground velocity measured at the geophones. The correct definition of this threshold is of great importance and depends on many factors (Abancó et al., 2012; LaHusen, 2005a). In contrast, other monitoring systems switch into the "event" mode, when rainfall starts (e.g. Coe et al., 2008). This approach avoids the problem with the definition of a threshold, but generates many "triggers" without debris-flow occurrence.

One of our major technical problems arisen during the monitoring tasks concerns the power supply. Because of the remote location of the site and the limited duration of

direct sunlight large solar panels and batteries were installed and sensors with low power consumption were selected. Large solar panels present an important weakness as they become an exposed element, which can be stolen or damaged by a rockfall, debris flow or snow avalanche. A wireless sensors network seems to represent an ideal technology to resolve the problem of power consumption, since the wireless nodes work with small batteries during several years. Apart from the low power consumption, another major benefit of the wireless technique is the independence from wiring and the subsequent opportunity to collocate sensors at long distances almost everywhere in the catchment without using bulky expensive cables. For example, the crossing of the channel by wires, which is laborious and vulnerable to debris flows or other mass movements, can be avoided by a wireless network.

In the Rebaixader torrent, the rockfall events stand for an unexpected problem. Mass movements like rockfalls or snow avalanches should never be neglected in the design of a debris-flow monitoring system, since they can represent an important danger for the installation and persons working in the site. This drawback specially occurs, when the devices are collocated in the higher parts of the channel. However, the installation of sensors in that area might be scientifically interesting, because initiation processes and the formation of debris flows can be better observed. In contrast, the data recorded at Rebaixader also show drawbacks of monitoring the upper reaches of a torrent, since the features of mature debris flows were principally visible at the downstream devices close to the fan apex. In conclusion, the adequate locations of the sensors should be initially evaluated in detail, because they depend on various factors like the characteristics of the catchment or the goals of the research.

The selection of appropriate sensors is of particular interest for the debris-flow detection. Our experiences showed that the geophones offer numerous advantages over other sensors. First, they are very robust non-invasive sensors and thus can be placed some distance apart from the torrent. Moreover, visibility of the torrent is not required, they are simply placed into the ground, and consequently no complex structures to sustain them are required. Because geophones cannot provide information on flow height, additional sensors like ultrasonic, radar or laser devices are necessary. Regarding stage measurements, a problem encountered in the Rebaixader torrent is given by the fact that debris floods many times not exactly pass below the ultrasonic device, and thus flow height are underestimated. This aspect must especially be considered for the stage measurements of small events in wide channels.

A correct interpretation of the recorded data is many times complex; in particular when visual information is missing. Therefore, the installation of a video camera is very recommendable, because many uncertainties will be clarified. Video images are helpful to confirm an event and to distinguish between different processes (in our case debris flow and debris flood). However, video technologies have multiples drawbacks like the rather elevated cost, the quite high power consumption and the large data volume. Moreover, a video camera only covers a limited reach of the torrent. That's why periodic field observations of the entire catchment are compulsory tasks, which strongly improve the interpretation and understanding of the data measured by the monitoring system.

2.5. Conclusions

Between summer 2009 and autumn 2012, a total of 6 debris flows and 11 debris floods were detected by the monitoring system installed in the Rebaixader torrent. While our experiences on monitoring have been discussed in the previous section, here we principally summarise our conclusions regarding the processes.

The distinction between debris flows and debris floods was performed by the analysis of the recorded data and field observations. While debris flows can principally be characterised by a sharp increase of ground vibration and flow height, when the front is passing, the recordings of debris floods had smoother shapes and no steep front.

The recordings of the ground vibration signals show that the debris-flow features were best visible at the most downstream geophone located near the fan apex. At this geophone, a positive relation between maximum values in the *IS* time series and the event volume was observed. Even the distinction between debris flows and debris floods seems to be possible with this variable at that location. This outcome would be essential in a future warning or alarm system.

The analysis of the rainfall measurements showed that most events were triggered by short high-intensity rainstorms that occurred during summer. Results indicated that a preliminary threshold for debris-flow initiation of about 15 mm in one hour may be adequate for the summer season. However, some events took place in spring, when the melting of snow cover and frozen soil may have played an important role in the

triggering mechanisms. Therefore, another rainfall threshold should be defined during spring; certainly with a lower critical value. In addition, a positive correlation between the volume of debris flows and debris floods and both the amount and the intensity of the triggering rainfall were observed.

The Rebaixader catchment seems to be an ideal site for debris-flow monitoring because of the high frequency of events. The magnitude – cumulative frequency relationship, which was established for the debris flows and debris floods observed during the first four years, indicates that large events of several thousands of cubic meters can be expected every year. Additional advantages of the Rebaixader site are the absence of countermeasures and infrastructures along the torrent and the short distance between the initiation and the accumulation zones.

3. Transformation of ground vibration signal for debris-flow monitoring and detection in alarm systems

3.1. Introduction

Debris flows are fast movements formed by a mixture of water, solids (sand, boulders, gravel and silt) and, on some occasions, woody debris. Their behaviour is similar to that of liquid concrete (Johnson and Rodine, 1984). Debris flows threaten people and infrastructures in mountainous areas worldwide, as they travel at high velocities (several meters per second) and can generate great damages due to their high impact forces (Jakob and Hungr, 2005).

Several torrents worldwide have been instrumented with different kinds of sensors and for distinct purposes (Arattano and Marchi, 2008). On one side, monitoring aims to gain knowledge about the flow behaviour, while on another, instrumentation seeks to detect the occurrence of events in order to alert the people exposed to the risk. According to the authors' knowledge, right now, in Europe, debris-flow monitoring stations are mostly located in the Alps: Italy (Berti et al., 2000; Marchi et al., 2002), Austria (Hübl and Kaitna, 2010), France (Navratil et al., 2012) and Switzerland (Badoux et al., 2009; Hürlimann et al., 2003b), but also in the Icelandic fjords (Bessason et al., 2007) or the

Spanish Pyrenees (Hürlimann et al., 2011). There are other stations in China (Zhang, 1993), Japan (Lavigne et al., 2000; Suwa et al., 2009), Taiwan (Yin et al., 2010) and USA (Hadley and LaHusen, 1995; LaHusen, 2005a), as well as monitoring stations for other types of rapid mass movements, such as lahars (Lavigne et al., 2000; Marcial et al., 1996; Tuñgol and Regalado, 1996), bedload transport (Rickenmann and Fritschi, 2007; Rickenmann and McArdell, 2007) or avalanches (Leprettre et al., 1996) throughout the world.

Geophones are widely used for detection in debris-flow monitoring stations and alarm systems. However, besides instrumentation to monitor flows, they are also used for other types of processes, such as rockfalls (Amitrano et al., 2010; Hürlimann et al., 2012). They are a type of ground vibration sensor that records the velocity of small ground movements because of the passage of debris flow. The ground vibration is caused by the energy dissipation of the passing debris flow, due to the impacts of solid material against the channel bed or the interaction between grains. Geophones are generally used as triggering sensors to activate other monitoring sensors or for detection in alarm systems. Their main advantages over other types of sensors being, among others, their robustness, low power consumption or the fact that they can be installed at safe distances, protected from the debris-flow destructive effects. The seismic sensors used in debris-flow monitoring and their features are explained in depth in Section 2.1.

The geophone signal data acquisition process and its analysis show the relevant complexities in the field of debris-flow monitoring. On one hand, the characterization of the measured signal requires high frequency ground vibration sampling rates. Usually the power available in the monitoring stations is limited, which makes the installation of PCs and fast processors difficult (PCs can scan and log at high frequencies). On the other hand, it is crucial to define an appropriate level of vibration to distinguish between the seismic noise of the site which can be originated by many other factors (e.g., wind, lighting strikes, human actions), and the vibrations generated by a debris flow. The definition of such a threshold level for ground vibration is a key task in both monitoring and alarm systems, but defining the optimal threshold value at a specific site remains uncertain. It is important to bear in mind the risk of an unintentional activation, especially when dealing with alarm systems.

The main purpose of this paper is to present a method intended to transform the complex ground vibration velocity signal measured by geophones into a simpler signal,

which permits one to detect debris flows and identify their main characteristics. The advantages and drawbacks of this new method will be also evaluated against the registration of the original seismic signal by the sensor. Other minor goals focus on the definition of a threshold value, the factors affecting the seismic signals caused by debris flows and how different types of processes might be distinguished.

The paper is structured into three main parts. First, the characteristics of the available ground vibration sensors are presented and evaluated. Second, the basis of the transformation and its implementation into the hardware are described. Additionally, the influence of the threshold is discussed and some advice for its definition is given. Finally, data recorded in three catchments are shown, and the possibilities of the proposed technique are discussed in detail.

3.2. Ground vibration sensors for debris-flow monitoring and detection in alarm systems

3.2.1. Types of sensors

The collision between particles within a moving debris flow and the impact of the boulders against the bedrock generate seismic signals and underground sounds (Arattano and Moia, 1999; Huang et al., 2003). There are several types of sensors used to detect this ground vibration. Seismometers are extremely sensitive, and detect a wide range of frequencies (including low frequencies). They have been used in several test sites, such as the Moscardo torrent in Italy, e.g.,(Marchi et al., 2002) (Arattano and Moia, 1999). Nevertheless, geophones are the most common ground vibration sensor in debris-flow monitoring systems (Arattano and Moia, 1999; Badoux et al., 2009; Berti et al., 1999; Hürlimann et al., 2011), due to their advantages over other kinds of ground vibration sensors (e.g., robustness, low consumption). They measure the velocity of ground motion. Acoustic sensors have also been tested to register the sound generated by the motion of a debris flow. Microphones to register underground sound (Itakura et al., 2000) or infrasonic devices (Kogelnig et al., 2011a; Zhang et al., 2004) are some examples of acoustic sensors used for debris-flow monitoring. According to recent advances the combination of acoustic sensors and seismic sensors increases the detection probability of events (Kogelnig et al., 2011c).

There are different types of geophones which can record 1D or 3D measurements: piezoelectric geophones and moving-coil geophones. In order to apply the method

presented in this work, 1D moving-coil geophones were used. Moving-coil geophones consist of a magnetic moving mass oscillating inside a wire coil, a mechanism that generates an output voltage proportional to the velocity of the ground vibration in the direction of the coil. The data from the geophone (continuous output voltage) is obtained and stored in a CPU memory, by means of a specific data recording system. This aspect will be more extensively described in the following sections.

3.2.2. *Factors influencing the ground vibration record*

The geophones or seismometers used for debris-flow monitoring are generally installed outside the wetted area, to avoid them being damaged when an event occurs. Normally they are placed in a protected location next to the channel. Both the amplitude and frequency of the signal measured by the sensors depend on several site-specific factors, especially their placement and assembly. Furthermore, other external elements can affect the vibration signal (e.g., meteorological elements, or human/animal actions). Normally the influence of some external factors is avoided with structures that cover the geophone and by means of information leaflets to avoid vandalism. But, the effects of site-specific influencing factors are still unknown, which leads once again to the problem of accurately defining ground vibration thresholds.

The threshold has to be defined for each individual geophone location. Until now, it was established empirically, following the experience of technicians and researchers (Genevois et al., 1999; Hadley and LaHusen, 1995; Hürlimann et al., 2003b). Therefore, should the effect of the different factors be quantifiable, the process of distinguishing debris flows from seismic noise in the site would be easier and more reliable. There are three main important issues that affect the vibration measured by ground vibration sensors: (1) distance between sensor and the flow path of the debris flow; (2) characteristics of the underground material at sensor location and between sensor location and channel (Figure 18), and (3) type of sensor assembly (Figure 19).

The distance between sensor and flow is key, as the vibration waves are attenuated with the distance (LaHusen, 2005b) and the wave does not travel long distances. It is for this reason that geophones should be installed, at the most, a few tens of meters far from the channel or at its stream banks. Diminishing the vibration signal strongly depends on the physical properties of the transmission medium (Itakura et al., 2000). For example, P-wave speed ranges from about 350 m/s in alluvium up to 700, m/s in rock (Arattano and Moia, 1999). Therefore, if the flow runs over the bedrock and there

is no colluvium between the flow and the sensor (Figure 18a), the signal does not attenuate as much as in the cases where colluvium is present (Figure 18b).
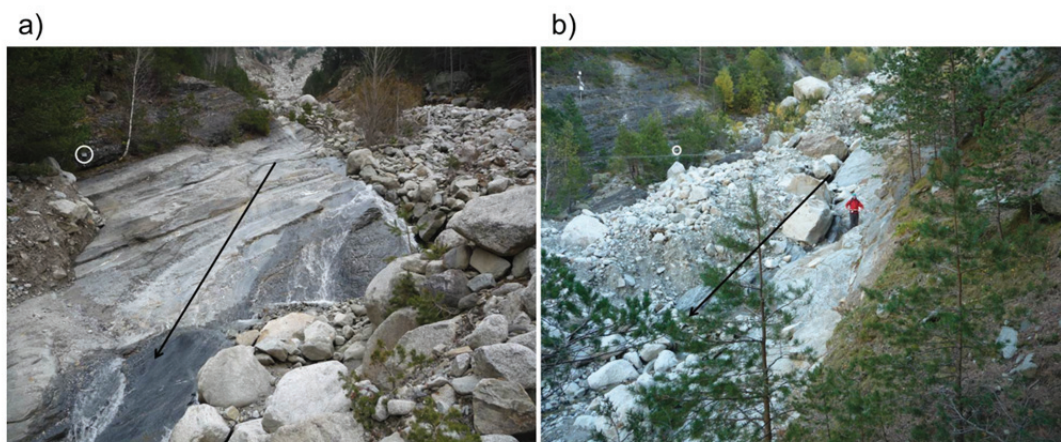
Figure 18: Factors affecting the ground vibration signal: characteristics of transmission medium between geophone and flow path. The transmission medium can be bedrock (a) or colluvium (b). The location of geophones is indicated by a circle; while the flow direction, is expressed by an arrow.

Regarding the assembly of the sensor, two important aspects should be taken into account: (1) the type of material the sensor is located in, and (2) the assembly system. The specifications of the geophones normally limit the assembly angle to a specific value (e.g., 25° in GEOSPACE geophones GS-20DX) with respect to the direction in which the ground vibration is measured. Since the surfaces of assembly are often irregular, different assembly systems are designed in the existing monitoring stations (Figure 19). The assembly structures can show a resilient vibration (Figure 19a), therefore affecting or conditioning the signal registered. In contrast, the geophones assembled using either a special structure or directly on the ground (Figure 19b) and Figure 19c are not thus affected.

3.2.1. Data recording systems

Data recording of ground vibration sensors in monitoring stations is normally done by means of an external device (data recording device). The output of the geophone is a continuous voltage proportional to ground velocity, as mentioned above. This voltage can be recorded in different ways, depending on the device used for data recording and the purpose of monitoring. Three different general data recording systems are described below.

First, analog signal recording consists in continuous logging of the voltage measured at the sensor. This technique was applied in the monitoring station of the Moscardo

torrent (Arattano and Moia, 1999), but it is not in use anymore. At Moscardo, a magnetic tape recorder was used, and changed periodically when full.
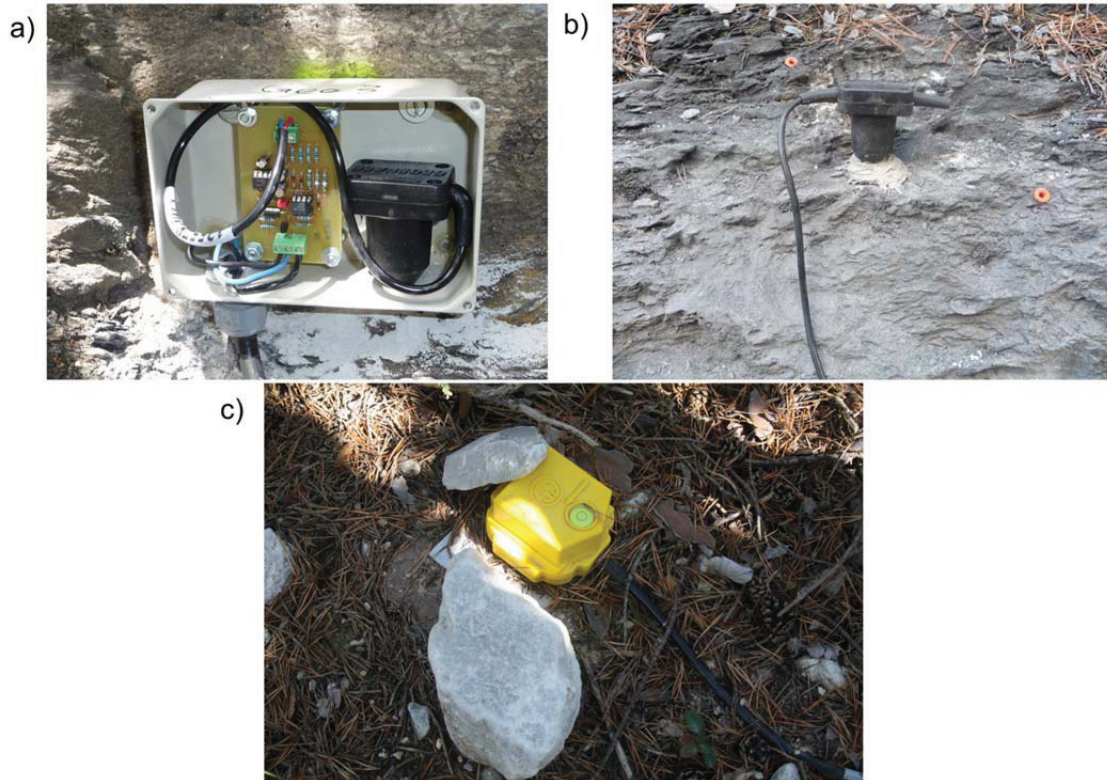
Figure 19: Factors affecting the ground vibration signal: assembly of sensors: (a) geophone fixed inside a metal sheet box (a signal conditioner can also be seen in the box), (b) fixed directly on the bedrock, and, (c) nailed down in the soil. Normally the geophone is additionally protected from the rainfall or hailing.

Second, digital signal recording consists of non-continuous voltage samples from the output signal measured at the geophone (Arattano, 2000). The acquisition device gathers the sample values at a specific frequency. According to the signal processing theories, the sampling rate (f_s) to avoid aliasing problems must be greater than the Nyquist sampling rate, which is twice the highest frequency (f_{max}) of the signal:

$$f_s > 2f_{max}$$

(Equation 6)

The typical frequencies of the strongest ground vibrations induced by the passage of a debris flow correspond to a range of some 20 to 50 Hz (LaHusen, 2005b). However, the signal registered by the geophones depends on the characteristics of the geophone, as well as other factors related to the device placement, as mentioned in

the previous section. Therefore, the frequency content can diverge from these values. That is why the minimum necessary sampling rate (≥100 Hz) is often a problem, especially when the device used for data recording is a standard datalogger, which normally has a limited sample rate. This type of data recording is thus generally associated with a PC. The problem concerning the use of a PC instead of a standard datalogger is the higher power consumption.

The third type of data recording system is defined as a general case that includes different types of transformations applied to the original ground velocity signal measured by the geophone. To the authors' knowledge, two different transformations of the ground velocity signals were used: (1) the one presented in this work (transformation into impulses), (2) the one used in the Moscardo Torrent (transformation into amplitude of the velocity signal (Arattano and Moia, 1999)).

Moreover, the amount of continuous data is very large, and thus, in the field of rapid mass movement monitoring, it is common to have two different recording frequencies: lower frequency ("no-event" mode) and higher frequency ("event" mode). For that reason, a trigger is used, defined as an algorithm that checks the variations of the signal that could indicate an event. Defining a reliable trigger for a monitoring system can avoid false alarms that can be caused by factors such as lighting or thunderstorms (Hürlimann et al., 2011). The simplest triggers, widely used in seismology, are: (a) level triggers, in which a high frequency recording ("event" mode) starts whenever the ground velocity threshold is reached; (b) short-term average-long-term average trigger (STA/LTA), which changes from no-event into event when the ratio between STA and LTA exceeds a given threshold. STA is the average of the values of ground velocity in a short term period (typically less than a second or a few seconds) and LTA is the average of ground velocity in a long term period (normally some tenths of seconds) (Havskov and Alguacil, 2004). Other than the simple triggers, more sophisticated ones are also used. They can include different parameters, focusing in amplitude and or frequency of the signal (Bessason et al., 2007).

In this work, we present a data recording system which consists of transforming the ground velocity signal measured continuously by a geophone (voltage), into a pulse signal (two voltage values). This transformation is useful for data gathering due to its simplicity, as it will be explained in detail in the following sections. This transformation is not specifically associated with a trigger, as mentioned above. However, in those monitoring stations that use this transformation (see following sections), the trigger

implemented is a level trigger over a time interval. The level trigger is implemented over the transformed signal (Hürlimann et al., 2011).

3.3. Transformation of the geophone signal into impulses

3.3.1. *The concept of transformation of ground vibration velocity into impulses*

The aim of the transformation of the geophone voltage signal is twofold. On one hand, it removes ground vibration noise and external malfunction/disturbing factors. On the other, it converts the continuous signal from the geophone into a simple digital one. The procedure consists of two parts: firstly a signal conditioner transforms the continuous signal into a pulse signal, and then, a counter records the number of impulses. Thus, the resulting transformed signal can be registered by a datalogger with a lower sample rate at a lower consumption, without losing the reliability of detecting the event occurrence and its different phases.

Removing the noise, as well as transforming the original geophone signal, depends on the existence of a threshold value of voltage, which defines the critical ground velocity. This threshold value allows distinguishing between non-desired seismic vibration and the ground velocity induced by debris flows by means of a comparator. The transformed signal has a value of 0V, if the ground velocity threshold is exceeded in the geophone, or the value of the power voltage (normally 12V), if the threshold is not exceeded (Figure 20).
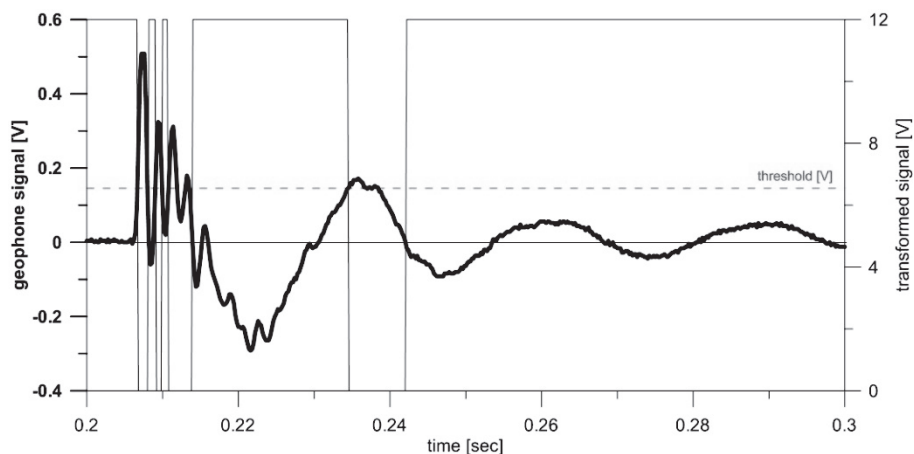

Figure 20: Transformation of the geophone signal (thick line) into a pulse signal (thin line) by the signal conditioner using a previously defined threshold value (dashed red line).

The gathering device counts one impulse every time the output signal from the Schmitt trigger (the output of the circuit is retained in the upper value until the threshold is exceeded) (Schmitt, 1938) changes from the upper voltage to 0 V. The 0 V value of the transformed signal lasts until the geophone signal crosses the line of 0 V. Finally, the counter integrated in the data recording device counts the impulses. In our case, the datalogger saves the number of impulses per second [IMP/s].

3.3.2. The signal conditioner

The signal conditioner (Figure 21) consists of a printed circuit board that is connected to the geophone and to the datalogger (see Figure 19a). The circuit has a power-consumption below 10 mA, which is provided by the datalogger battery. The power voltage is normally 12 V, because this is the standard voltage source required by the datalogger, and the values of voltages presented in this work are relative to a 12 V source voltage. However, the system can work with lower voltages.

The transformation of the ground velocity signal into a pulse signal is the main objective of the signal conditioner. This transformation is controlled by the threshold of the vibration, which is set by means of a group of three electrical resistors (R11, R12, R13 in Figure 21). The signal conditioner board has five components: (1) an amplifier, which increases the input signal from the geophone directly at the entrance of the circuit. This amplifier has the function of magnifying the ground velocity signal by a certain factor (in our case: ×30); (2) a comparator, which checks if the voltage exceeds the threshold voltage established by the resistors; (3) a transistor, which regulates the closure of the circuit (threshold exceeded) and consequently the pulse signal value is 0 V or open (threshold not exceeded) and the pulse signal has the value of the power voltage, 12 V; (4) a voltage suppressor, that regulates the input voltage from the datalogger battery and protects the circuit from external factors potentially causing malfunctions; and (5) a voltage converter, that transforms the input voltage coming from the battery (12 V) into the working voltage of the signal conditioner board (-5 V to $+5$ V).

[53]
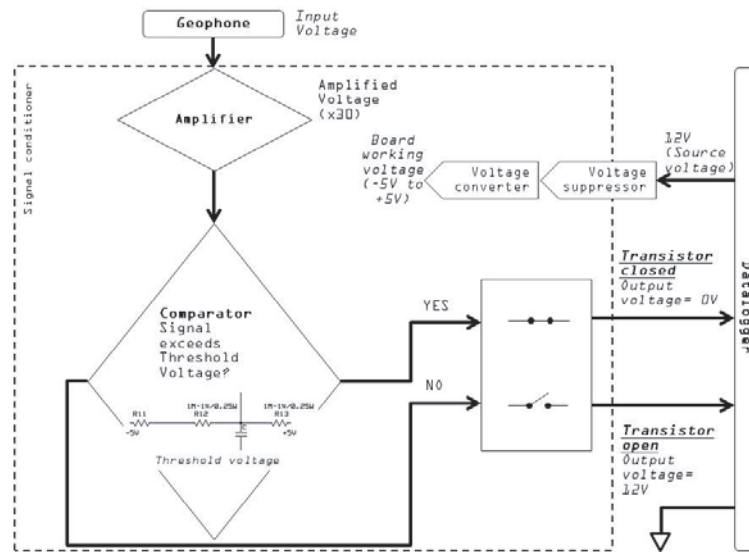
Figure 21: Simplified diagram of the signal conditioner and its interaction with the datalogger and the geophone.

3.3.3. Selection of the ground velocity threshold

The definition of the threshold is essential for debris flow detection. The threshold should be chosen in such a way that ground vibration induced by seismic noise should be ignored, while the ground vibration caused by the passage of debris flows is preserved. In order to satisfy these two conditions, the definition of the threshold has to be performed at each geophone location taking into account the local influencing factors described in Section 2.2.

As mentioned above, the threshold value is controlled by the signal conditioner, in particular electrical resistor R11 (Figure 21). The resistance value of R11 regulates linearly the threshold of ground vibration velocity (Figure 22). The correlation between the resistance value of R11 and the corresponding voltage level can be obtained by applying Ohm's Law. This threshold voltage depends on the value of resistance R11 (the values for R12 and R13 should be fixed at 1 MΩ), and it can be transformed into ground velocity using the transduction constant inherent in the geophone model (e.g., 0.28 V/cm/s in GS-20DX, http://www.geospacelp.com/).
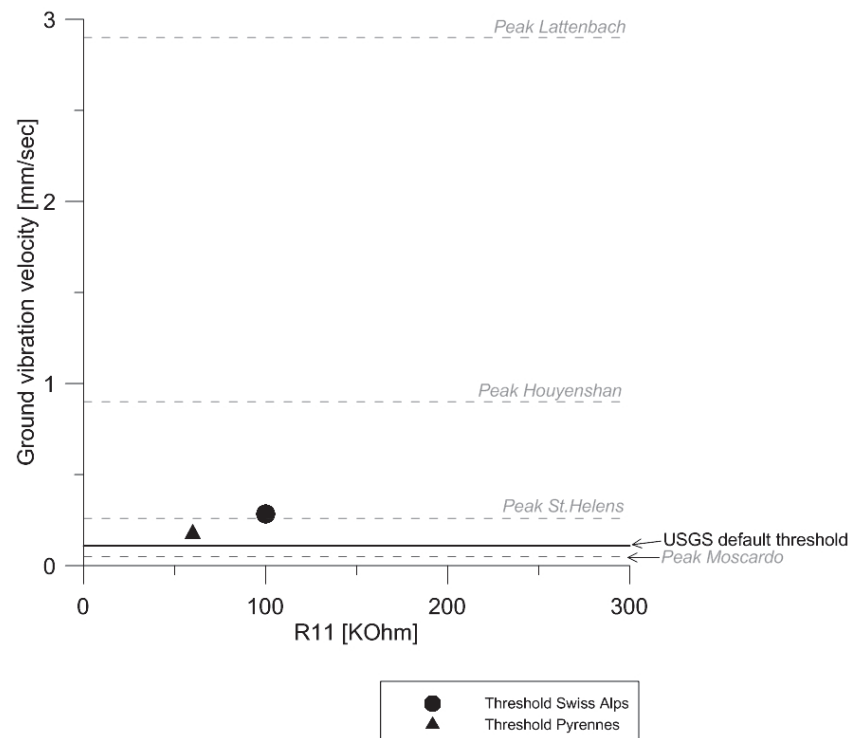
Figure 22: Common threshold values of the monitoring stations in the Pyrenees and the Swiss Alps (indicated by dots), linearly dependent on value R11. Values of ground vibration velocity peaks (dashed grey lines) and thresholds (black continuous line) are given for comparison (see text for detailed explanation on each value).

While peak values of ground velocity due to debris-flow occurrence are often found in the literature, threshold values are still rarely published (Figure 22). In Figure 22, the thresholds from the test sites in the Swiss Alps and the Pyrenees are compared with the default threshold value of the USGS Acoustic Flow Monitor (Hadley and LaHusen, 1995). Moreover, some peak values of ground velocity from other monitored sites are included in the plot. In the Mount St. Helens (USA) event of 16 October 2004, the maximum ground velocity was about 0.25 mm/s (LaHusen, 2005b). In the Moscardo torrent (Italy), the peak value of the ground velocity was 0.05 mm/s during the debris flow occurred in 22 June 1996 (Arattano and Marchi, 2005). In Houyenshan (Taiwan) the peak value of ground velocity was 0.9 mm/s (Chou et al., 2010). In Lattenbach (Austria), the peak value of ground velocity registered reached the 2.9 mm/s (Kogelnig et al., 2011b).

The low peak value of ground velocity from Moscardo can be attributed to the placement of the geophone, buried into the ground and separated about 20 m from the flow path. In general, the peak values of ground velocity exceed the threshold values, as it could be expected. However, it is important to notice that the values of the velocity

registered in the geophones are clearly affected by the influencing factors commented in Section 3.2.2, but also for the magnitude of the event. Therefore, it emphasizes once more the importance of the good adjustment of the threshold value, depending on the placement and the magnitude order of the events occurring in the instrumented torrent.

3.4. Application to debris-flow monitored sites

3.4.1. Site description and data analysed

The signal transformation method proposed in this work is or was in use in several running or abandoned monitoring stations located in the Pyrenees (P; Figure 23a)) and the Swiss Alps (SA; Figure 23b)): Ensija (P), Erill (P), Rebaixader (P), Illgraben (SA), Dorfbach (SA), Preonzo (SA), Riascio (SA) and Schipfenbach (SA). The monitoring systems in the Pyrenees were installed in 2009 (Hürlimann et al., 2011), and only a few debris flows have been registered until now. In contrast, an extensive database of debris-flow events was gathered in the Swiss Alps during the last decade. In the following sections, data from debris-flow events recorded in the Illgraben and Dorfbach monitoring systems are presented. Moreover, a comparison of the seismic data collected in the Rebaixader torrent shows, how to distinguish between the different processes occurred in the torrent.
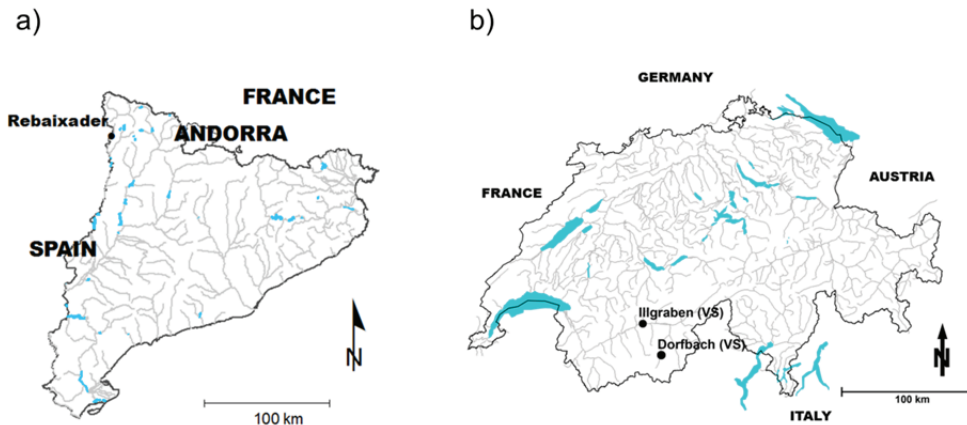

Figure 23: Location of the monitoring stations applying the signal transformation method. (a) Catalan Pyrenees (b) Swiss Alps.

3.4.1.1. Illgraben

The Illgraben catchment (9.5 km2) is well-known for its high debris-flow activity and frequent sediment transport (Badoux et al., 2009; Hürlimann et al., 2003b). It is

characterized by steep slopes and a huge amount of sediment originated by the weathered bedrock that forms a large anticline. Debris flows are mainly triggered by high-intensity, short-duration storms (McArdell and Badoux, 2007). Tens of debris flows, in a wide range of different flow types, were registered by a sophisticated monitoring system. Although many were the types of devices installed, including several types of flow depth sensors, geophones, erosion sensors, etc., only the data recorded at three geophones (located at check dam 27 and its surroundings) were analysed in this work (Table 3 and Figure 24a). Two data recording systems for the geophone signal were used: (1) digital sampling, as explained in Section 2.3, and (2) signal transformation applying the method proposed. The geophone known as "geoCD27IMP" (fixed on the wall of the check dam, Figure 24a), recorded the transformed signal. In contrast, "geoCD27DIG" (buried in the channel bed upstream of the check dam, Figure 24a) and "geoSoilDIG" (nailed in the soil, 15 m far from the flow path at the check dam) were connected to a PC and digitized the signal at 2 kHz without applying any transformation. These data were used to compare both data recording systems.

3.4.1.2. Dorfbach

The Dorfbach catchment (5.7 km2) is located in the Mattertal valley, in the Canton of Valais (Switzerland). The Dorfbach has been monitored since 1993 by changing and enlarging the equipment, even though observation was interrupted from 2007 to mid-2010, when a new modernized system was installed. Some small debris flows occurred during the late spring and summer of 2011. These debris-flow events were registered by several devices, which include flow depth sensors and geophones with different thresholds. The geophone signal was gathered by means of signal transformation into IMP/s. In this study, data corresponding to geophone Geo3L and the event in late spring 2011 were analysed (Table 3 and Figure 24c). This geophone signal is transformed by 10 different thresholds in parallel. Each one of these thresholds is controlled by a different electrical resistor.
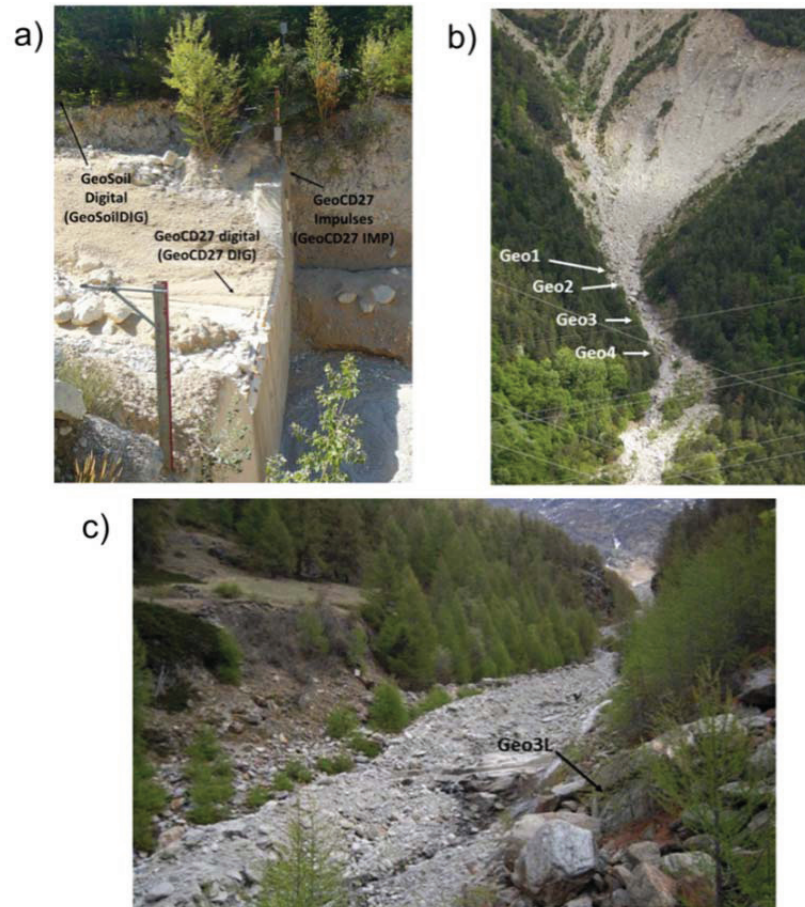
Figure 24: Location of the geophones in the three sites (a) Illgraben torrent (Swiss Alps), (b) Rebaixader torrent (Central Pyrenees, Spain), (c) Dorfbach torrent (Swiss Alps).

3.4.1.3. Rebaixader

The Rebaixader torrent has a catchment area of 0.53 km2 and is located near the village of Senet in the Central Pyrenees. The torrent runs over a glacial moraine and bedrock (slates) outcrops. The monitoring system consists of a meteorological station and a flow station. The latter includes one ultrasonic device to record the flow depth, a video-camera and five geophones. Data from four of them were analysed in this work applying the signal transformation method presented in this chapter (Figure 24b). All of these geophones are assembled in a weatherproof box. The distances to the channel and type of material available are given in Table 3.

Table 3: Main characteristics of the location of the geophones analysed in this work.

Catchment	Geophone code	Material in the flow path	Assembling of geophone	Distance to the flow path [m]	Threshold [mm/s]
Rebaixader	Geo1	Colluvium	Box on bedrock	25	0.17
	Geo2	Colluvium	Box on bedrock	15	0.17
	Geo3	Colluvium	Box on bedrock	20	0.17
	Geo4	Slates (bedrock)	Box on bedrock	8	0.17
Dorfbach	Geo3L	Colluvium	Box on bedrock	15	0.4; 0.6 ; 0.8; 1.1; 1.6; 2.3; 3.1; 4.5; 6.4; 8.9
Illgraben	geoCD27IMP	Concrete check dam	Box on check dam	5	0.71
	geoCD27DIG	Colluvium	Buried in the channel bed	0	No impulse transformation
	geoSoilDIG	Colluvium	Nailed in soil	15	No impulse transformation

3.4.2. *Comparison between ground velocity signal (GVS) and impulse per second (IS) data*

The ground vibration induced by the event occurred in 27 July 2009 in Illgraben was measured by the two geophones located at check dam 27 and a third one placed in the surrounding area (Figure 24a). On the one hand, the signal measured by geoCD27DIG and geoSoilDIG was digitized at 2 kHz and stored on a hard disk. The signal measured by geoCD27IMP was transformed by the signal conditioner into impulses using a threshold of 0.71 mm/s. It was stored in a datalogger (Campbell Scientific CR10X) every second.

[59]

Additionally, a MATLAB 7.9 (released in 2009) code was developed to perform the same transformation as the signal conditioner, but as a post-process. This was done using the original signal of geoCD27DIG and geoSoilDIG, digitized using a PC. Subsequently, it was possible to compare three different time series: (1) ground velocity signal (GVS) recorded digitally at 2 kHz by geoCD27DIG and geoSoilDIG (Figures 25a and 25c), (2) impulse per second (IS) time series obtained by the MATLAB code from the ground vibration data recorded by geoCD27DIG and geoSoilDIG (Figure 25b and Figure 25d), (3) IS time series recorded by geoCD27IMP (Figure 25e).

Figure 25(a,c) corresponds to GVS time series from each of the two geophones that register the original ground velocity data. In both figures, different stages of the event can be identified. A spindle shape is common in both time series, describing the general trends: (a) Low vibration in the beginning of the time series, which can be attributed to an hyperconcentrated flow stage and the initiation of the debris flow; (b) Sudden increase of ground velocity, which corresponds to the front passage close to the geophone (Kogelnig et al., 2011c). The amplitude of the ground velocity signal increases as the flow incorporates more mass, mainly by the sediment entrainment (Suriñach et al., 2005); (c) After the passage of the main mass near the geophone, a decreasing can be observed. Additionally, precursory and post-front waves (both smaller than debris-flow front) can be identified (Arattano and Moia, 1999).

Note that the GVS signal in Figure 25a shows high ground velocities, especially compared to values in Figure 22. Although data in Figure 25a are vastly higher than in Figure 25c, the stages of the event are better identified in Figure 25c than in Figure 25a. The proximity to the source of vibration (debris flow) results in this high amplitude signal measured at the geophone (which is buried only at 0.5 m in depth) and difficults the distinction of increments/decrements in ground velocity.

Figure 25(a,b) corresponds to the geophone buried in the channel bed (geoCD27DIG). The IS corresponding to this geophone shows elevated values (Figure 25b), when using a threshold of 0.71 mm/s. The distinction between phases of the event in geoCD27DIG is plainly impossible using this threshold. However, if we use a higher threshold, such as 6 mm/s, the characteristics of the flow are visible, as in the other geophones.

Figure 25(c,d) show that both GVS and IS from geoSoilDIG reveal three stages of the event: (1) The initial phase between the beginning of the recording and the pass of the flow front (between 0 and approx. 225 s). This period is characterized by background vibration produced by the flow with the lowest sediment concentration, previous to the flow front. Several separated precursory surges, indicated by small increments of the background vibration can also be identified. (2) The passing of the flow front, indicated by a high, rapid increment of the vibration, followed by a gradual decrease (from 225 until 350 s). (3) The after flow with background vibration produced again by the flow with low sediment concentration (after 350 s).

The IS time series from geoCD27IMP (Figure 25e) also depicts the three phases mentioned before: the transition between the hyperconcentrated flow and the initiation of the debris flow (from 0 to 225 approximately), the flow front pass (between 225 and 300 s), and the after flow (after 300 s). However, the precursory surges before the flow front are not evident, and the background noise is lower than the one measured by geoSoilDIG. The differences in the signal measured at the three geophones (geoCD27DIG, geoSoilDIG, geoCD27IMP) can be explained by the differences in factors discussed in Section 2.2.

Thus, both GVS and IS time series are suitable to detect the phases and characteristics of the debris flow. The main difference between methodologies is that the impulses method removes the seismic noise. This noise removal is done by means of the threshold in the signal conditioner. Once again, it is important to remark the importance of the threshold, which has to be adjusted for each geophone, depending on the site-specific effects.

Moreover, there are other important differences between methodologies. Data corresponding to GVS measured by geoCD27DIG and geoSoilDIG is recorded in a higher frequency sampling rate, resulting in a file more than 400 times larger than the IS data file (Table 4). One of the most important advantages of the impulses method is related to this data reduction and concerns the power consumption. The power consumption can be considerably lower, because a standard datalogger can be used instead of a (industrial) personal computer. However, the transformation method also presents disadvantages. The main disadvantage is that it does not provide the exact value of ground velocity neither the frequency content of the signal, because the data are transformed into a pulse signal. This simplification obviously leads to a loss of information.

[61]
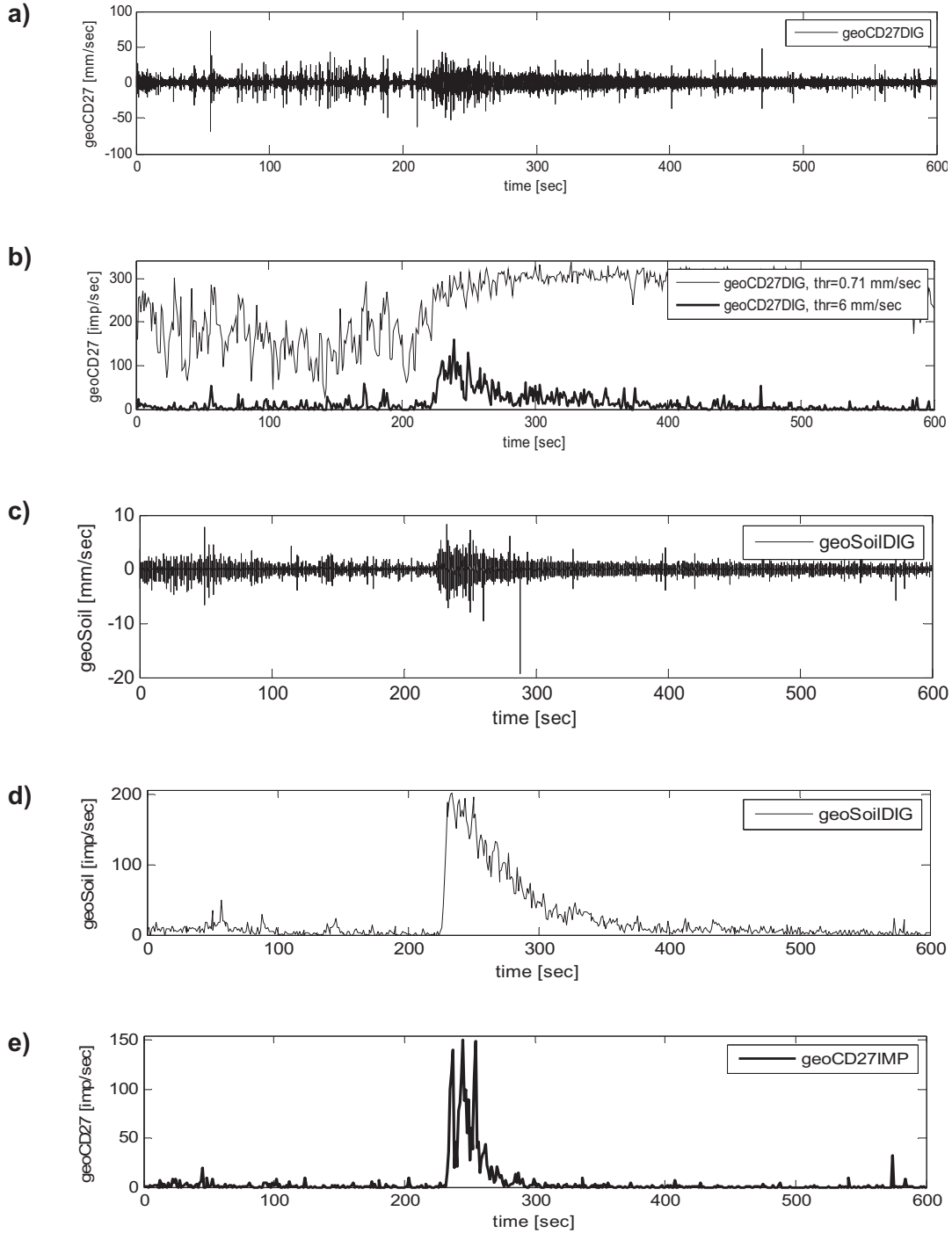
Figure 25: Data recorded in Illgraben during the event occurred in 27 July 2009. (a) Ground velocity signal (GVS) measured by geoCD27DIG (sample rate: 2 kHz) (b) Impulse per second (IS) time series obtained by post-processing geoCD27DIG data using the MATLAB code (thin line: 0.71 mm/s threshold, thick line: 6 mm/s threshold) (c) GVS measured by geoSoilDIG (sample rate: 2 kHz). (d) IS time series obtained by post-processing geoSoilDIG data using the MATLAB code (0.71 mm/s threshold) (e) IS time series measured at geoCD27IMP applying the transformation by the signal conditioner (0.71 mm/s threshold).

Table 4: Details of the data recording systems of the three geophones in Illgraben with regards to the event of 27 July 2009.

Geophone code	Recorded data	Data recording system	Data recording device	File size [kB]	Number of records	Estimated power consumption of the recording device
geoCD27DIG, geoSoilDIG	Ground velocity signal	Digitization at 2 kHz	PC	114,263	1,200,000	3 A (standard embedded computer system)
geoCD27IMP	Impulses per second time series	Transformation by the signal conditioner	CR10X Campbell Datalogger	251	600	56 mA (6 mA signal conditioner + 50 mA datalogger)

3.4.3. *Influence of the vibration velocity threshold*

In order to analyse the effect of the velocity threshold value in the transformation of the GVS into impulses, the IS time series obtained from two different debris-flow events were compared using five different threshold values: (a) 0.4 mm/s, (b) 0.6 mm/s, (c) 0.8 mm/s, (d) 1.15 mm/s, and (e) 1.6 mm/s (Figure 26). The first event is the one occurred in 4 June 2011 in Dorfbach. The ground vibration signal measured at geophone Geo3L was directly transformed by the signal conditioner with the multiple thresholds indicated in Table 1. The second event is the Illgraben debris flow in July 2009 presented in the previous sections. Here, the GVS measured at geoSoilDIG was transformed by processing the data with the MATLAB code.

In the Dorfbach event (Figure 26a), the threshold clearly influences on both the duration of the vibration and on the number of impulses. Using a threshold of 0.4 mm/s, the peak of the IS time series almost reaches 300 IMP/s and the vibration lasts 150 s approximately. As the threshold increases, the peak vibration decreases drastically (Figure 27) as well as the vibration time, until it reaches the point of no vibration, should a threshold of 1.6 mm/s be applied in the signal conditioner.

In Illgraben (Figure 26b), the relation between peak impulse values and threshold values is clearly visible again (Figure 27). This relation could be of great importance to

detect the precursory surges, because they appear in the time series of the lowest thresholds, as they almost disappear in the higher thresholds. The time of vibration is almost not affected by the threshold, as opposed to the shape, which is actually affected. The shape of the time series and duration of the signal after the flow front has clearly a different aspect depending on the threshold value. The signal duration can be more than 400 s long in case of a 0.4 mm/s threshold, while only 50 s long if the threshold equals 1.6 mm/s.
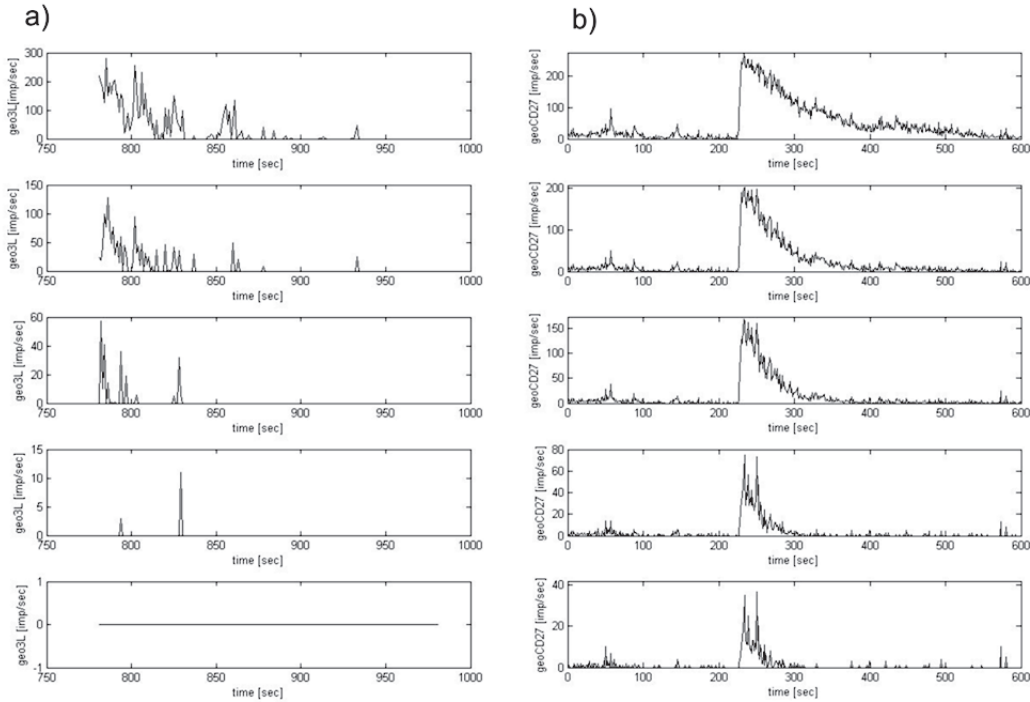
Figure 26: IS time series corresponding to different thresholds of ground velocity (from top to bottom: 0.4 mm/s, 0.6mm/s, 0.8 mm/s, 1.15 mm/s, 1.6 mm/s). (a) Dorfbach event (4 June 2011) and (b) Illgraben event (27 July 2009).

In general, the relation of peak *vs.* threshold is visible in both events, but the signals in Dorfbach (transformed by signal conditioner) show a much higher variability (Figure 26). Thus, the results are strongly dependent on the threshold defined. There are still many uncertainties associated with the definition of the threshold. There is not yet a guideline to establish a general threshold, but nowadays it resorts to calibration or the experience of technicians and researchers. To optimize the definition of the ground velocity threshold, many aspects should be taken into account, such as ground vibration that is influenced by several factors. For example, in the two examples shown in Figure 27, we could establish that: (1) in Dorfbach the threshold should not be higher than 0.6 mm/s in Geo3L, otherwise the signal would disappear completely; (2) with a

threshold up to 1.6 mm/s in geoSoilDIG, in Illgraben would still be useful to detect the signal.
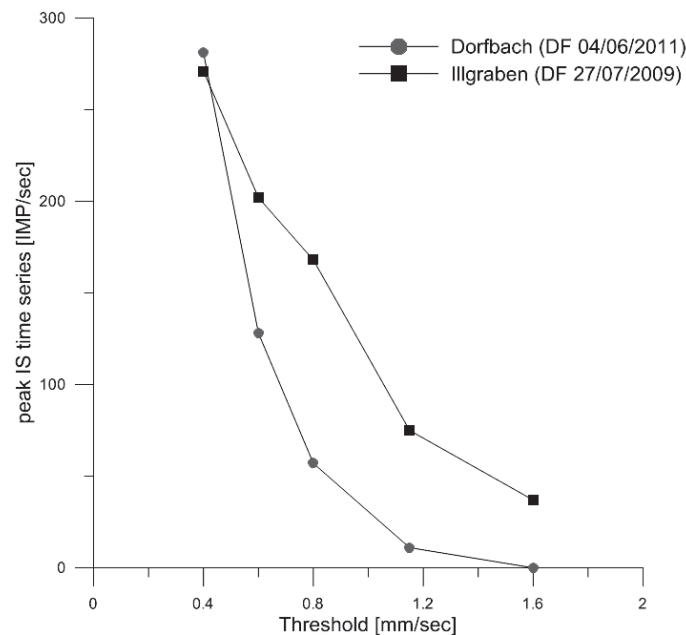
Figure 27: Relation between the threshold value in mm/s and the peak value of the IS time series obtained from the different cases of Figure 26.

3.4.4. Other uses of the method

Several types of mass movements have occurred at the Rebaixader monitoring station since its installation in 2009 (until January 2012). The processes monitored include two rockfalls (Hürlimann et al., 2012), two debris flows and multiple other flows with lower sediment concentration (Hürlimann et al., 2011). The events were monitored by different types of sensors.

The different characteristics of rockfalls and debris flows were compared by the IS time series obtained at the four geophones. The following parameters were selected for this analysis: the peak of the IS time series [IMP/s], the mean value of IS over time [IMP/s], the sum of the seconds with IS different to null [s], the maximum slope of the IS time series within a 5 s interval [s^{-1}], the slope of the IS time series within a 1 s interval [s^{-1}].

In Figure 28, the correlation between the sum of seconds with measured IS time series and the peak value of IS are shown, for the four geophones. There are two important points to be mentioned: first, at geophone Geo1 (closest to the rockfall source, Figure 24b), the rockfalls show shorter duration and higher peak values than debris flows. The explanation is that rockfall signals are typically rapid increments of vibration generated by the impacts of the boulder detached to the ground. In contrast, debris flows produce

[65]

a continuous signal with the typical characteristics of time series showed in Figure 25. Second, at Geo2, Geo3 and Geo4 (in the channel zone, Geo4 is located near the apex of the fan), the debris-flow events have longer durations and higher peak impulses. This is attributed to the fact that geophone 1 is too close to the source area and the flow is still not well developed. In all the geophones, a distinction between the processes could be established. However, Geo2 and Geo3 show closer signals for both processes than Geo1 and Geo4. This can be explained with the location of Geo2 and Geo3, in the middle of the travel path between the initiation area and the deposition fan. This part is where the sediment content in the flows increases the most, as well as it is a part reached by most of the rockfalls. In contrast, debris flows are not always well formed where Geo1 is placed, and at the same time, some rockfalls do not reach geo4 (Hürlimann et al., 2012).
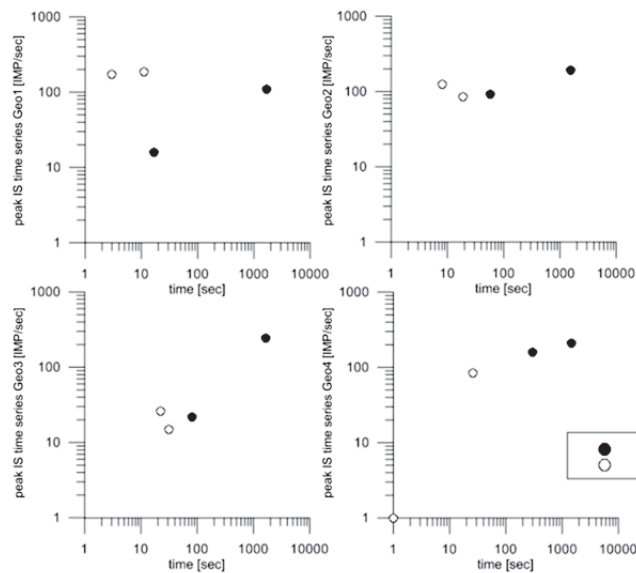
Figure 28: Distinction of processes in Rebaixader by using two parameters: the sum of seconds with registered impulses from the geophone and the peak value of the IS time series.

3.5. Conclusions

In this work, a method to transform and simplify the ground vibration velocity signal originated by debris flows and other rapid mass movements was presented. Based on the results shown, it can be concluded that:

(1) In spite of not registering ground velocity signals and, consequently, losing the frequency content of the signal, the method can visualize much information

concerning flow behaviour (not only the flow front, but also precursory waves or secondary surges, impact of big boulders, *etc*.);

(2) Due to the transformation, the seismic noise can be avoided. That is why the size of the data file can be reduced hundreds or even thousands of times. Moreover, this method reduces the problem related to the limit of power available in the monitoring stations;

(3) The definition of a suitable threshold value is a key point of the method presented, in order to avoid seismic noise but to detect debris-flow occurrence. Both too high and too low thresholds can generate important lacks of information, such as missing events or losing their different stages (Figure 25b). It still presents many uncertainties, because the ground vibration signal is affected by many factors. That is why the threshold value of ground velocity has to be defined and calibrated for each geophone location

(4) Data from the Rebaixader station pointed out interesting applications of this method to distinguish different rapid mass moving processes in a monitoring station. The results presented here, showed that the peak of the impulses per second time series [IMP/s] and the duration of the vibration [s] can be used to distinguish between debris flows and rockfalls, especially in two of the four geophones of the Rebaixader monitoring station.

[67]

4. Analysis of the ground vibration produced by debris flows and other torrential processes at the Rebaixader monitoring site

4.1. Introduction

Debris flows are one of the most hazardous geomorphologic processes. In order to improve the understanding of debris-flow mechanisms, torrents are being instrumented with an increasing variety of sensors. The data collected by the sensors are not only needed to calibrate numerical models, but also to develop and adjust warning and alarm systems.

In torrential catchments, other geomorphic processes can occur besides debris flow, like debris floods or rockfalls. Besides the Rebaixader monitoring site was installed with the purpose of monitoring debris flows, other type of torrential processes were recorded by the sensors.

Torrential processes, especially debris flows generate seismic waves in the ground, originated by the collision between boulders or between boulders and the bedrock.

These vibrations can be measured by several seismic and sonic devices (such as geophones, seismographs or infrasounds (Itakura et al., 2005; Kogelnig et al., 2011a)). Geophones are the most common seismic sensors used in debris-flow monitoring because of their robustness and low power consumption. These features make them also very suitable not only for monitoring, but also for alarm purposes. All over the world, several sites have been instrumented with geophones: Illgraben in Switzerland (Hürlimann et al., 2003b), Lattenbach in Austria (Kogelnig et al., 2011a), Moscardo (Arattano et al., 2012), Acquabona (Berti et al., 2000) or Gadria (Marchi et al., 2012) in Italy, Manival or Réal in France (Navratil et al., 2011), Mount St Helens in USA (LaHusen, 2005b), Houyenshan (Chou et al., 2010), Fong-Ciou Creek or Ai-Yu-Zi Creek (Fang et al., 2011; Huang et al., 2007) in Taiwan, and Jiangjia in China are some examples.

Many analyses of geophone signals induced by debris flows have been published during the last decades (Arattano et al., 2012; Arattano and Moia, 1999; Berti et al., 2000; Chou et al., 2010; Huang et al., 2007; Hürlimann et al., 2003b). All these studies have substantially increased our knowledge on the dynamic behaviour of debris flows and the ground vibration they provoke. However, there are still many open questions, as the distinction between debris flows and debris floods or the definition of thresholds for data recording or warning.

The ground velocity signal can be recorded by two different approaches: a) continuously (e.g. in Moscardo torrent (Arattano and Moia, 1999)); and, b) by switching from "no-event" mode into an event-mode (e.g. in the Swiss torrents (Hürlimann et al., 2003b)). The latter approach needs the incorporation of threshold and the definition of its value. Normally this threshold is established empirically analysing the signals of past events and expert criteria. The threshold has to be defined at each geophone, as there are several site-specific factors that influence the vibration registered. An accurate assessment of the threshold is of crucial importance; especially in alarm systems, when some actions must be performed or alarm messages to the stakeholders emitted. However, there are only very few studies dealing with the influence of site-specific factors that affect the vibration registered by the geophones (Huang et al., 2007; Navratil et al., 2011).

Different types of thresholds can be found on the literature: a) ground velocity values (LaHusen, 2005a), b) values of a transformed signal (Badoux et al., 2009; Hürlimann et al., 2011); or c) more sophisticated thresholds focusing in the frequency of the signal

(Bessason et al., 2007). The type of threshold mainly depends on the data recording system implemented at the site. Several systems have been used historically: a) analogical recording (Arattano and Moia, 1999), b) digital sampling (Arattano, 2000; Kogelnig et al., 2011b); and, c) transformations of ground vibration velocity signal (Abancó et al., 2012; Navratil et al., 2011).

In this study the features of the ground vibration signals registered at two monitoring stations located in the Rebaixader torrent are analysed. The main difference between the two stations is the data recording system, but also some other aspects regarding the mounting and the location of the geophones. The major purpose of this work is to define the main characteristics of debris flows and other torrential processes using the two recording systems installed in the site. Another objective is the analysis of the influence of some site-specific factors on the ground vibration signal. The outcomes of this research improve our knowledge on some current issues (i.e., process differentiation, geophone location, recording method or threshold assessment) and should help for the set-up of future debris-flow monitoring or alarm systems.

4.2. Debris flow characterization by ground vibration monitoring

4.2.1. Debris-flow features

Debris flows are rapid landslides formed by water and solid material poorly sorted from boulder to clay (Iverson, 1997). Pierson (1986) describes a typical debris flow by 3 parts: the front, the fully developed debris flow (also called "body"); and the tail. The front carries the biggest boulders and is followed by the debris flow body, with a high sediment concentration, in a turbulent regime. At last, there is the tail, with much less solid material concentration, which can also be characterised as a hyperconcentrated flow. Many debris-flow events occur in a series of surges, each one showing a front, a body and a tail (Johnson and Rodine, 1984; Pierson, 1986). Finally, it usually ends with a muddy water tail (*afterflow*), typically turbulent (Arattano and Marchi, 2008; Hungr, 2000; Iverson, 1997).

The coexistence of torrential processes has also been noted in the Rebaixader site. Debris floods are defined as episodes of massive bedload transport, characterized by a limited maximum grain size (Aulitzky, 1982). Debris flood is a very rapid surging flow of water in a steep channel, heavily charged with debris (Hungr et al., 2001). A debris flood may transport quantities of sediment comparable to a debris flow, in the form of massive surges. However, the transport is carried out by the tractive forces of water

overlying the debris. As a result, the peak discharge of a debris flood is comparable to that of a water flood (perhaps multiplied by a factor up to 2). This contrasts with peak discharges of debris flows which are tens of times greater than major water floods (Hungr et al., 2001; VanDine, 1985).Another difference between debris flows and debris floods is the absence of the bouldery front, and levees along the channel margins.

Ground vibration produced during the pass of a debris flow has its origin in the impacts between boulders or between boulders and the channel bed. A change of sediment concentration and boulder content alters the energy transmitted to the ground as seismic waves in such a way that debris flows can be distinguished from other torrential processes, but also parts of a debris flow and surges (Huang et al., 2007).

References to rockfall occurrence in debris-flow prone catchments are rare in the literature. Rockfalls documented in such setting were produced by the failure in bedrock (Berger et al., 2011) and by the instabilisation of boulders in till deposits (Hürlimann et al., 2012).

4.2.2. Monitoring of debris-flow induced ground vibration

Ground vibration is transduced by a geophone to a voltage that is (generally linearly) related to the ground velocity. The digital measuring of the geophone output is done by sampling the signal with a certain frequency. To avoid aliasing problems, the sampling rate must be greater than the Nyquist frequency, which is twice the highest frequency of the signal. Not only digital sampling is used to record the data from the geophones, but also other techniques based on the transformation of the original signal into simpler data have been developed. These data acquisition systems are widely described in the following sections.

Several physical parameters of moving debris flows have been estimated analysing ground vibrations. For instance, the correspondance between the hydrograph and the ground vibration signal (Arattano and Moia, 1999), or the increase of the amplitude of the ground vibrations as the flow front approach to the seismic sensor (Arattano and Moia, 1999). Furthermore, the flow volume was correlated with the time integral of the acceleration amplitude (Suwa et al., 2000). Other authors found some general patterns in the frequency domain. For instance, LaHusen (1996) described the typical peak frequency range of the debris flows between 30 and 80 Hz, or Huang et al (2007) suggested this range from 50 to 100 Hz.

4.2.3. Ground vibration influencing factors

Both the amplitude and frequency of the signal measured by the geophones depend on several site-specific factors. The main influencing factors are the distance between the sensor and the passing debris flow, the ground material below and between them, and the assembly of the geophone.

Geophones are generally installed outside the channel bed, in a protected location to avoid damage when a torrential event occurs. However, the distance between sensor and flow is crucial, as the vibration waves are attenuated with the distance and the wave does not travel long distances (LaHusen, 2005b). For this reason, geophones must be installed maximum a ~30-40 metres from the active channel or on its lateral banks. Diminishing the vibration signal strongly depends on the physical properties of the transmission medium (Itakura et al., 2000). For example, P-wave speed ranges from about 350 m/s in alluvium up to 700 m/s in rock (Arattano and Moia, 1999). Field tests have been performed in Manival torrent (France) in order to improve the understanding of material and distance (Navratil et al., 2011). Boulders of 10 kg were thrown from a height of 2 m. The comparison of the distance versus the peak of the signal showed that there is a linear or exponential decrease of the maximum ground vibration with longer distances. Such correlation strongly depended on the placement of the geophone (inside the soil, in lateral banks or on big boulders placed in the soil).

When geophones cannot be buried in soil, the sensors must be fixed on bedrock, big boulders or existing concrete structures (e.g. check dams). In this case, the method of fixing the geophones to these hard surfaces controls the transfer of vibrations to the sensor and, consequently, has a strong influence on the signal recorded. Since the surfaces are often irregular, different assembly systems are designed in the existing monitoring stations (e.g. metal box). The assembly structures can show a resilient vibration, therefore affecting and conditioning the signal registered.

4.3.   Description of the Rebaixader site

4.3.1. General settings

The Rebaixader catchment is a first order basin, with an extension of 0.53 km^2, which is located at the Central Axial Pyrenees, near the village of Senet (Figure 29). The catchment has the typical morphology of a torrential basin formed by three zones (erosional source area, channel zone and fan). The source area has a steep slope (average of 29º), an area of 0.09 km^2 and is located between 1425 and 1710 m.a.s.l

(Figure 29). The channel zone has an average slope of 21° is 250 m long and about 20 m wide, and is located between the 1425 and 1350 m.a.s.l. Downstream the channel zone, there is a fan with an area of 0.082 km^2 and a mean slope of 17°. The Noguera Ribagorçana River defines the lower boundary of the fan. There is no protection works in the Rebaixader torrent.

The geology of the source zone consists of a thick till deposit over a bedrock of slates and phyllites of Devonian age. The bedrock crops only locally out in the source and forms the margins of the channel zone. The till corresponds to a lateral moraine of the glacier that occupied the Noguera Ribargorçana Valley during the Last Glacial Cicle(Vilaplana, 1983).

The meteorological conditions of the site are affected by the proximity of the Mediterranean Sea, the influence of the Northern-Atlantic winds and the orographic effects of the Pyrenees. The debris flows and debris floods analysed in this study are mostly triggered by convective storms in the summer, which are characterised by short and intense rainfalls (Hürlimann et al. 2011).
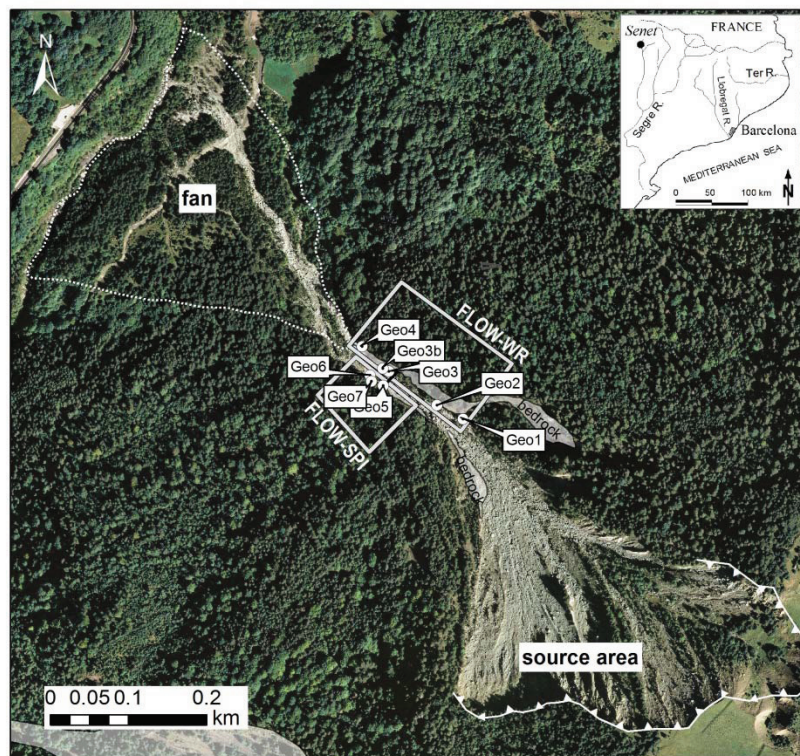

Figure 29: The Rebaixader torrent, its fan and source area. Seismic stations (FLOW-WR and FLOW-SPI) and the corresponding geophones are indicated and labelled. The ultrasonic device is represented by a black line in the middle of the channel reach. Inset shows the location of the Rebaixader site.

[74]

4.3.2. Flow monitoring network

The monitoring system installed in the Rebaixader torrent includes on one side four stations measuring the meteorological and hydrological conditions in the catchment and in the upper reach of the channel zone for the analysis of the debris flow initiation, and on the other side two stations regarding the detection and characterisation of the flows. Further details about the instrumentation can be found in (Hürlimann et al., 2011). Herein, we focus on the two stations measuring the ground vibration (FLOW-WR and FLOW-SPI in Figure 29) to characterise the flow dynamics. The geophones of both stations are 1D vertical, moving coil geophones (Geospace 20-DX) with a natural frequency of 8 Hz and a spurious frequency of 200Hz. The main difference between the stations is the data acquisition system. The data acquisition in station FLOW-WR is based on a low sampling rate of a transformed signal, meanwhile in station FLOW-SPI the high sampling rate provides data on the original ground velocity signal.

The station FLOW-WR includes five geophones, an ultrasonic device for stage measurements and a video camera. The sensors are connected by wires and controlled by a Campbell CR1000 datalogger, which is powered by a 12V 24Ah battery, charged by a 30W solar panel. The data are transmitted via GSM modem to our server in Barcelona. The geophones are distributed along 175 m at the right side of the torrent (looking downstream; Figure 29), between 1415 and 1345 m.a.s.l. Inter-geophone distances are up to 75 m, and the distances between the sensors and the active channel range from 8 to 25 m (Table 5). Four of the five geophones are mounted by a sheet metal box to the bedrock (geophones Geo1 to Geo4 in Fig. 2b). Each box is protected by a plastic structure in order to avoid the impact of raindrops or hail on it. The fifth geophone (Geo3b) is fixed directly on the bedrock without a box. It is also protected by a plastic structure like the other geophones. The setup of the station started in July 2009 and was completed in June of 2011 with the installation of the video camera.

The station FLOW-SPI was set up in June 2012 in order to record the ground vibration by an additional method. The station contains three geophones, which are located at the left side of the channel (looking downstream; Figure 29). The geophones are located between 3 and 5 m from active channel much closer than those of station FLOW-WR (Table 5). In this station, all the geophones are fixed directly to the ground. Two of them (geophones Geo6 and Geo7) are buried in the soil (granular colluvium) at a depth of about 20 cm (Figure 30d), while the third one (Geo5) is fixed on bedrock

[75]

(Figure 30c) and protected by a plastic structure by the same system as in the other station. Data logging is carried out by a 24 bits broadband seismic recording unit (Spider Worldsensing s.l.), powered by a battery of 12V, 22Ah, and charged by a 50W solar panel. The Spider communicates the data to a gateway, where they are resent to our server via GSM modem.

Figure 30: a) Downstream view from inside the channel indicating the places where the geophones are placed. Pictures of the detailed assemblies are shown in (b) to (d).

4.4. Data analysis by Impulses per Second time series

4.4.1. Methods

The data recording system at the FLOW-WR station is based on the transformation of the original signal, a voltage signal proportional to the ground vibration velocity, into a signal of impulses per second (Abancó et al., 2012). The signal transformation is carried out by an electronic conditioning circuit board that is connected to each geophone (Figure 30b). The aim of the transformation is twofold. On one hand, it removes ground vibration noise. On the other hand, impulses per second (IS) data constitute a simple discretised signal, which can be more easily analysed and which need much lower memory requirements.

Table 5: Summary of main characteristics of the geophones analysed in this work.

Geophone	Mounting	Station (data recording system)	Distance to active channel (planimetric distance)	Material on the cross section
Geo3	Sheet metal box attached to bedrock	FLOW-WR (IMP/sec)	25	Colluvium and bedrock
Geo3b	Bedrock	FLOW-WR (IMP/sec)	25	Colluvium and bedrock
Geo4	Sheet metal box attached to bedrock	FLOW-WR (IMP/sec)	8	Bedrock
Geo5	Bedrock	FLOW-SPI (complete signal)	3	Bedrock
Geo6	Buried in soil	FLOW-SPI (complete signal)	3	Colluvium and bedrock
Geo7	Buried in soil	FLOW-SPI (complete signal)	5	Colluvium and bedrock

The procedure of signal transformation involves the filtering, and the conversion to impulses. The original voltage measured by the geophone is, firstly, filtered to remove low ground velocities, which are assumed to correspond to noise. Filtering is analogically done by means of electrical resistors in the conditioning circuit board. Two values of ground vibration threshold (GVth) are used at Rebaixader site depending on the geophone assembly. For the geophones mounted in a sheet metal box (Geo1, Geo2, Geo3, Geo4), the threshold corresponds to a vibration velocity of 0.17 mm/sec. The other geophone (Geo3b), which was fixed directly to bedrock and for which no resonance effect of the metal box is expected, the velocity threshold is much lower

[77]

(GVth = 0.019 mm/sec). After this filtering, the signal is transformed into impulses per second by the conditioning circuit (for further details, see Abancó et al.2012).

The frequency of measuring is controlled by the CR1000 datalogger, which was programmed to scan the geophones of the station every second. To optimize the memory management of the data files, the recording is not carried out continuously, but only when the number of impulses per second exceeds a threshold. This threshold is called "event mode threshold" (EMth) and is based on the number of impulses per second counted during a certain duration. Therefore, this "event" mode threshold includes two components: a) the number of impulses of the EMth (EMth$_{IMP/sec}$), and b) the duration of the EMth (EMth$_{dur}$). The "event" mode threshold was defined progressively by analysing the data of the first year of the monitored period. Since August 2010, the EMth$_{IMP/sec}$ was fixed to 20 IMP/sec and the EMth$_{dur}$ was established on three consecutive seconds. When the threshold is exceeded in any of the geophones of the station, the "event" mode is triggered by the datalogger code and the signal is recorded each second. "event" mode is deactivated after two minutes with vibration smaller than EMth$_{IMP/sec}$ scanned in any of the geophones. The recording is also carried out during the "no-event" mode to monitor the noise and the performance of the system; although at a much lower frequency (each hour).

As it is shown below, several types of events (debris flows, debris floods and rockfalls) were recorded in the torrent. The analysis of the IS times series revealed different types of responses (IS curve morphologies) to torrential processes. They were assigned to different types of events by means of cross-checking the vibration gathered in the five geophones, the flow depth measured by the ultrasonic device, the video images (available only for 10 events) and periodic field trips (31 campaigns), carried out after some events to identify geomorphic changes in the site.

4.4.2. Results

Between July 2009 and December 2012, the "event" mode was triggered 363 times. The trigger was mostly (216 times) provoked by malfunctions in one of the geophones, which was affected by a rockfall in 2010 (Hürlimann et al., 2012). Another 126 triggers were attributed to small mass movements at the upper part of the channel, that didn't progress downstream, as it was suggested by periodic field reconnaissance carried out during this period, which indicated no apparent geomorphic changes after some of these triggers. Consequently, 342 of the 363 events were not considered as torrential

events and classified as "other triggers", both the malfunctions and the small movements that triggered the system. Indeed, the EMth was calibrated during the first monitoring year to minimise the recording of this type of triggers. For the whole monitoring period, 21 torrential events were recorded by the station. Regarding the shape of the IS time series curve, three types of curves were distinguished (Figure 31).
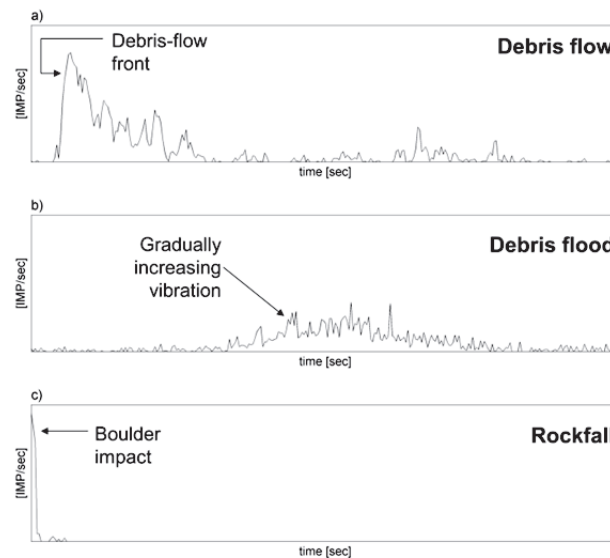
Figure 31: Typical shapes of the IS signal registered during a debris flow (a), debris flood (b) and rockfall (c). Horizontal and vertical scales are the same in the three cases.

Type A curve is characterised by three flow phases (Figure 31a): a) a first phase of stationary level of no or very low IS values, b) an abrupt increase of the impulses, reaching values over 100 IMP/sec in less than 5 seconds, followed by c) a slow exponential decrease. In some debris-flow events, this type A curve was observed (Figure 32b, 32d, 32f, 32h). Nevertheless, some of the events only show clear A-curves in Geo4, the geophone located in the most downstream position in the channel zone. In the other geophones, located upstream, the A-curve is often not observed, especially in the "small-magnitude" debris flows (Figure 32a and Figure 32e and Table 6). It is interpreted that debris flows generate type A curve, but the former facts suggests that only when the flow mass reach the location of Geo4 debris flows are fully developed, showing a well-defined front. It should be noted that geophones 1 to 3 are located at greater distances from the active channel (15 to 25 m) than Geo4 (8 m) and the attenuation of the vibration with distance may probably play a role in the record of debris flows by geophones more distant from the flow path, as it is shown below.

[79]

Type B curve consists of a first phase of gradual increase of IS, which is followed by a gradual decrease (Figure 31b). The peak number of impulses of this type of curves strongly depends on the geophone location along the channel and the characteristics of the event (distance between geophone and the flow path or volume of the event). This type of curve is considered as associated with debris floods or immature phases of debris flows. Besides the shape of the curve, the peak of IMP/sec time series at Geo4 is useful to distinguish between debris flows and debris floods. The values of peak vibration in this geophone never exceeded 100 IMP/sec for debris floods, while the values are from 130 up to 211 IMP/sec for debris flows.

Type C curve is defined by a very short duration (2 to 5 sec) and a high maximum (up to 190 IMP/sec; Figure 31c). Video images and geomorphological reconnaissance show clearly that this type of curve is related to rockfalls (see Hürlimann et al, 2012). Highest values of vibration corresponding to rockfalls and the shortest durations of vibration were recorded in Geo1, the uppermost geophone.

Most of the records shown in Figure 32 present similar durations. In general, the events last several hundreds of seconds, around 10 minutes. Exceptionally, the debris-flow event registered on the 11th of July 2010 lasted approximately 10 times this common value. An unusually long and high intensity rainfall (~50 mm/h as peak hourly rainfall intensity) event accompanied this debris flow and generated many flow surges. Except the July 2010 case, the registers suggest that there are no differences between debris flows and debris floods in terms of duration of the IS signal.
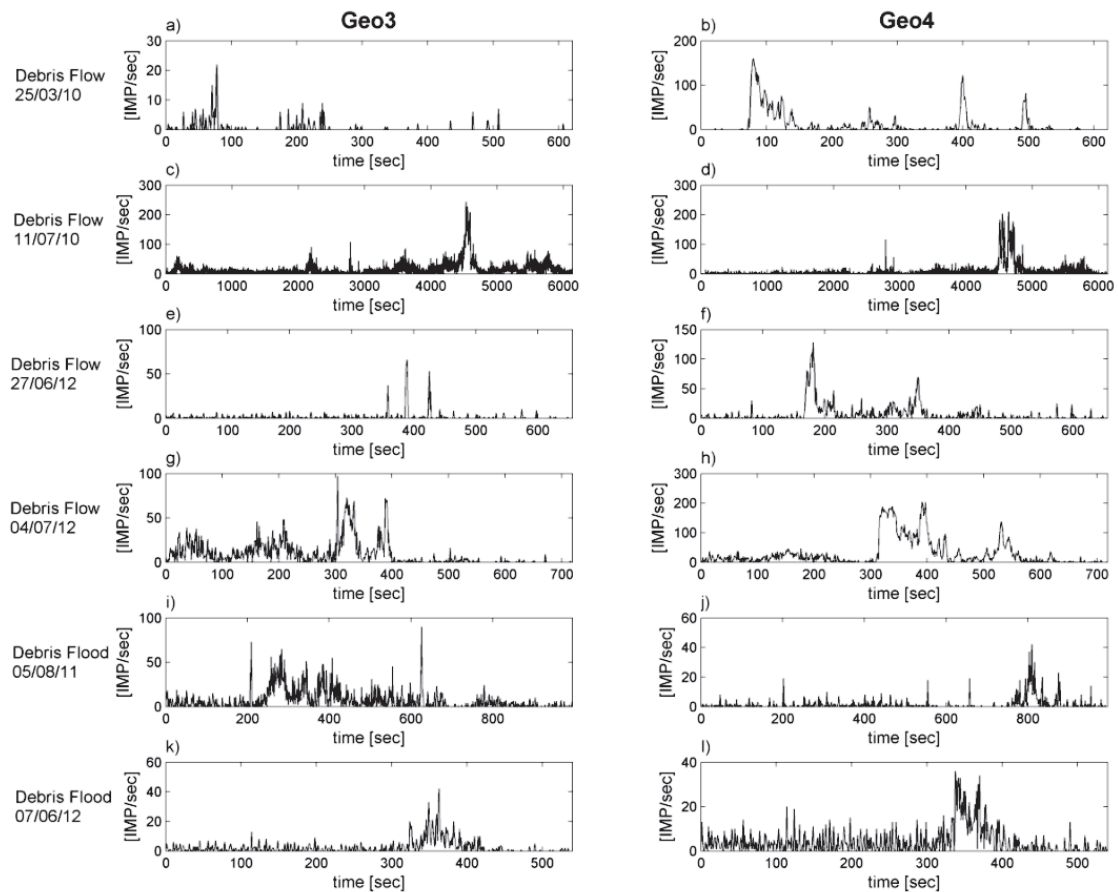
Figure 32: Plots of the ground vibration in (time vs. IMP/sec) during some debris flows and debris floods occurred in the Rebaixader monitoring site. Left column (a, c, e, g, i, k) corresponds to Geo3 and right column (b, d, f, h, j, l) to Geo4.

Table 6: Characteristics of the events analysed in this work

Date	Type	Volume (m^3)
04/07/2012	Debris flow	16200
11/07/2010	Debris flow	12500
27/06/2012	Debris flow	4000
05/08/2011	Debris flood	2500
25/03/2010	Debris flow	2100
05/07/2012	Debris flood	1000
07/06/2012	Debris flood	750

[81]

4.5. Data analysis by Ground Vibration Signal

4.5.1. Methods

In the station FLOW-SPI the geophone signal is recorded directly as a voltage and represents the vertical vibration velocity of the ground. The velocity was calculated using the geophone transduction constant (0.28 V/cm/sec for GEOSPACE-20DX). A base line correction was applied in order to correct the possible deviation of the "zero" value.

FLOW-SPI station provides data that has two main characteristics making it different from the FLOW-WR station: a) the recording of ground velocity signal (GVS) is continuous without distinction between "event" and "no event" modes; and b) the signal is recorded without filtering the noise. The data is stored in "mseed" files, a typically seismological format. Each of these files contain approximately 30 minutes of data sampled at 250 Hz (250 samples per second).

One of the key points of the recording by digital sampling is the sampling frequency, which has to be at least the double of the peak frequency of the vibration (as it was above-mentioned). This is a site-specific characteristic, which depends on the nature of the process and the characteristics of the geophones and its placement. In the Rebaixader catchment, the sampling frequency of 250 Hz is clearly enough to sample the records, according to the results of the spectral analysis carried out.

FLOW-SPI station was installed recently, in 2012, and for this reason only three events were recorded. Due to the small numbers of events recorded, an empirical approach to distinguish the type of events as the used for the IMP/sec time series was not possible for the analysis of GVS data set. Video images were available only for one of the events because the first two events occurred at night and the infrared spot used to light the scene were damaged by one of the events. The interpretation of the GVS signals recorded during the events was carried out mainly by crossing the data from both stations (FLOW-WR and FLOW-SPI), by analysing the flow depth recorded by the ultrasonic device, which is located very close to the three geophones of FLOW-SPI station (Figure 29), and by field reconnaissance.

4.5.2. Results

The events were characterized by different phases that define the progression of the flowing mass over time: a) Phase 0 (P0) is a pre-event phase, characterized by stationary low values of GVS and also low stage measured by the US; b) Phase 1 (P1)

is characterized by a rapid increase of the flow stage as well as the values of the GVS and corresponds to the pass of the debris-flow main front; c) Phase 2 (P2) is defined by GVS values lower than the flow front but some peaks are still visible, as well as punctual flow-depth increases; this phase is related to the passing of the flow main body; and, d) Phase 3 (P3) where GVS and stage gradually decrease to go back to the pre-front values, but still some small increments can be observed; this later phase is interpreted as corresponding to the flow tail or afterflow (turbulent muddy flow).

Phase 0 was observed in all of the events (Figure 33a, Figure 33b and Figure 33c and Table 7). The typical values of the GVS for Phase 0 are of hundredths of mm/sec. For all the geophones and events, these values represent between 1 and 25% of the highest peak of the event signal. Duration of this phase is variable (from tens to hundreds of seconds).

Phase 1 was only visible in the bigger debris flow (Figure 33a). The GVS records of this phase are the highest ones of the event. For this event, duration of Phase 1 was short compared to the other phases, but all the geophones reached the maximum values.

Phase 1 was only visible in the bigger debris flow (Fig 33a). The GVS records of this phase are the highest ones of the event, up to 1.6 mm/sec. For this event, duration of Phase 1 was short compared to the other phases (only ~40 sec).

Phase 2 was observed for the three events and it is characterized by high values of vibration compared to Phase 0 and Phase 3, although lower than Phase 1. Typical values are of tenths of mm/sec for debris flows and lower for the debris flood. Duration of this phase was similar for the three events, around 100 seconds.

The Phase 3 is characterized by low values of vibration but however, some peaks could be observed, as it could be noticed at the event of the 27th of June, where the highest peak at Geo5 was recorded at Phase 3 (Table 7). Besides the decrease of the vibration and the discharge, some big boulders or small waves could take place along this phase.

The comparison between the three geophones suggests that Geo5 provides a clearer signal, especially for the small-magnitude events. For the large debris flow, the three geophones present similar characteristics. Although the peak observed at Geo7 was the highest, the values of the peaks were similar for the three geophones.
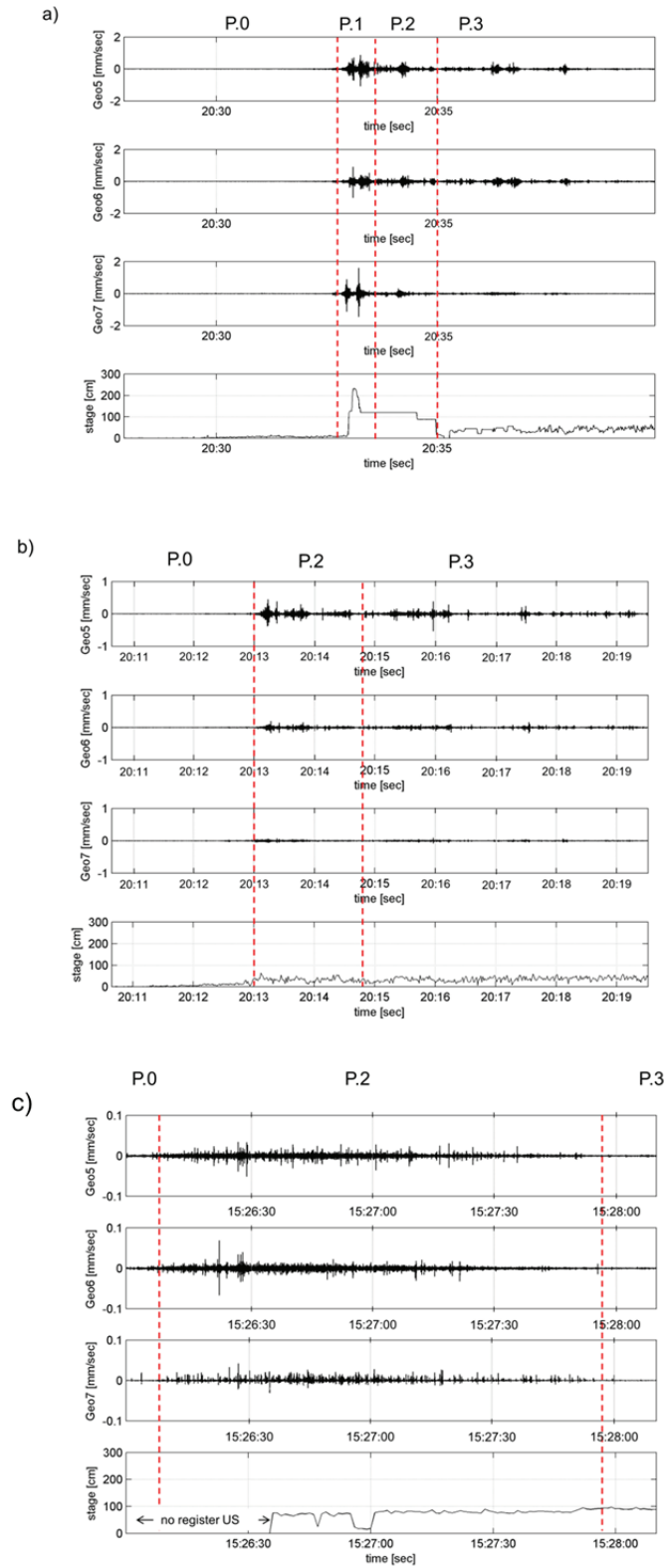
Figure 33: Ground vibration signals registered previously and during the debris flows occurred on 4th July 2012 (a), 27th of June 2012 (b) and the debris flood occurred on 5th July 2012. For all the events, data from Geo5 (a), Geo6 (b), Geo7 (c) and the US device are shown respectively.

[84]

Table 7: Summary of characteristics of the GVS recorded during the debris flows (04/07/2012 and 27/06/2012) and the debris flood (05/07/2012) from Figure 33.

		Phase 0			Phase 1			Phase 2			Phase 3		
		Geo5	Geo6	Geo7	Geo5	Geo6	Geo7	Geo5	Geo6	Geo7	Geo5	Geo6	Geo7
04/07/2012	Max value [mm/sec]	0.03	0.01	0.02	0.86	0.91	1.61	0.45	0.37	0.33	0.45	0.26	0.11
	Normalized peak value	0.02	0.01	0.01	0.54	0.57	**1**	0.28	0.23	0.20	0.28	0.16	0.07
	~Duration [sec]		~120			~40			~85			~120	
27/06/2012	Max value [mm/sec]	0.02	0.01	0.02				0.45	0.19	0.07	0.53	0.15	0.09
	Normalized peak value	0.04	0.03	0.05				0.85	0.36	0.13	**1**	0.28	0.17
	~Duration [sec]		~150						~110			~280	
05/07/2012	Max value [mm/sec]	0.01	0.01	0.02				0.04	0.07	0.03	0.01	0.01	0.01
	Normalized peak value	0.12	0.09	0.27				0.61	**1**	0.49	0.19	0.16	0.09
	~Duration [sec]		~10						~105			~15	

4.6. Effects of site-specific factors

The vibration registered by the geophones in both seismic stations of the Rebaixader torrent is conditioned by the placement of the geophones. Some factors such as the distance to the flow path, the underground material, the assembly of the geophones or the ground vibration threshold used in FLOW-WR will be studied and discussed in this

section. The influence of each factor was analysed by means of applying different approaches.

4.6.1. Distance and underground materials (field tests)

We carried out field tests at station FLOW-SPI in summer 2012 in order to record the GVS under specific conditions. We released a 9 kg sledgehammer from a height of 1.5 m at different distances from the three geophones Geo5, Geo6 and Geo7 (from 0 to 20 m) along the corresponding cross-section of the torrent. We performed the tests mostly twice to improve data quality. Similar tests have also been used in other studies (Kogelnig et al., 2011b; Navratil et al., 2011).

The results demonstrate a clear attenuation of the peak ground velocity signal with increasing distance in all the cases (Figure 34). The differences on attenuation between the different geophones can be attributed to the underground material not only in the location of the geophone, but also all over the cross section where the test was carried out.

Geophone Geo6 presents the highest peaks, while the attenuation curve is similar to Geo5. These two geophones have in common that bedrock outcrops at most of the cross section. However, the difference between them is that geophone Geo6 is buried into a thin layer of colluvium. Whereas geophone Geo5 is directly assembled to the bedrock. The comparison of the results from the tests carried out near these two geophones suggests that the thin colluvium layer produces an amplification effect of the sledgehammer impacts.

In a different way, geophone Geo7 shows much lower vibration peaks and minor attenuation with the distance. Colluvium appears practically all over the cross-section where the impacts of the sledgehammer were performed, which could be the reason of the attenuation.
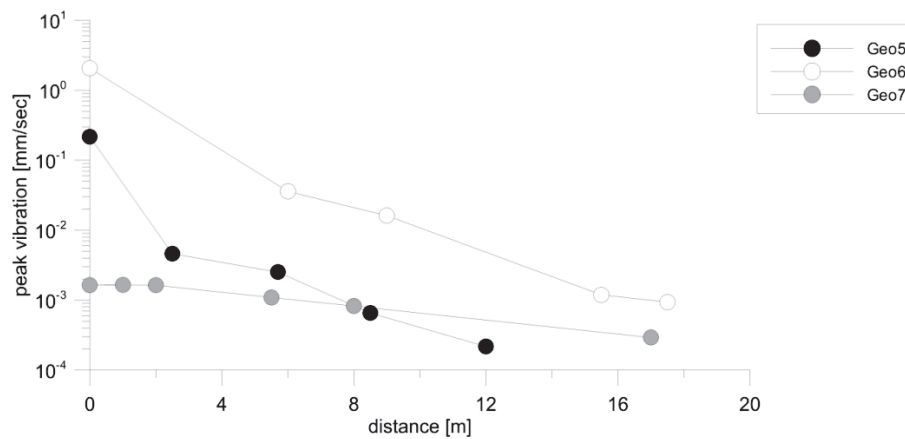
Figure 34: Distance vs. peak of the ground vibration signals registered during field tests.Geophones Geo6 and Geo7 are installed in colluvium and Geo5 is installed in bedrock.

4.6.2. Assembly of the sensor and distance

In order to identify the influence of the geophone assembly and the distance to the flow path, the signal registered at three different geophones was compared. These three geophones were selected because of their location. On one hand, they are installed approximately at the same cross-section of the channel. Geophone Geo3 and Geo3b are located at the right margin of the channel and very close together (they are only 50 cm apart). Geophone Geo5 is placed at the left margin of the channel, 35 m upstream from Geo3 and Geo3b (Figure 29). On the other hand, all of them are mounted on bedrock. Geo5 and Geo3b are fixed directly on bedrock and Geo3 is mounted in a sheet metal box, which is fixed on bedrock.

As it was mentioned above, the signal at Geo5 is recorded directly as GVS. Thus, the Geo5 data were transformed into IS in order to be compared with the data from Geo3 and Geo3b, which were recorded as IS. This transformation was carried out as a post-process by a self-made MATLAB code (MATLAB, 2009). The code applies the same transformations to the GVS that is done by the signal conditioner of the FLOW-WR station. As a preliminary stage, a baseline correction was performed to avoid offsets derived from the analog-to-digital converter (ADC) Then, the GVS below a certain GVth is filtered and the GVS over the threshold is transformed into IS signal. The GVth is applied by means of electrical resistors in the signal conditioner for Geo3 and Geo3b, but as an input of the MATLAB code for Geo5. The GVth used for the transformation into IS are: 0.17 mm/sec in Geo3 and 0.019 mm/sec at Geo3b. It is worth noting that the GVth used for the transformation into impulses at Geo3b (which is fixed directly to bedrock) is 10 times lower than at Geo3 (which is mounted in a sheet metal box). Both

thresholds (0.17 and 0.019 mm/sec) were applied for the transformation of the GVS measured at Geo5.

The comparison of the four resulting IS time series shows the influence of the distance and the effect of the sheet metal box. In Fig. 7 the ground vibration of the July 4th 2012 debris flow are represented for the three geophones Geo3 (Figure 35a), Geo3b (Figure 35c) and Geo5 (Figure 35b and Figure 35d).

The results show that the sheet metal box has a strong effect of amplification of the signal. The peak at Geo3 is observed at time 200 sec, and it is 75 IMP/sec approximately (Figure 35a). At the same moment Geo3b shows 15 IMP/sec (Figure 35c), that is, about 5 times smaller. The significant difference of the records of Geo3 and Geo3b can only be explained by the effect of the sheet metal box, which works as a resonant structure magnifying the vibration registered by the geophone. The influence of the sheet metal box produces an increase of the values of the IS signal at Geo3 up to 10 times the values of IS at Geo3b. It is important to remind that the threshold used for the transformation into IS at Geo3 was 10 times greater than in Geo3b (GVth 0.17 versus 0.019 mm/sec, respectively). Therefore, the results suggest that effect of the box could be described as an amplification of factor 100. The effect of the distance to the flow path can be noticed by comparing the data from Geo3b (Figure 35c) and Geo5 (Figure 35d). Both geophones are directly mounted on bedrock and the velocity threshold, GVth, is the same in both cases. However, the distance between the geophones and the active channel is greatly different (25 m at Geo3b and 3 m at Geo5). The comparison of these figures suggests that the distance can produce an important effect on the IS signal, a reduction factor of the vibration peaks up to 3.5.

To summarize, the influence of the box assembly and the distance greatly affect the IS signal registered at the geophones. Although the evaluation of the effects numerically is difficult, it can be stated that the effect of the sheet metal box generates an amplification of the signal that cannot be reached by reducing the distance between sensor and vibration source 5 times.
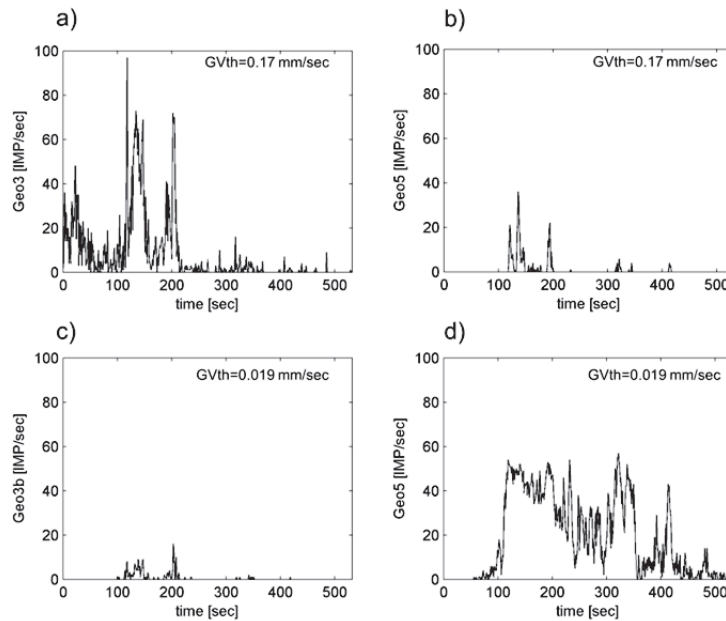
Figure 35: Comparison of the IS signal observed during the 4th of July 2012 debris flow. Data registered at Geo3 (a), Geo3b (c) and signal obtained by transformation of data from Geo5 (b and d).

4.6.3. Detection threshold

The most important point on the development of a reliable alarm system is the definition of the detection threshold, in such a way that false alarms are reduced to a minimum. In the FLOW-WR station at the Rebaixader monitoring test site, we defined a "detection threshold" (Dth) for the monitoring system, calibrated for research purposes. The Dth is based on two thresholds: on one side the GVth, and on the other side the EMth, which is formed by EMth$_{dur}$ and EMth$_{IMP/sec}$ (see Section 4.1.). The detection threshold Dth could be used for alarm purposes; however the values of GVth and EMth should be calibrated with more restrictive intentions. As it is suggested by the results in previous sections, the site-specific factors influence the vibration recorded by the sensor, and the values registered can be widely different from one geophone to another. For this reason, the values of GVth and EMth should be defined for each specific geophone, according the placement of the geophone.

Using the data from the debris flows occurred on the 27th of June of 2012 and 4th of July of 2012, a sensibility analysis of the three Dth parameters was carried out. Different values of GVth and EMth were tested using data recorded by the geophones of FLOW-SPI station, where the complete register of the ground velocity signal was available (Geo5, Geo6, Geo7). First, the data was transformed into impulses using 10

different values of GVth. Then, two values of $EMth_{IMP/sec}$ (10 and 20) were chosen and the number of seconds over it was obtained for each GVth value and $EMth_{IMP/sec}$. The number of seconds over $EMth_{IMP/sec}$ corresponds to the maximum value of $EMth_{dur}$ that could be defined for each combination of $EMth_{IMP/sec}$ and GVth.

In Fig. 8 it can be observed that, as the GVth increases, the number of consecutive seconds that the signal exceeds the $EMth_{IMP/sec}$ decreases exponentially for both values of $EMth_{IMP/sec}$ (10 and 20) and for both events.

It is worth noting that any of the debris flows would not have been detected for the Dth parameters used in the station FLOW-WR (GVth = 0.17 mm/sec; $EMth_{IMP/sec}$ = 20; $EMth_{dur}$ = 3). This fact enforces the outcomes of the previous section on the effect of the metal sheet metal box, which strongly amplifies the ground vibration. Assuming a GVth – value of 0.019 mm/sec (as used at Geo3b, where there is no box), the big event (04/07/12) would have been detected by the three geophones, while the small event (27/06/12) would only have been detected by Geo5 and Geo6.

A reliable threshold should detect the desired events as early as possible but filter the ground velocity that does not correspond to an event. The definition of an incorrect combination of the tree threshold parameters ($EMth_{dur}$, $EMth_{IMP/sec}$ and GVth) could signify missing an event, such as it can be observed in the data from the event of 27th of June (Figure 36a and Figure 36b), where $EMth_{IMP/sec}$ was almost never exceeded.
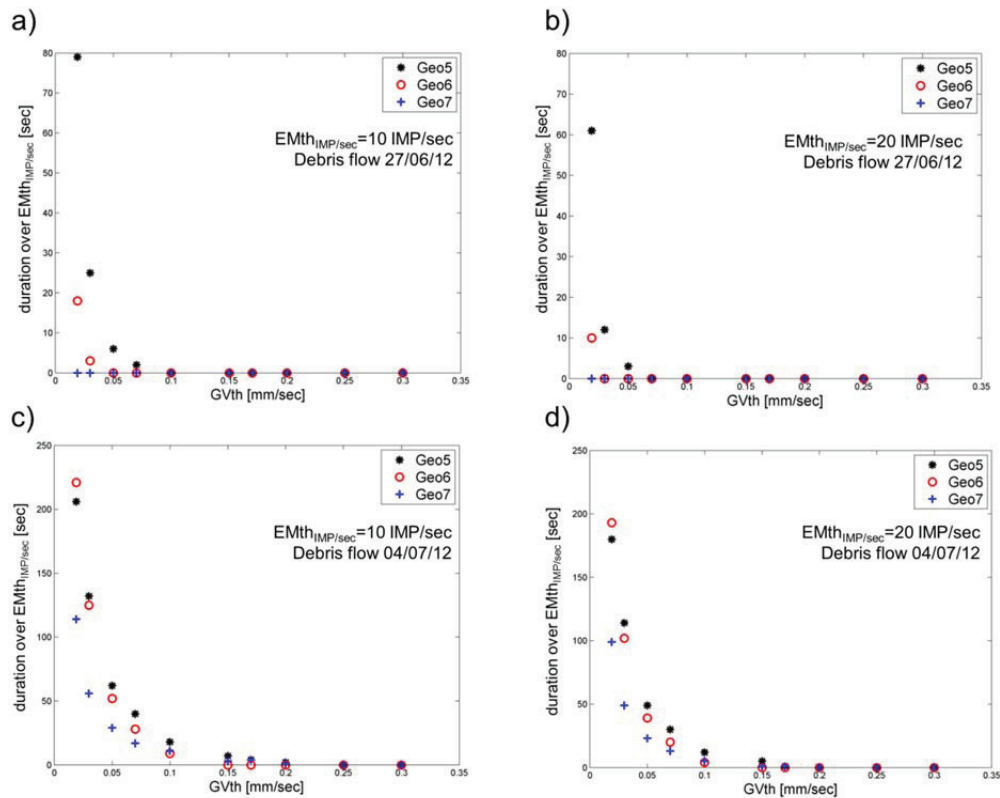
Figure 36: Influence of the three parameters of the detection threshold (Dth): ground velocity threshold (GVth) vs. duration over the IMP/sec threshold of the "event" mode (EMth$_{IMP/sec}$) (a and c). The value of EMth$_{IMP/sec}$ is 10 IMP/sec for (a) and (c) and 20 IMP/sec for (b) and (d).

4.7.   Conclusions

Monitoring torrents prone to debris flows is an increasing activity all over the world. The efficiency of the geophones to monitor the occurrence of torrential processes has been widely proved, and so it is their convenience for alarm purposes (Arattano and Moia, 1999; Badoux et al., 2009; Bessason et al., 2007; Huang et al., 2007; LaHusen, 2005b; Suwa and Okuda, 1985). However, there is a great variety of data recording systems, highly conditioned by the technical details of each monitoring station.

In this work, two different recording systems have been compared, both of them installed in the Rebaixader torrent (Central Pyrenees). One of the data recording systems consists of collecting the entire ground velocity signal (GVS), digitized at a high frequency rate, while the other is a more simplified system, which records a transformed signal (IS). Both recording systems demonstrated their efficiency on recording the typical debris-flow features including the different phases of the events. Thus, both techniques should be considered suitable for debris-flow monitoring. On

one hand, GVS data recording technique provides more information about the signal generated by the debris-flow passing, but it generates a great amount of data and subsequently consumes more electric power and time of analysis. On the other hand, IS data recording technique provides less information about the signal, but it has been demonstrated that it is reliable for detection. Moreover it requires less power and simplifies the data collecting and gathering. These latter issues make the transformed signal especially useful for an alarm system.

The data analysed suggests that for GVS and IS signals, the differences between debris flows and debris floods can be identified. For IS the differences are mainly based on the shape of the IS signal, while for the GVS signal the values of the ground velocity are the main distinctive feature. In both stations (FLOW-WR and FLOW-SPI), the results point out that the geophones that better show the debris-flow features are the closest to the active channel. It is also worthwhile that the active channel runs over bedrock on the cross-section. The geophones located at cross-sections where the active channel runs over colluvium show less clearly the characteristics of debris flows, especially if they are placed relatively far from the active channel. All these results suggest that the optimum position for a geophone to obtain reliable records of debris flows would be as closest as possible to the active channel, and preferably where it runs over bedrock.

The site-specific factors that influence the ground vibration measured at the geophones were evaluated by field tests and the comparison of the GVS registered at three geophones. Two major conclusions were obtained: a) the distance attenuates the signal exponentially, b) the seismic waves travelling in colluvium stronger attenuate than in bedrock, although a fine colluvium layer over bedrock could amplify the signal; and, c) the assembly of the geophone can strongly condition the amplification of the signal. This last conclusion was clearly observed by comparing one geophone directly fixed at bedrock with another one mounted at a sheet metal box, which is attached to the bedrock. The results suggest that the sheet metal box amplifies the signal by a factor up to 100x. Therefore, from all these effects it is pointed out that some amplification is useful for the detection of events, especially where the geophones cannot be placed close to the active channel. However, other amplification system (like an electronic amplifier in the circuit board) should be considered, where the amplification factor could be known and controlled.

Finally, the choice of a correct Detection Threshold (Dth) is fundamental, since it could produce the loss of an event or a great number of false alarms. In this study a sensibility analysis of the parameters of the Dth was carried out. The results point out that the number of seconds (duration threshold $EMth_{dur}$) over the number of IMP/sec (IMP/sec threshold $EMth_{IMP/sec}$) threshold 10 and 20 IMP/sec decrease exponentially as the ground velocity threshold (GVth) increases. Small differences in GVth can provoke a high decrease of the number of seconds over a certain number of IMP/sec, which could result in missed events. Therefore, it enforces again the necessity of calibration of the threshold at each specific geophone considering all the site specific effects.

Although many uncertainties are still remaining, the outcomes of this research improved knowledge on the use of seismic sensors for the detection of debris flow and other torrential processes and helped on the design of an alarm system using geophones as key sensors.

5. Rockfalls detached from a lateral moraine during spring season. 2010 and 2011 events observed at the Rebaixader debris-flow monitoring site

5.1. Introduction

Rockfalls represent a significant geomorphological hazard in mountainous areas. Generally, they are related to failures in rockwalls and only to a lesser extent to instabilities of superficial deposits (e.g. Cruden and Varnes, 1996; Dorren, 2003; Evans and Hungr, 1993). Although the glacial deposits in the Rebaixader catchment (Central Pyrenees, Spain) are affected by different types of mass-wasting processes such as debris flows, the present study only focus on the two rockfalls occurred in 2010 and 2011.

Nowadays, slope failures initiated in glacial deposits represent an important research topic due to future climate changes and associated consequences like glacier recession or the possibility of thawing permafrost (Allen et al., 2011; Blair, 1994; Clague and Evans, 2000; Gruber and Haeberli, 2007; Harris et al., 2009; Hugenholtz et al., 2008; Soldati et al., 2004). While shallow slope failures in moraine deposits have

been analysed by different approaches (Curry et al., 2009; Springman et al., 2003; Vedie et al., 2010), detailed research studies on rockfalls detached from glacial deposits have not yet been published. Another research topic related to mass movements in high mountain areas, which has not yet been solved, is the effect of snowmelt on the destabilization of natural slopes (Decaulne et al., 2005; Flageollet et al., 1999; Van Asch et al., 1999).

The two rockfalls that will be presented in this work occurred both in spring (May 2010 and April 2011). Both events initiated by the detachment of large boulders from a steep lateral moraine (Figure 37). Detailed data are available, because the rockfalls took place in a debris-flow monitoring site. Although the monitoring system was not designed for rockfall observation, interesting and new data on rockfall mechanisms were recorded by the devices installed. While sensor measurements or visual data of artificially triggered rockfalls can be found in literature (e.g. Vilajosana et al., 2008), only very general information is available on naturally-induced events. The same conclusion can be drawn for slope failures in glacial deposits (e.g. Springman et al., 2003).

The major goal of this study is the presentation of monitored data and field observations related to the two rockfalls. This information firstly improves the general understanding of the stability of glacial deposits; and secondly, it also shows the need of monitored data on the dynamic behaviour of rockfalls to calibrate simulation models. The need of such calibration data was recently stated as a major conclusion at an international workshop on rockfall protection: "*Detailed calibration is more urgent today than refining the mathematics*!" (Hungr, 2011). In addition, the results also exposed some helpful aspects related to alarm and monitoring systems for debris flows and other mass movements, in particular if they can be affected by rockfalls.

5.2. Settings

The rockfalls occurred in the Rebaixader catchment (WGS: 42°32'47.07"N, 0°45'19.50"E; Figure 37), which is located near Senet, a village in the Axial Pyrenees. The Rebaixader is a small tributary of the Noguera Ribagorçana river valley. During the Last Glacial Cycle, this latter valley was occupied by an alpine glacier that reached a maximum length of 27 ^{km} and a thickness greater than 500 m at the confluence with the Rebaixader torrent (Vilaplana, 1984). A debris-flow monitoring system runs in this

catchment since the summer of 2009 (Hürlimann et al., 2011), though rockfall events were not considered during the design and installation of the system. The unexpected occurrence of rockfalls caused the destruction of some sensors and required the adaptation of the monitoring systems to avoid future damage.
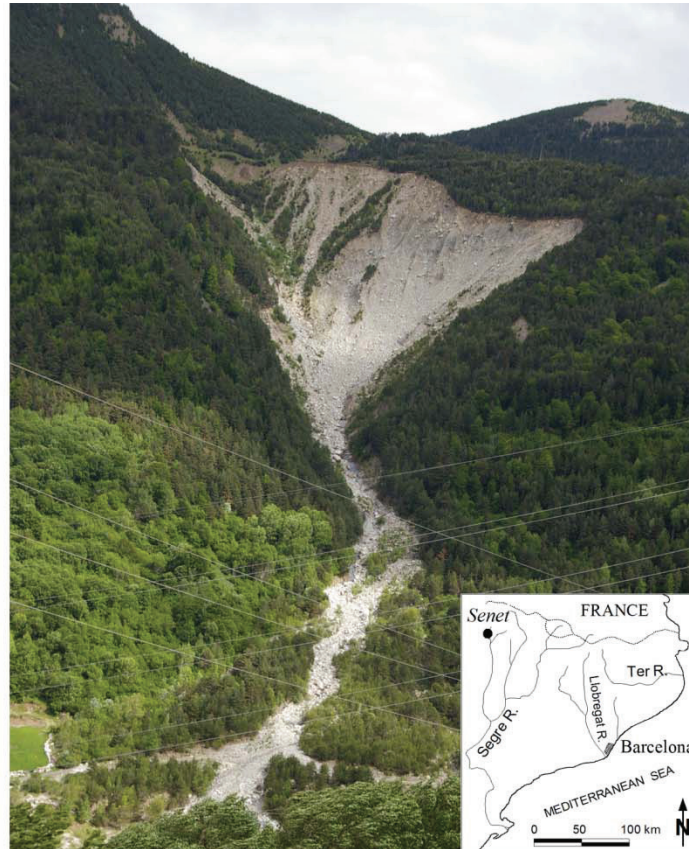
Figure 37: Oblique photo of the Rebaixader catchment with the large scarp in the lateral moraine where the rockfalls detached. Inset shows the location of the Senet, a village close to the catchment.

5.2.1. Morphology, geology and climate

The Rebaixader catchment is characterised by a typical high-mountain morphology affected and formed by glacial and periglacial processes (Figure 38a). The drainage basin covers an area of 0.53 km^2 and can be divided into different parts: 1) the area between 1720 and 2475 m a.s.l. with steep slopes and a limited layer of colluvium; 2) a relatively flat area located between 1710 and 1720 m a.s.l. formed by torrential deposits; 3) a steep scarp between 1425 and 1710 m a.s.l. developed in the lateral moraine, which is the source zone for debris flows and boulder detachments; 4) a channel or track zone located between 1350 and 1425 m a.s.l., and 5) a debris fan that links the Rebaixader creek with the floor of the Noguera Ribagorçana valley. The

[97]

glacial deposit (till) that forms the lateral moraine is built of two different layers (Bordonau, 1992): 1) the lower subglacial materials consisting of unsorted gravel, sand and silt, and 2) the supraglacial materials containing large granitic boulders in a sandy matrix. The rockfalls observed in the Rebaixader catchment initiated in the scarp of the supraglacial layer. Thus, a sample of the matrix of the supraglacial layer was collected in the highest part of the scarp for a grain-size analysis. The particle-size distribution curve shows that the matrix of this sample is mainly formed by gravel and sand (Figure 39). The comparison of the Rebaixader sample with the grain-size distributions of other moraines shows that the Rebaixader material is coinciding with the characteristics of glacial tills from other mountainous areas.

The bedrock of the catchment is built by Paleozoic metamorphic rocks, which are typical for the Axial Pyrenees (Muñoz, 1992), and mostly consists of Devonian slates and phyllites formed during the Hercynian orogeny.

The regional weather conditions depend on three factors: the vicinity of the Mediterranean Sea, the influence of the west winds from the North-Atlantic and the orographic effects of the Pyrenean mountain range. The annual precipitation in this area of the Pyrenees is between 800 and 1200 mm, while a strong orographic influence and an inter-annual variability can be observed (CAC, 2004; Novoa, 1984). Two general types of precipitation patterns can be distinguished: 1) long-lasting and moderate-intensity precipitation in autumn, winter and spring, and 2) convective, short and high-intensity rainstorms in summer.

At present time, the existence of permafrost at the moraine can be excluded, because lower limits of permafrost in the Pyrenees normally range from 2700 to 2900 m a.s.l. (Julián and Chueca, 2007).
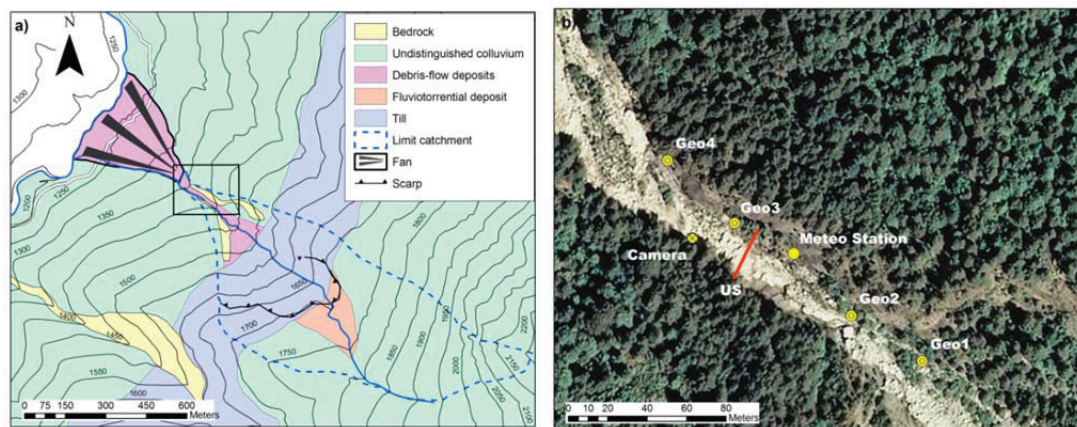
Figure 38: a) Geomorphological-geological map of the Rebaixader catchment (rectangular area shows area represented in b). b) Ortophoto of the monitored channel reach and location of the sensors. Geo indicates geophone, while US stands for ultrasonic device.
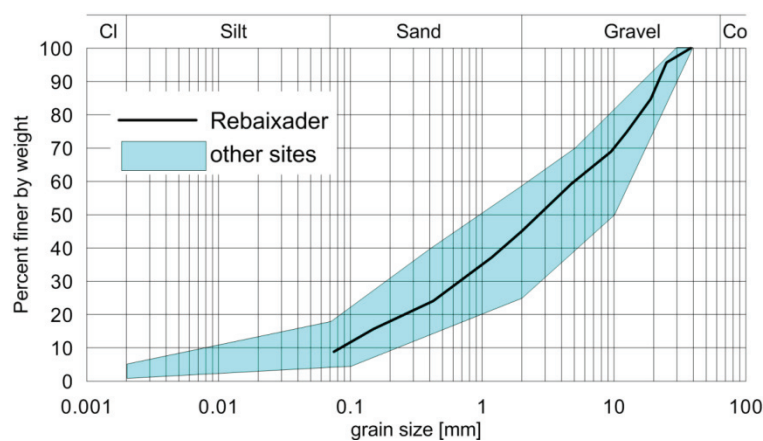
Figure 39: Grain-size distribution of the matrix material sampled in the supraglacial layer, where the large boulders detached (maximum particle size: 40mm). Comparison with other moraines in the European Alps and the Pyrenees (Lebourg et al. 2003; Springman et al. 2003; Curry et al. 2009).

5.2.2. Description of the monitoring system

As previously mentioned, a debris-flow monitoring system was installed in the catchment in the summer of 2009. The monitoring system includes two main parts: the meteorological station and the so-called "flow station". The meteorological station measures at 5 minute intervals the values recorded by both a standard unheated tipping bucket rain gauge and a temperature sensor. The flow station, which is designed for the measurement of the dynamic behaviour of debris flows, records at a scan rate of 1 Hz (each second) the values of four geophones, which acquire the

[99]

ground vibration, and an ultrasonic device, which measures the flow depth. In the summer of 2010, a video camera was incorporated to obtain visual information. The location of each device is illustrated in Figure 38b.

Sensors measurements in each station are recorded by data loggers, while GSM modems are used for data transmission to the university server in Barcelona. The monitoring system is powered by batteries, which are recharged by solar panels.

An important aspect is the fact that, the ground vibration detected by the geophones is directly transformed by an electronic signal conditioner into a number of impulses per second (IMP/sec). This transformation takes place at each geophone and helps to reduce the volume of data that reaches the data logger. Detailed information on the technical aspects of the monitoring system can be found in Hürlimann et al. (2011).

5.3. Field and monitoring data

5.3.1. Methods applied and data available

Two types of information were analysed to reconstruct the two rockfall events: 1) geomorphic field observations obtained by recurrent surveys of the torrent, and 2) data recorded by the sensors of the monitoring system. In addition, complementary information measured at surrounding meteorological stations was also analysed.

The trajectory of the fallen boulder was reconstructed by locating of the initiation point, the major impacts on the ground and the final position of the boulder (Figure 40). While the trajectory and final position of the boulder was defined by direct observations in the channel (using information on the damage to trees and shrubs, impact marks on bedrock and fresh rock flakes close to impact marks), the access to the detachment point of the boulders in the steep moraine scarp was problematic due to rockfalls and other mass movements. Thus, the initiation points of the boulders were obtained by interpretating the photographs periodically taken during the control of morphologic changes in the channel and the moraine scarp (Figure 41).

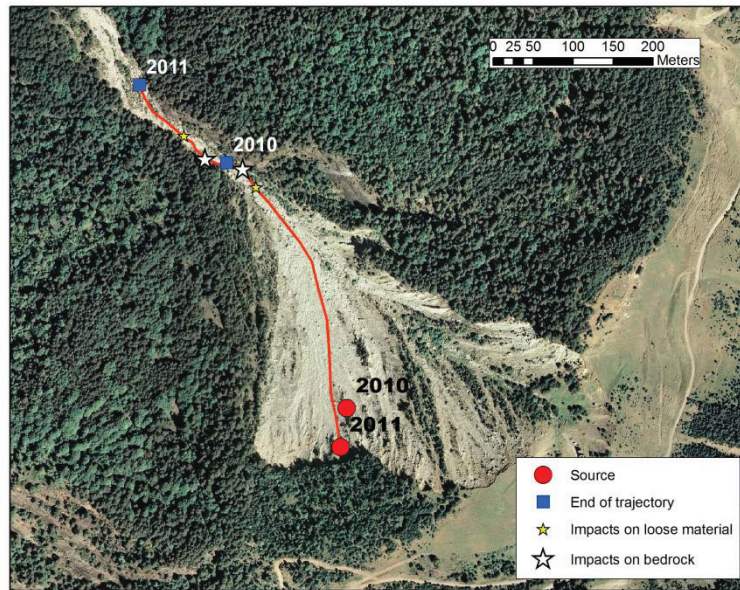**Figure 40: Assumed trajectory and major impacts of the 2011 rockfall. Initial and final position of the 2010 rockfall is also indicated.**

Figure 41: Overview of the steep moraine scarp containing large boulders. The red circle indicates the location of the detachment point of the 2011 rockfall. a) Pre-event photo taken on March 18th 2011, and b) post-event photo taken on May 31st 2011.

The data recorded by the different sensors include, on one side, the meteorological information and, on the other side, the measurements related to the rockfall movements. Regarding the meteorological data, an important drawback is the lack of information on the amount of snowfall. Because the rain gauge installed in the Rebaixader test site is an unheated device, snowfall cannot be correctly measured. However, the two rockfalls took place in spring and late snowfalls can occur at this site. Thus, additional data of snow height were incorporated in the analysis in order to obtain information on the amount of snowfall and snowmelt. The meteorological station closest to our test site is Boí, at 2535 m a.s.l. The Boí station forms part of the Catalan Meteorological Service network and is located 11 km to the South-East of the Rebaixader catchment.

Regarding the data on the dynamic behaviour of the rockfalls, the ground vibration recorded at the geophones is available for the 2010 and 2011 events. These measurements can be used to determine the exact time of the rockfall and to roughly estimate the mean velocity of the process between each sensor. In contrast, information recorded by the ultrasonic device and the video camera are only available for the 2011 event. In fact, the interpretation of the video frames added important information on the movement of the rockfall and revealed an additional data on the velocity.

A digital elevation model with a resolution of 5x5 meters was used to determine the longitudinal profile and the slope angles of the rockfall trajectory (Figure 42).
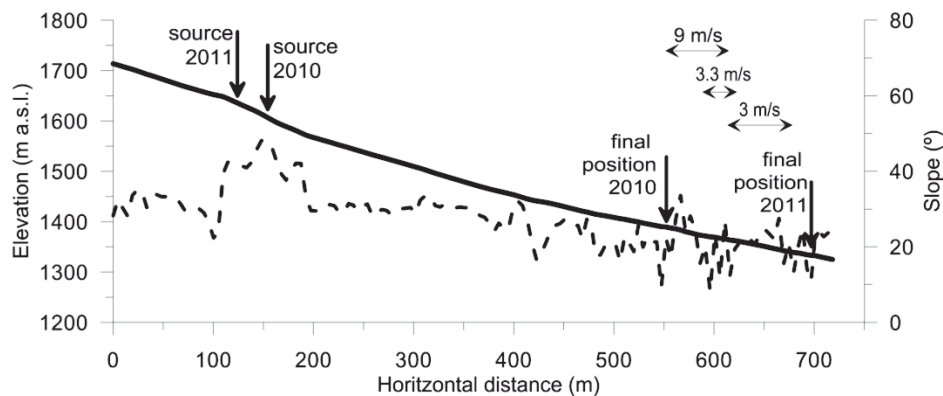

Figure 42: Topographic profile along the 2011 rockfall trajectory and information on the slope angles. Velocity estimates obtained from the monitoring devices are also indicated. Source and final position of the 2010 rockfall are illustrated for comparison.

5.3.2. *2010 rocfkall*

The 2010 rockfall was detected by the ground vibration recorded at the two uppermost geophones at 10:04 UTC on May 13th (Table 8). The volume of the boulder was calculated as 55 m3 (approx. 2.7 x 4.5 x 4.5 m3; Figure 43a), which seems to be an upper bound of the size of the boulders visible in the actual moraine scarp. The source point of the boulder at ~1610 m.a.s.l. is characterised by a slope angle of about 46º, while its final position is in the upper part of the channel zone, at ~1390 m a.s.l. (Figure 40 and Figure 42). The rockfall damaged the meteorological station and destroyed the ultrasonic device, both of them installed at that time near geophone Geo2 (Figure 38b). That's the reason why these sensors were subsequently installed further down-slope.

Figure 43: a) Boulder of the 2010 rockfall at final position (up-slope view), and b) boulder of the 2011 event at final position (down-slope view). The scale in front of the boulders has a length of 2 meters.

The field survey after the rockfall focussed on the last section of the trajectory. There, most of the vegetation was destroyed and several boulder impacts were observed. The most important impact was detected on a rockwall located in the right (northern) side, at the uppermost reach of the torrent channel (Figure 40). This wall directly faces the most active source area of rockfalls. The falling boulder was strongly deflected by this rockwall. The analysis of the boulder shape at its final position revealed several fresh and shallow fractures on its surface. This fact suggests a minor fragmentation and may represent a volume reduction of about 1 to 2 m3.

The meteorological data recorded at the Rebaixader station shows a rather low temperature and only insignificant rainfall both at the moment of the rockfall and also

several hours previous to the event (Table 2). The temperature near 0 ºC also supports the hypothesis that freezing-thawing effects may have affected the release of the boulder. Antecedent precipitation may have played an important effect, since about 100 mm were measured during the four days preceding the event (Figure 44). Some of this precipitation probably felt as snow in the higher part of the catchment, and thus the effect of snowfall-snowmelt may have influenced the detachment of the boulder.
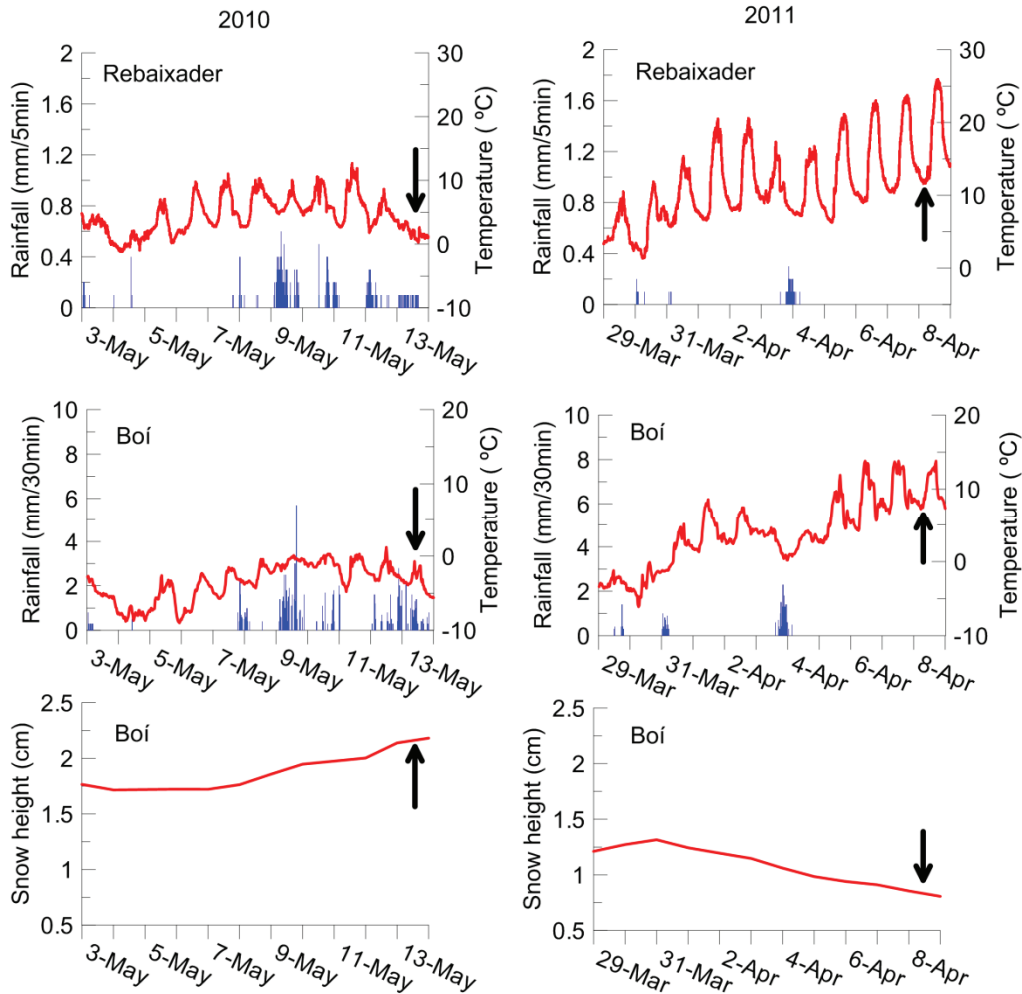
Figure 44: Rainfall, temperature and snow height measurements related to the 2010 and 2011 rockfalls. Data recorded at Rebaixader (1380 m.a.s.l.) and Boí (2535 m.a.s.l.). The arrow indicates the moment of the rockfalls.

Because the final position of the boulder is near geophone Geo2, the analysis of the ground vibration focuses on the measurements of the two uppermost geophones (Geo1 and Geo2). The ground vibration lasted about 8 seconds and was characterised by a high number of impulses per second (Figure 45). These limited data on the ground vibration do not allow a velocity estimate and unfortunately video images of this event

are not available (as mentioned above, the video camera was installed in the summer of 2010).
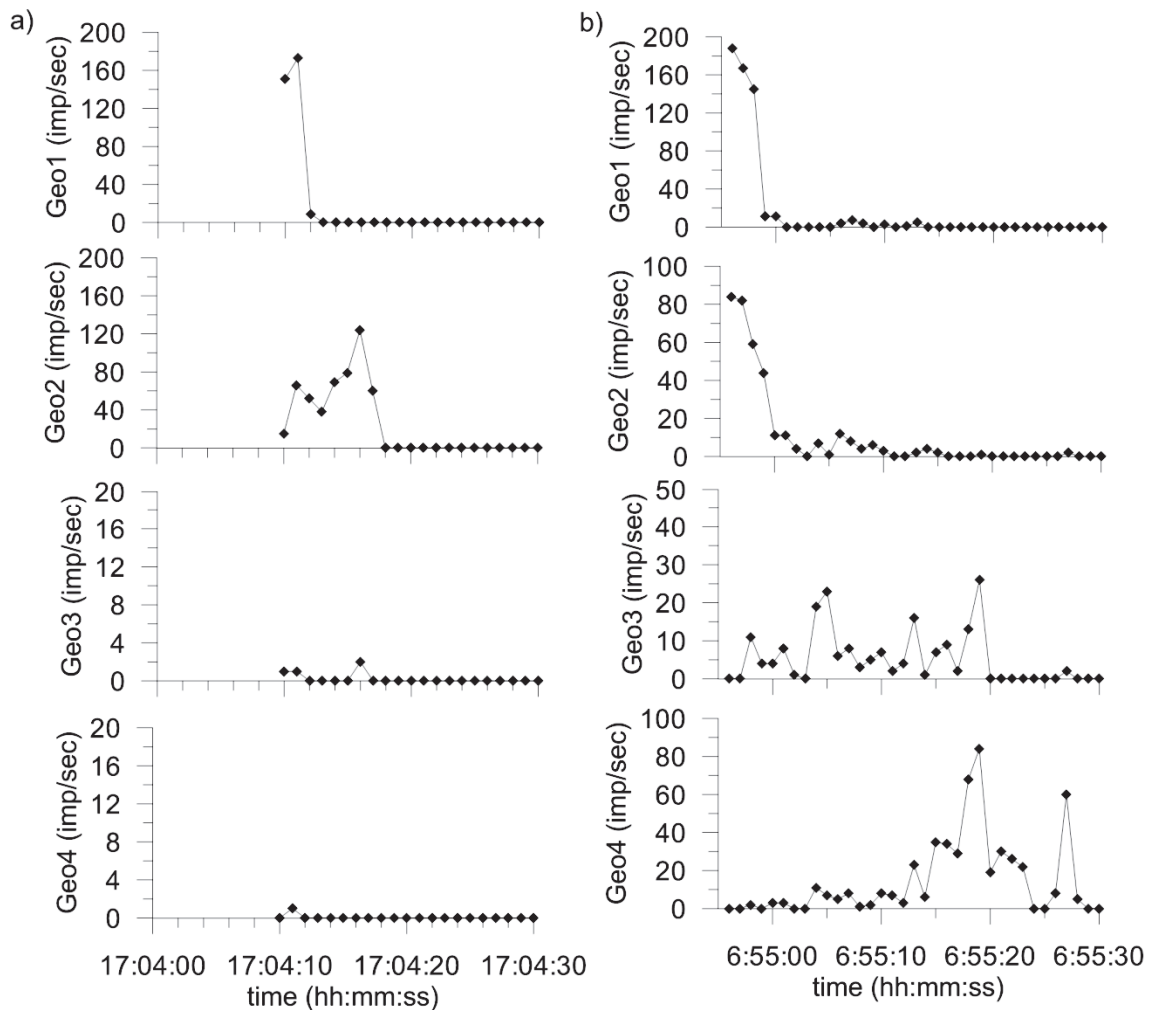
Figure 45: Ground vibration recorded by the geophones during the 2010 rockfall (a) and the 2011 rockfall (b). Ground vibration is illustrated by number of impulses per second (IMP/sec). Note the different scales at the axes of ground vibration.

5.3.3. 2011 rockfall

The vibration provoked by the 2011 rockfall was detected at the geophones on April 8th at 6:54 a.m. (Table 8). The volume of the boulder was calculated as 18 m3 (approx. 2.0 x 2.5 x 3.5 m3; Figure 43b). The detachment area was located almost at the crest of the moraine scarp at ~1630 m.a.s.l., where slope angles are about 42º (Figure 41). The rockfall crossed the entire monitored section of the torrent channel and stopped just down-slope the fan apex, at 1333 m.a.s.l. (Figure 40 and Figure 42).

The field survey after the rockfall showed several impacts along the trajectory, but no damage at the monitoring system. As in the 2010 event, the size of the boulder was

[105]

slightly reduced during the movement due to the impacts on bedrock and subsequent minor fragmentation of the boulder.

Table 8: General information on the two rockfalls.

Date (dd.mm.yyyy)	Time (UCT) (hh:mm)	Volume of boulder (m³)	Runout, L (m)	Falling height, H (m)	Angle of reach, H/L (-)
13.05.2010	17:04	55	399	220	0.55
08.04.2011	06:54	18	569	297	0.52

In contrast to the May 2010 event, the April 2011 rockfall was triggered at a higher temperature and without any precipitation (Table 9). The temperature evolution of the 3 weeks before the event indicates an important fluctuation with increasing mean values (Figure 44). The average temperature of the 24h preceding the event was 16.1 ºC. Thus, in this case, freezing-thawing and also snowfall-snowmelt effects associated with the boulder detachment should be neglected.

Table 9: Cumulative rainfall, *P*, and average temperature, *T*, recorded at the Rebaixader meteorological station regarding different time intervals previous to the rockfall events.

Rockfall event	P_{1h} (mm)	P_{1d} (mm)	P_{3d} (mm)	P_{10d} (mm)	T_{1h} (ºC)	T_{1d} (ºC)	T_{10d} (ºC)
May 2010	2.0	14.0	50.4	105.7	0.9	2.8	4.6
April 2011	0.0	0.0	0.0	18.5	12.8	16.1	11.2

The monitored data, which refer to the dynamic behaviour of the 2011 rockfall, include ground vibration from the geophones, visual information from the video camera and data from the ultrasonic device. The ground vibration was measured at the four geophones, since the boulder stopped down-slope the geophone Geo4. As in the 2010 event, the vibration was generally characterised by a high number of impulses per second and a short duration (Figure 45b). Velocity estimates were obtained from the measurements recorded at the geophones and the ultrasonic device. The distances between the sensors and the time intervals between the recorded peaks revealed

mean velocities of about 9 m/s in the upper part of the monitoring reach and about 3 m/s in the lower part (Figure 42). These estimates were crosschecked with the information gathered by the video camera, which provided velocity estimates of 3.3 m/s. In addition, a detailed analysis of the dynamic behaviour of the rockfall was carried out by the interpretation of the video images. Six different frames are illustrated in Fig. 10. The complete movie can be downloaded at www2.etcg.upc.es/prj/debriscatch. The first frame indicates the moment just after the energetic impact of the boulder on the bedrock between geophones Geo1 and Geo2 (see high peaks in Figure 45b), which produced a large cloud of dust. The following frames shows the boulder moving with a combination of rolling and some small bounces along a zigzag trajectory inside the torrent channel.
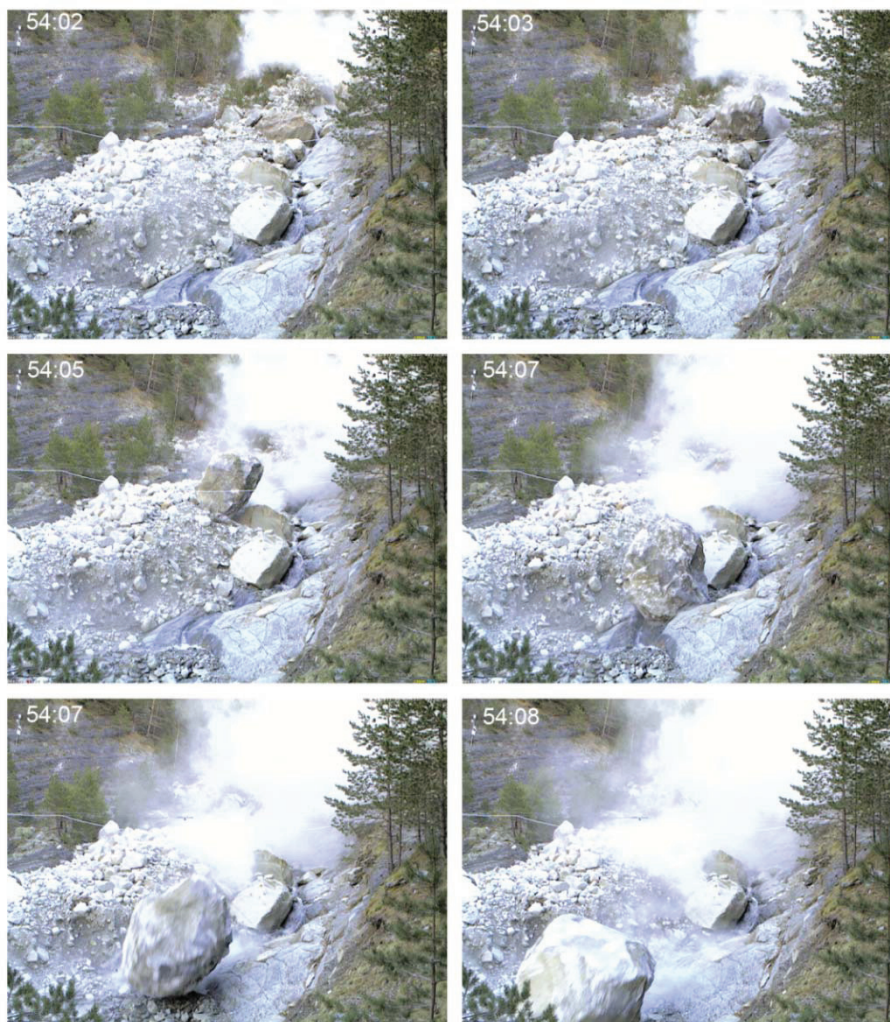

Figure 46: Video frames of the rolling and bouncing block during 2011 rockfall. The time of each frame is given in mm:ss.

[107]

5.3.4. Simulation of the 2011 rockfall

The back-analysis of the 2011 rockfall mainly aims to show the importance of exact monitored data for the calibration of the different input parameters. No detailed study of the parameter calibration and other modelling aspects will be presented herein.

The 2011 rockfall was back-analysed by the ROFMOD model (GEOTEST AG, 2006), which is a two-dimensional physically based model originally developed by Zinggeler et al. (1991) and subsequently improved by GEOTEST AG. The model inputs contain a longitudinal profile, the exact boulder size, which is defined by both the length of its three major axes and the degree of roundness, and the ground parameters related to damping and surface roughness. The output data of ROFMOD include bounce height, energy values, velocity and travel distance.

While the boulder size and the trajectory of the 2011 rockfall were fixed using the field data, modelling focussed on the calibration of the ground parameters using, on one side, the maximum runout observed in the field and, on the other side, the velocity estimates obtained from monitoring. In addition, the simulated bounce heights of the boulder were compared with the video information. Figure 47 shows the simulation results obtained using the best-fit model parameters: a damping value of 15 and a surface roughness value of 2. The simulated runout distance, velocity and bounce height of the rockfall coincide rather well with the data gathered in the field and recorded by the monitoring system. The difference between the simulated and monitored boulder velocity may be attributed to the drawback of the two-dimensional model. A two-dimensional model is not able to incorporate the energy loss due to the impact of a boulder on a sub-vertical wall at a deflection point (see impacts points in Figure 40). This effect could only be included by the application of a three-dimensional model (Agliardi and Crosta, 2003).
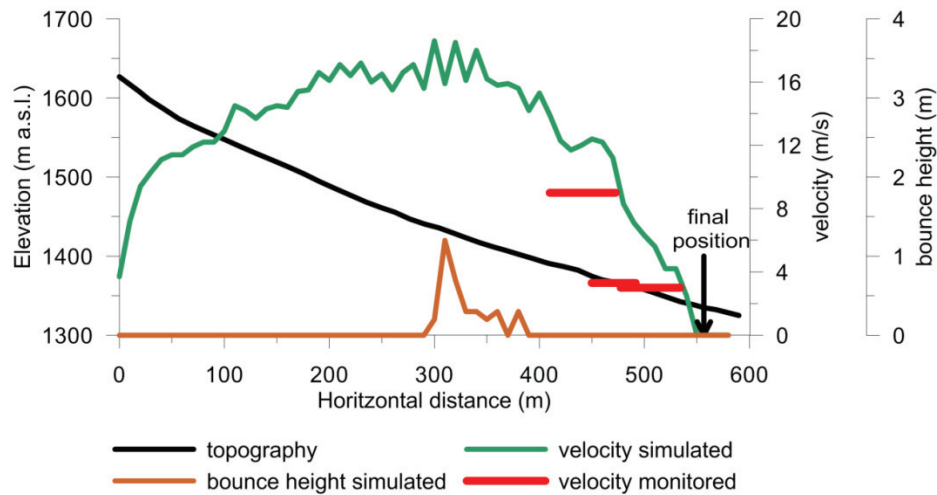
Figure 47: Back-analysis of the 2011 rockfall indicating simulated velocity and bounce height. Velocity estimates obtained from the sensors are also illustrated.

5.4.   Discussion and conclusions

The data gathered on the two rockfalls represent unique and interesting information. Subsequently, three general topics will be briefly outlined: 1) the instability processes in glacial deposits; 2) the dynamic behaviour and back-analysis of the 2011 rockfall, and 3) the implications for debris-flow monitoring and alarm systems.

Boulders detached from a lateral moraine represent one of the manifold instability processes that can affect the mountain slopes debuttressed due to the past, recent and ongoing recession of glaciers. The meteorological data show that the rockfall initiations in the moraine scarp cannot be directly associated with important rainfall amounts, since the 2010 event occurred with insignificant precipitation and the 2011 event without any precipitation. However, there might be an influence of antecedent precipitation. In contrast, the 2010 rockfall may be related with the freezing-thawing effect, because the temperature preceding the event was around 0 ºC. Although no detailed analysis of the detachment mechanisms was carried out, the present study suggests that there is a complex combination of different geomorphic processes affecting the stability of glacial deposits. These processes may include 1) freezing and thawing; 2) snowfall and snowmelt, and 3) water infiltration, subsurface flow and water outflow or seepage among others.

The data recorded by the monitoring system also provided essential information on the dynamic behaviour of the boulder rolling and bouncing down the channel. Because the

[109]

calibration of input parameters for rockfall simulations commonly focuses only on field observations, the monitored data providing velocity estimates and bounce heights are unique information. The back-analysis of the 2011 rockfall showed that the simulated velocity and bounce heights coincide rather well with the recorded data. However, the results obtained from the two-dimensional rockfall simulation indicated that a sophisticated three-dimensional model may be necessary to improve the incorporation of energy loss due to the impacts of the boulder on the lateral sub-vertical walls along the zigzag rockfall trajectory.

The results of the present study also reveal useful information on debris-flow monitoring and alarm systems in mountainous torrents. The possibility of rockfalls must especially be taken into account in the design and running of debris-flow alarm systems. Rockfalls can trigger false alarms, because they do not necessarily reach the elements at risk endangered by debris flows, which usually show a much longer runout. The separation between rockfall and debris flow should not cause problems, because the first process generates short and high-intensity records of ground vibration, while the second process produces longer and less intense records. Finally, another aspect to be considered is the fact that rockfalls can damage or even destroy the monitoring and alarm system.

Part II: Geomorphologic characterization

6. Estimate of debris-flow entrainment using field and topographical information

6.1. Introduction

Debris flows are fast mass movements, formed by a mix of water and solid materials, which mostly occur in steep torrents. They represent a major risk for human settlements and infrastructures in mountainous areas. The basal entrainment of channel-bed material is a common feature of debris flows. Debris-flow torrents often consist of colluvium and other types of coarse sediment, which can be partially or totally incorporated into the flowing mass (Hungr et al., 2005; Pierson and Scott, 1985). The entrainment of loose and unconsolidated material along the flow path affects fundamental parameters used for debris-flow hazard assessment, since it directly influences the volume and flow dynamics (Iverson et al., 2011; Mangeney et al., 2010).

The total volume of the debris-flow can be considerably enlarged due to the entrainment (Berger et al., 2011; Guthrie et al., 2009; Hungr et al., 2005). For example, the well-documented Glyssibach event (2005) in the Swiss Alps involved a total volume of 80000 m^3, from which 50000 m^3 were related to the entrainment (Scheidl et al., 2008). Furthermore, recent topographic data revealed that the material entrained along

the flow path reached up to 92% of the total volume of the event (Theule et al., 2012). For this reason, it is a key question to predict the potential volume that can be entrained along the flow path. However, debris-flow entrainment is a complex phenomenon and there are still many uncertainties remaining in the definition of the process. While case studies on individual events are available in literature (e.g.Scheidl et al., 2008), only a few studies present results on entrainment obtained from large, regional datasets (Fannin and Rollerson, 1993; Gertsch, 2009; Hungr et al., 2005).

The main goals of this research are twofold: First, data of entrainment from recent debris-flow events are analysed in order to determine the governing factors of this process. Second, an approach to estimate the amount of material, which can be entrained from the channel bed along the flow path, is developed. This approach should be easy to apply. In addition, a minor goal consists of a review of published approaches to estimate the total volume of debris flows and the associated entrainment.

The first part of the paper provides the review of available approaches on total volume and entrainment estimate. Then, the database and the governing factors of the study are described. After that, a simple statistical analysis of the governing factors, and a data mining analysis using two different techniques are presented. Finally, a comparison of one of the techniques with other methods is shown and the definition of our final approach is given.

6.2. Approaches to estimate debris-flow entrainment and total event volume

There are various methodologies to estimate the volume that can be involved in a debris flow event. Below a review of approaches is presented, which are divided into four types: 1) empirical, 2) hydrograph-based ones, 3) field or geomorphological methods; and, 4) physically-based formulae. The main part of this review focuses on estimating the material potentially movable regardless of the hydraulic conditions, as this is the objective of this paper.

The empirical methods consist of simple equations, usually based on few parameters. These equations are normally used to estimate the total volume of the event (Table 10). VanDine (1985) observed a positive correlation between the catchment area and the debris-flow volume. Analogously, some authors described approaches to estimate the debris-flow volume as a function of the catchment area only: Marchi and D'Agostino

(2004), Zeller (1985), Dong, et al. (2009), Franzi and Bianco (2001) and Takei (1984). Other authors included one or two additional parameters. For instance Kronfellner-Kraus (1985) described some estimates of the total debris-flow volume based on the catchment area, the torrent slope and an adimensional factor of torrentiality (K). Three values were defined for this torrentiality factor for specific areas of the Austrian Alps. The factor is based on several aspects of the geology, geomorphology, climatology, etc. In a similar way D'Agostino (1996) and, and suggested other expressions to estimate the total event volume based on alike factors. Rickenmann (1995) developed a similar expression but based on the runout distance instead of the catchment area. These approaches are defined to be applied at entire torrent scale, without considering local changes in torrent characteristics.

The second type of approach is the hydrograph-based one. The estimation of the total volume in this case is based on the runoff hydrograph, which is calculated by a hydrological model such as HEC-HMS or others (Gregoretti and Fontana, (2008). The clear water hydrograph is then transformed into a debris-flow hydrograph including a sediment concentration by physical or empirical formulae. Finally, the volume eroded or deposited can be considered (e.g. Degetto et al., 2011) or neglected (e.g. Gostner et al., 2003).

The so-called field methods consist of geomorphological descriptions of the torrents to identify, and quantify in some occasions, the potential sediment sources (Table 11). On one hand, the potential erosion volume can be estimated from the general characteristics of the torrent. Fannin and Rollerson (1993), for instance, developed a methodology based on a database of 449 torrents from British Columbia (Canada), which were grouped into seven different types according to similar characteristics. For each type of torrent, an average yield rate was derived from the geometric mean of the entrainment defined for each torrent of the database. On the other hand, some authors establish their methodologies on torrent reaches. Firstly, Hungr et al. (1984) described five different types of torrent reaches depending on the geomorphological and geological characteristics. An estimated yield rate is designed for each type of reach. Secondly, Spreafico et al. (1999) suggested dividing the channel into reaches with an erodible layer of similar thickness in the channel bed and potential failures of lateral slopes. The equation of Table 11 only focuses on channel bed erosion, without including the part of large channel banks failures.

[115]

Table 10: Summary of empirical formulae for the estimate of the total debris-flow volume.

Authors	Equation	Area of Study
Marchi and D'Agostino (2004)	$V = 70000A$ (upper limit) $V = 1000A^{0.3}$ (lower limit)	Eastern Italian Alps
Zeller (1985)	$V = cA^{0.78}$	Swiss Alps
Dong et al. (2009)	$V_{out} = 7273A^{0.582}$	Central Western Taiwan
Franzi and Bianco (2001)	$V = 8959A^{0.765}$	French, Swiss and Italian Alps
Takei (1984)	$V = 13600A^{0.61}$	Japan
Kronfellner-Kraus (1985)	$V = KA\theta$	Austrian Alps
Rickenmann (1995)	• $\theta_f < 15\%$ $V = (6.4\theta_f - 23)L$ • $15\% < \theta_f < 40\%$ $V = (110 - 2.5\theta_f)L$	Swiss Alps
D'Agostino (1996)	$V = 45A^{0.9}\theta^{1.5}(I.G.)$	Eastern Trentino (Italy)

V(m3): total volume of the event ; K (-): torrentially factor; A (km2): catchment area; θ (%): mean slope of the channel; c (-): constant; θ$_f$ (%): mean slope of the fan; L (m): runout distance; I.G. (-): geological index

A more complex approach was defined by Fannin and Wise (2001). The governing factors of the model are: flow behaviour, which depends on the channel shape; slope and path azimuth. The model determines the volume eroded or deposited in a certain reach depending on the channel properties. The computation is based on an equation obtained by regression analysis. This model requires information on the debris flow path and the deposit to define the reaches, which makes it more appropriate to be used for backanalysis than for prediction purposes.

The fourth type includes the approaches based on physics. The physics of the entrainment process still include many uncertainties and most of the existing approaches are based on experiments performed in the laboratory (Egashira et al., 2001; Papa et al., 2004; Rickenmann et al., 2003) or in a large outdoor flume (Iverson et al., 2011). Others are based on data registered in monitored catchments or on monitoring. The understanding of entrainment is fundamental for numerical modelling,

but only some of the codes available for the debris-flow simulation have the option to incorporate this aspect (e.g. FlatModel (Medina et al., 2008) or RAMMS (Bartelt et al., 2012)).

Table 11: Summary of field or geomorphological approaches to predict the total volume of a debris flow.

Authors	Working scale	number of classes	Governing factors to define class	Equation	Study area
Fannin and Rollerson (1993)	T	7	• slope morphology • initiation mechanism • shape of channel section • deposition patterns inside the channel	$V = Le_{torrent}$	Queen Charlotte Islands (BC, CA)
Hungr et al. (1984)	TR	5	• slope • bed material • erodibility of side slopes • stability condition	$V = \sum_{i=1}^{n} a_i^{\frac{1}{2}} L_i e_i$	southern coast ranges (BC,CA)
Spreafico et al. (1999)	R	nd	nd	$V = \sum_{i=1}^{n} L_i b_i \, d_i k$	Swiss Alps

T: torrent; TR: torrent reach; e_i (m3/(m·km2)): yield rate of reach i; $e_{torrent}$ (m3/m·): mean yield rate of torrent; a_i (km2): drainage area of reach i; L_i (m): length of reach i; n: total number of torrent reaches; b_i (m): mean torrent section width of reach i; d_i (m): mean erosion depth of reach i; k (-): reduction factor; nd: no data

There are mainly two approaches to physically describe the entrainment mechanism: the static approaches and the hydrodynamic approaches. In the first case, the incorporation of material into the flowing mass can be explained by the failure of the channel bed material. The failure is produced by undrained loading during the passage of the debris-flow mass (Hutchinson and Bhandari, 1971). The volume of material

involved in the failure depends on the depth of sediment and the relation between the undrained loading and the resistant forces of the channel bed, according to simple equilibrium methods, such as Mohr-Coulomb. The second case is based on the bedload transport formulae of fluvial hydraulics. In this case, the particles on the channel bed are accelerated to the velocity of the flow when the flowing mass generates a shear stress higher than the resistant shear stress (Egashira et al., 2001; Iverson et al., 2011; Quan Luna et al., 2012; Rickenmann, 1990; Smart and Jäggi, 1983; Takahashi et al., 1992).

As it can be seen by the previous review, the estimation of the debris-flow material is a complex process, especially the entrainment of material along the debris-flow path. The estimation of the potential volume to be entrained has been solved, up to now, by simple empirical expressions, extensive field surveys or equations that define the physics of the process according specific hypotheses. However, there are some drawbacks and limitations to the use of these technics. On the one hand, the empirical techniques are rather simple, but may include a large error. On the other hand, the physical approaches strongly depend on the uncertainties related to input parameters.

Besides the suitability of the different types of approaches, many uncertainties still remain with regards to the conditioning factors of the entrainment. Some authors have tried to find correlations between some geomorphological parameters (such as slope or drainage area) and the erosion occurred in certain torrents, but the results show high dispersion (Hungr et al., 2005).

6.3.   Study regions and database

Entrainment data on 17 granular debris flows (Coussot and Meunier, 1996) were collected in this study. Data collection was carried out during field surveys and was complemented using a geographic information system (GIS). The surveyed debris-flow torrents are located in the Pyrenees and the European Alps (Figure 48). The events selected for this study are constituted by reaches with a wide range of erosion rates. Therefore, the database includes a large variety of governing factors and erosion. The database contains events initiated both by a landslide and by runoff, and the final volumes range from hundreds of cubic meters to tens of thousands (Table 12). These final volumes of the events were estimated from our field data or taken from technical reports (Marquis, 2006; Marquis, 2008; Oller and Pinyol, 2009; Pinyol, 2008). The field

surveys were mostly carried out days or weeks after the events. Only in a few cases the data collection took place after a longer period of time.

Figure 48: Location of the surveyed debris-flow torrents in the Pyrenees (a) and European Alps (b). All the torrents used in this study (training set, validation set and test set) are shown.

The estimates of erosion rates were based on the field observations of erosion evidences and reconstruction of the sediment disposition before the event (Figure 49). For some reaches an airborne LIDAR digital elevation model was available. Finally, for each event, two types of input data were incorporated into the database: 1) field observations, and 2) morphometric data derived from digital elevation models (DEM) with pixel size ranging from 1 to 5 m.
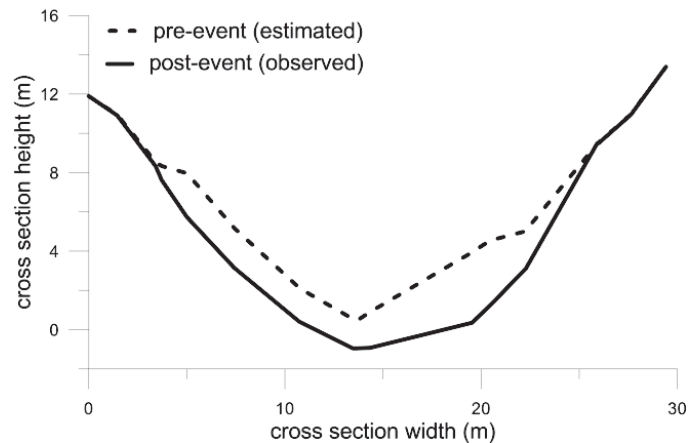
Figure 49: Sketch of the cross-section of a channel reach indicating how erosion was estimated.

The Central-Eastern sector of the Pyrenean mountain range limits the Spanish autonomy of Catalonia from France and also includes the Principality of Andorra. The highest peaks show altitudes slightly over 3000 m a.s.l. and are located in the Central Pyrenees. From a geological point of view, the bedrock of the Axial Pyrenees mainly consists of a basement of igneous and metamorphic Paleozoic rocks folded, intruded and metamorphosed during the Hercynian orogeny(Muñoz, 1992). The southern outer part of the range, coinciding with the Pre-Pyrenees, is composed of sedimentary sequences mostly of Mesozoic ages. The superficial deposits predominantly consist of colluvium with a maximum thickness of a few meters. All the events occurred during a short period of time and high intensity rainfall episodes related to convective summer storms.

Four debris flows occurring in the European Alps (A) were analysed (Table 12). The European Alps cross Western Europe along ~1200 km and include many peaks over 4000 m.a.s.l. (the maximum elevation is 4810 m). In short, they comprise different nappes (Pennine, Helvetic and Austroalpine) of sedimentary to metamorphic rocks and a crystalline basement. The three Swiss events are located in areas where the Helvetic nappe, and partially the crystalline basement crop out, while the Austrian event is situated in the National Park 'Gesäuse' within the northern limestone Alps. All events occurred during the summer and were triggered by convective storms with high rainfall intensities.

Table 12: Main characteristics of the debris flows included in the database.

Name	Date of the event (mm/yyyy)	Estimated[1] V (m^3)	Catchment area (km^2)	Averaged erosion rate (m^3/m)	Mean channel slope (°)	n° of reaches	Initiation mechanism	Area of study
Varradòs	11/2011	~1500	0.2	1.5	35	7	R	AP
Sant Nicolau	05/2008	1800	0.7	0.87	19	4	L	AP
Llebreta	~2000	2350	0.03	0.56	22.5	4	L	AP
Port Ainé	09/2008	26000	5.6	2.12	15	8	R	AP
Reguerals	08/2009	1500	4.4	1.12	21.5	2	R	AP
Riu Runer	08/2008	14000	8.2	1.85	14	13	R	AP
Fontanals	08/2008	1500	0.4	1.37	31	6	R	AP
Setcases	08/2010	~800	0.9	0.25	27	2	R	AP
Montaup	07/2010	900	5.3	0.55	17	10	R	AP
Vilacireres	11/1982	11000	0.2	3	22.5	1	L	PP
Ensija	2006	1500	0.7	2.12	19.2	6	R	PP
Tagast	11/1982	5000	0.5	2.83	12.5	3	L	PP
Torrent de la Molina	~2011	12000-16000	0.8	3.74	17.1	18	L	AP
Torrent des Glariers	07/2006	4000-5000	1.3	1.37	33.5	4	R	EA
Torrent Sec	06/2008	20000	1.4	1.89	33	10	R	EA
Schipfenbach	08/2000	5000	1.4	2.1	45	7	R	EA
Gesäuse	2009	1200	0.01	2.8	32.5	5	R	EA

R: Runoff; L: Landslide; AP: Axial Pyrenees, PP: Pre-Pyrenees, EA: European Alps

6.4. Definition of governing factors

The 17 torrents were divided into reaches according to similar geomorphological features and erosion rates. Thus, the final database contains 110 reaches of debris-

flow torrents. The length of the reaches ranges from tenths of meters to more than one thousand meters.

In every reach, different geomorphological patterns were determined, herein called governing factors. Four governing factors were selected for each reach i: 1) reach-averaged slope (S_i), 2) sediment availability (SA_i), 3) cross-section shape (CS_i), and 4) upstream contributing area (UCA_i). These factors can be divided into two groups depending on the collecting method: 1) three field factors (S_i, SA_i, CS_i), and 2) one topographical factor (UCA_i). The factors can also be distinguished between numerical (S_i, UCA_i); and categorical ones (SA_i, CS_i). The choice of these factors was based on: 1) the simplicity of their collection, 2) field observations that proof their influence on the entrainment process (regarding the field governing factors) and 3) experiences obtained from previous studies (e.g.Hungr et al., 2005).

6.4.1. Field factors

a) Reach-averaged slope

The reach-averaged slope of a specific reach (S_i) is a numerical factor measured in degrees. In our work the slope of the reaches was measured in the field using a standard clinometer: one single measurement for short reaches (few tens of meters) and several ones for longer reaches, which are then averaged to obtain the reach-averaged slope. The slope of the longest reaches was compared to the one provided by the DEM. This comparison showed that the values obtained from both methods were similar.

Some authors studied the relation between the erosion rate and the slope of the torrent reaches or of individual points in the channel. In some cases the relation shows that the slope increases, as the entrainment rate enlarges (Guthrie et al., 2009; Rickenmann and Zimmermann, 1993). This result would stress the importance of the slope on the entrainment process. In other circumstances, however, it has been observed that there is a feedback effect, which means that the entrainment is higher at low slopes. The justification of this effect was the increasing flow concentration or peak discharge with longer distances, which is normally associated with slope decreases (Breien et al., 2008). Other studies contradict these two cases indicating that there is no clear trend, as the erosion rate is completely related to the availability of sediment in the reach (Hungr et al., 1984; Marchi et al., 2009).

b) Sediment availability

The sediment availability in reach i (SA_i) is a categorical factor. According to our observations in the field, it is one of the most influencing factors in the entrainment during a debris flow. In some torrents, reaches may show unlimited sediment (here called "unlimited" reaches). Thus, the erosion produced is totally conditioned by other factors. While in other reaches, the lack of sediment limits the entrainment.

In this work five classes were described depending on how much material is available in the torrent reach channel. The distinction of classes is based on the percentage of the cross-section that is covered by a certain thickness of sediment (Table 13).

a) Cross-section shape

The reach cross-section shape (CS_i) is a categorical factor that was considered to illustrate the degree of incision of the reach, despite no relationships between the shape of the torrent and the erosion rate were established in previous works.

In order to determine the shape of the cross-section the concept proposed by Gabet and Bookter (2008), who studied the shape of some gullies in southwest Montana (USA) based on a shape index, was adapted. The width was established at a certain height above the thalweg, being the relevant dimension to describe the reach incision. The height was chosen with expert criteria, as an estimate of the flow depth that achieved the debris flow in the specific reach. In order to simplify field work and subsequent data analysis, the cross-section shape factor was divided into the three classes "wide", "moderately incised" and "incised" instead of using the exact width (Table 14). The class limits were established based on the observation during the field surveys in the torrents.

Table 13: Sediment availability classes.
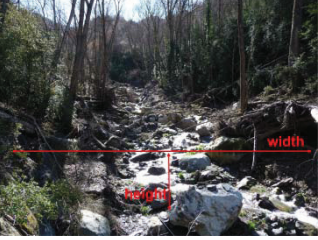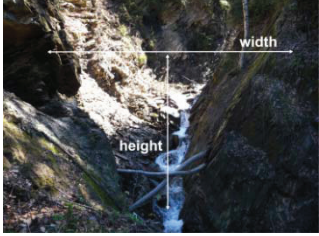
Class		Image	% of bedrock at cross section	% of colluvium at cross section	thickness of colluvium layer (m)
Complete limitation	(CL)		> ~90	< ~10	< ~0.5
High limitation	(HL)		> ~75	< ~25	< ~1
Medium limitation	(ML)		~50	~50	~1
Low limitation	(LL)		< ~25	> ~75	>~1
No limitation	(NL)		< ~10	> ~90	>~1

Table 14: Cross-section shape classes. (W: width and H: height)

Class	Wide	Moderately incised	Incised
Image			
Characteristics	W > 5H	2H < W ≤ 5H	W ≤ 2H

6.4.2. Topographic factor

a) Upstream contributing area

The reach upstream contributing area (UCA$_i$) is a numerical factor that can easily be determined in a GIS. It is calculated as the sum of map units (pixels) that drain water and other substances to the lowest point of a reach. The sum value of the pixels is obtained by means of the Flow Accumulation tool found in ArcGIS® (ESRI, 2005), using a DEM.

The upstream contributing area is applied in this work to illustrate the differences of discharge and sediment transport between reaches. For example, a debris flow can initiate with similar concentration as a hyperconcentrated flow in the upper reaches of the torrent (smaller upstream contributing area) and be totally developed to a mature debris flow lower at the fan apex, where the upstream contributing areas are larger.

6.5. Data mining

Data mining is the process of discovering patterns, sometimes hidden, in a database (Fayyad et al., 1996). In this work, the objective was to develop a methodology to predict an estimation of the erosion rates that can be produced by debris flows in a torrent reach.

[125]

Firstly, the general patterns were analysed for each variable, both the governing factors (S_i, CS_i, SA_i, UCA_i) and the target variable (e_i). The analysis was performed by means of histograms and correlations between variables for the entire database of 110 reaches. Secondly, data mining was carried out. It was done by means of two different learning techniques: a multiple linear regression analysis and the construction of a decision tree. The algorithms of both learning techniques were applied to a training set (93 reaches from the database). Two resulting models were obtained as a consequence of these learning processes: a formula obtained by the multiple linear regression (MLR) and a decision tree (DT). Then, the success of both models was evaluated. On one side, the comparison between the two learning techniques was done by means of a validation set (10 reaches from the database, representative for the whole dataset and randomly selected). On the other side, a test was realized in an extra torrent (7 reaches from the database), where also empirical methods were applied.

The basis of the two data mining learning techniques applied in this study and the parameters used for the evaluation of the success are presented in the following two sections.

6.5.1. Multiple linear regression

The multiple linear regression is a learning technique, whose intent is to find out the best linear relationship between the erosion rate in a particular reach (e_i) and the governing factors using the following expression:

$$e_i = a_1 S_i + a_2 SA_i + a_3 CS_i + a_4 UCA_i + b$$

<div align="right">**Equation 7**</div>

The coefficients a_1, a_2, a_3, a_4, and b are determined by minimizing the sum of the squared errors originated by the approximation of the erosion rate in every reach of the dataset. A numerical value was attributed to the categorical factors (CS and SA). For example: a "wide cross-section shape" is represented by 1, a "medium cross-section shape" by 2 and a "incised cross-section shape" by 3. The same was done with the SA, although numbers range from 1 (complete limitation of sediment) to 5 (no limitation of sediment). Therefore, the resulting erosion rate is a numerical value.

Previously to the application of the multiple linear regression to the training set, the distribution of the variables should be taken into account. If some of the variables in the dataset present a distribution far from normal, it is common to perform a transformation

of the dataset. By transforming the data, a normal distribution of the values of a certain variable can be achieved (Gartner et al., 2008).

6.5.2. Decision tree

Decision trees are a family of learning techniques that have been used by several authors in the field of natural hazards (Chevalier et al., 2013; Wan and Chiang Lei, 2009). Decision trees allow using categorical values directly. They are based on two main elements: nodes and leafs. At each node an attribute (governing factors) is tested. The procedure consists in comparing the attribute with a certain value (in numerical attributes) or choosing a specific category (in categorical attributes). At a certain level of the tree a leaf is reached, which means that a final category of the target variable is achieved.

To create the decision tree, we used the data mining software WEKA (Hall et al., 2009). WEKA incorporates a total of 77 algorithms of learning techniques, from which 16 are decision trees. Many of them were tested, achieving the best results in the J48 decision tree. The algorithms of the decision trees are not discussed herein but are explained in Breiman et al. (1984) .That is why herein only results from decision tree J48 are presented. We selected a 10-fold cross-validation method to optimize the tree.

The decision tree learning process can present problems, if the target variable is not equally distributed. For this reason, the cost matrixes are a common strategy in the definition of decision trees in imbalanced datasets (Witten et al., 2011).They are implemented as a metaclassifier during the learning process to force that all of the target classes appear in the tree. The matrix components provide a cost value for each class that would be misclassified into another class. Another problem in the definition of decision trees is the overfitting, which creates extremely complex trees. One of the strategies to avoid overfitting is pruning (Witten et al., 2011). The pruning parameters are set in the classifier, and affect the size of the tree and its complexity.

6.5.3. Validation and test of models

The evaluation of the success of the models was structured in two parts. Firstly, the two learning processes were assessed by comparing which of them fits better the validation set. Secondly, both models were implemented in a torrent where the final volume of the event is known. In this part, a comparison between the models (MLR and DT) and two existing empirical formulae was carried out.

The first part (validation) consists in evaluating the success of the models obtained by the learning techniques. The success of different predicting models is usually based on the receiver operating characteristics, also called ROC-analysis (Fawcett, 2006). Common parameters used for ROC-analysis are the True Positive Rate (TPR) and the False Positive Rate (FPR). Typically the values of the TPR and FPR are plotted in a ROC graph. Then, the values are compared to the diagonal line (y=x), in case the predicted variable has two classes.

Since our predicted variable (the erosion rate) has more than two classes, the ROC analysis and Precision-Recall curves become more complicated. Thus, the ROC-space is n-dimensional, being n the number of classes of the variable. The visualization in the bi-dimensional ROC space is also impossible. Thus, we used the F-measure parameter to test the performance of the models for each class of entrainment. This F-measure parameter can be expressed by:

$$F = \frac{2 \cdot precision \cdot recall}{(precision + recall)} \qquad \textbf{(Equation 8)}$$

This expression combines the precision (true positives over total positives) and the recall (true positives over the sum of true positives and false negatives) of each class. This is the weighted harmonic mean of these two parameters (Hripcsak and Rothschild, 2005). The comparison of the F-measure for each entrainment class illustrates, whether a model is especially advantageous for a certain entrainment class. This could be meaningful in case the class is especially representative in the database.

The second part (test) consists in applying the models to a torrent from the database that was not used neither in the training nor the validation processes. The Schipfenbach torrent (Fig 1b; Table III), which includes 7 reaches, was selected as test set because of its variability in the governing factors and the erosion rates. Both the two learning techniques and two simple empirical methods (Rickenmann, 1995) and (D'Agostino, 1996) (see Table I) were applied, to the Schipfenbach torrent in order to compare the results of each methodology to estimate the final volume of material entrained. The observed total volume of entrainment along the torrent is known from field observation after the event (Hürlimann et al., 2003b). For the decision tree, two different volumes were computed taking into account the minimum and maximum values of the erosion rate classes for all the reaches.

6.6. Results

6.6.1. Statistical distribution of the governing factors

The database contains a total number of 110 torrent reaches located in the Pyrenees (84) and the European Alps (19). Cumulated frequency graphs of the numerical variables and histograms of the four governing factors and the target variable are shown in Figure 50. In the same Figure 50 the histograms of the reaches in the test set are also shown.
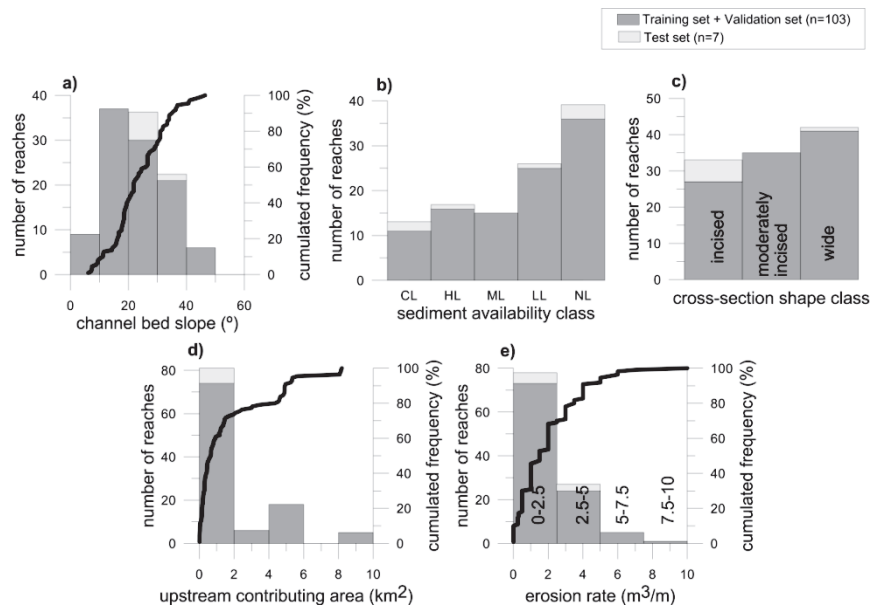
Figure 50: Histograms of the 4 governing factors (a, b, c, d) and the erosion rate (e) for the 110 reaches included in the database. The cumulated frequency is shown for the numerical governing factors (a, d) and erosion rate (e). See Table IV for abbreviations of SA classes.

The histogram of the reach-averaged slope distribution (Figure 50a) presents a peak in the slope bin of 10º to 20º. The most frequent values of the reach-averaged slope are between 10º and 40º, with a mean value of 23º and a standard deviation of 9º. Steeper (>40º) and smoother (<10º) reaches are of low frequency in our dataset, ~6% and ~8% respectively. These results fit other published works, in which channel slopes showing erosion range from 18º to 27º (Marchi and D'Agostino, 2004), or are higher than 15º (Hungr et al., 2005).

Almost 40% of the reaches in the database are unlimited (NL) in terms of sediment availability (Figure 50b) and more than half of the reaches have NL or LL. The cross-section shape distribution revealed that incised reaches are the most common ones in our database (Figure 50c).

[129]

The upstream contributing area of the reaches in the database takes values up to 8.2 km^2 (Figure 50d). This value and the total drainage areas (See Table III) support the hypothesis that a small catchment area is a typical feature for debris-flow occurrence (e.g.Rickenmann and Zimmermann, 1993). The histogram shape is strongly skewed to the left, and almost 60% of the reaches have an upstream contributing area lower than 1 km^2.

The erosion rate cumulated frequency graph shows a gradual increase: sharper for the lower values of the erosion rate and rising slowly for the higher ones (Figure 50f). The prevalence of low erosion rates (of less than 2.5 m^3/m) is also illustrated in the histogram. Although high erosion rates were reported in some reaches, the values reported in our database are similar to the lower classes of erosion rates from similar studies, such as Hungr et al. (1984). This can be justified by the exclusion of lateral bank failures and the glacial geological context of Hungr's work.

In order to identify possible relations between governing factors and the target variable or among themselves, many governing factors plots were visualized. Most of the plots show high dispersion. However, few general trends could be identified. Although the graph that correlates the reach-averaged slope vs. erosion rate shows high scatter, note that there is a general linear increasing trend between the slope and the erosion rate for the less limited sediment classes (NL and LL,Figure 51). In the case of more limited sediment classes, the trend cannot be observed. Figure 51b includes the influence of the cross-section shape. Although no clear trends visible, it seems that higher erosion rates occur preferably in incised reaches than in moderately incised or wide reaches.
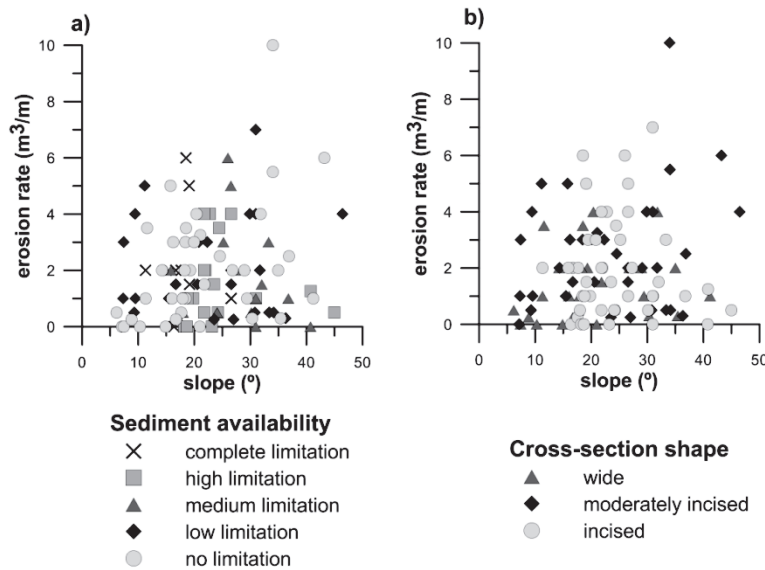
Figure 51: Relations between slope and erosion rate depending on sediment availability (a) and channel cross-section shape (b) for the 92 reaches of the database.

6.6.2. Multiple linear regression

The histograms of previous section show that some variables present a distribution far from normal, particularly skewed to one side: upstream area, erosion rate, sediment availability or cross-section shape. As mentioned above, a transformation of the values of these variables could help to get better results in the learning process. Only two of these variables are numerical, and therefore a transformation of the values could be applied to their values: erosion rate and upstream area. We performed two different types of modifications on these variables in order to transform them in normal-distributed variables. We carried out a log-transformation and ln-transformation. Moreover, to ensure the importance of each of the variables in the analysis, we carried out a step-by-step MLR analysis. In each step we added a new variable. Therefore, we can ensure that adding variables increases the success of the methodology.

The results of the MLR applied to the original training set (without transformation of area upstream and erosion) and the transformed training sets are shown in Table 15a. Two parameters were chosen to compare the three attempts: the R^2 and the standard error. The models with highest R^2 value and lowest standard error are the ones with best performance. Thus, when the erosion rate and the area upstream are log-transformed, best results are obtained. The purpose of the second part of the analysis was to verify if accuracy depends on the quantity of governing factors included in the

MLR. The results confirm that the best performance is achieved when using all the parameters Table 15b).

Therefore, the final equation obtained by the multiple linear regression is a first order polynomial expression of 5 variables and can be expressed by:

$$\log(e_i + 1) = 0.007S_i + 0.102SA_i - 0.066CS_i + 0.053\log(UCA_i + 1) - 0.312$$

(Equation 9)

The maximum weight (higher coefficient) of the linear regression corresponds to the sediment availability of the reach; followed by the cross-section shape and upstream contributing area, and finally by the slope.

6.6.3. Decision tree

The resulting tree applying the J48 algorithm to the training set is shown in Figure 52. The predicted erosion rate was divided into four classes with an interval of 2.5 m^3/m (the same classes as the ones shown in the histogram in Figure 50e). The interval of 2.5 m^3/m is considered to be a reasonable resolution of an erosion rate class for our database and the classification of this parameter to be favourable to the simplicity of the methodology.

On the one hand, with the intention to avoid the problems derived from the imbalance of the erosion rate distribution, a cost matrix was used. The cost matrix was defined in order to force that the four classes of the erosion rate appear in the final decision tree. It was done by means of attributing higher costs to the misclassification of reaches with larger erosion rates (less present in the database). On the other hand, after several attempts, the pruning was set by a confidence factor of 0.25. This confidence factor provided a decision tree with a maximum of three levels, which was acceptable according the aim of defining a simple model.

The first split of the tree is on the sediment availability, and the branches with fewer availability of sediment (CL and HL) already reach the final leaf, which correspond to the lower erosion rate classes. The branches with more sediment available (ML, LL and NL) need one or two additional levels to reach the leaf with the value of the erosion rate.

The shape is the second factor appearing in two of the classes of sediment availability, while the slope exists in one. In the following level of the tree, the slope or the upstream contributing area are located. In general, the dominant class in the decision tree is the lowest erosion rate class: "0≤e_i≤2.5 m^3/m", appearing in half of the leafs of

the decision tree. The maximum erosion classes only appear in reaches with unlimited sediment availability, in steep reaches (<32º).
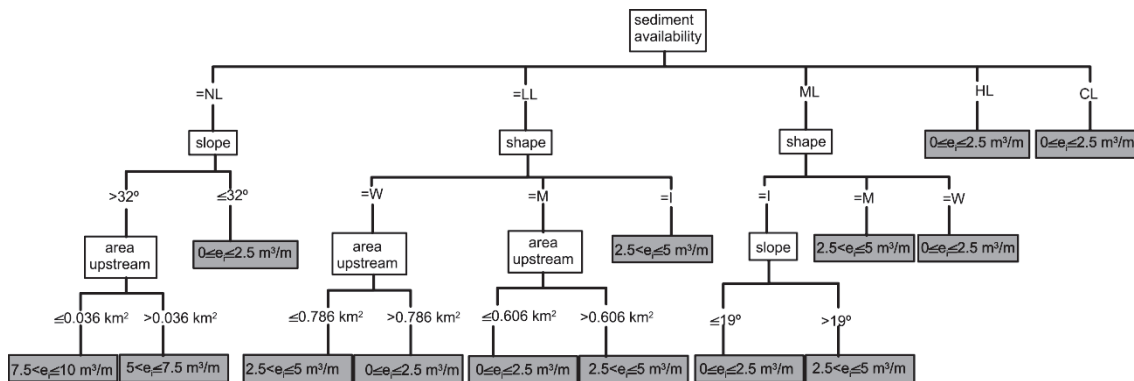
Figure 52: Decision tree for entrainment estimate using the training set of our database applying the algorithm J48.

Table 15: Results from multiple linear regression analysis: a) different attempts with different data-transformations; b) step-by-step analysis of the different parameters (log-transformed values of upstream contributing area and erosion)

a)

Attempt	Training dataset	R^2	Standard Error
1	Data not transformed	0.27	1.61
2	E and UCA log-transformed	0.3	0.22
3	E and UCA ln-transformed	0.3	0.5

b)

Step	Governing factors in dataset	R^2	Standard Error
1	SA	0.19	0.23
2	SA and CS	0.25	0.22
3	SA, CS and S	0.3	0.22
4	SA, CS, S and UCA	0.31	0.22

SA: Sediment availability; CS: Cross-section shape; S: Slope, UCA: Upstream Contributing area; E: Erosion

6.6.4. Validation and test of models

The validation of the two models was based on the F-measure parameter, as mentioned in previous sections. The F-measure was obtained for each of the classes of the erosion rate, both in the training set and the validation set. The values in Table 16 show that both techniques show good performance in the lowest class of erosion rate (up to 2.5 m^3/m) in both training set and test set. This is a reasonable result, as this is the most frequent erosion rate class. However, for the larger erosion rate classes, MLR does not offer good results. Thus, the weighted average of the F-measure was calculated to get an overall evaluation. Regarding the weighted average, the decision tree learning technique showed better results, especially in the training set, but also in the validation set.

On one hand, the results show that the volumes determined by the two empirical relationships strongly overestimate the observed volume by more than one order of magnitude (Figure 53). This result can be attributed to various facts. First, empirical equations always have a large scatter, and the results can consequently have important errors. Second, the empirical techniques were developed in a specific area, and their application to other regions may generate inaccuracy. On the other hand, multiple linear regression shows the best-fit results. In contrast, the two options of the decision tree (minimum and maximum values of every erosion rate class) define an interval in which the real volume observed is included.
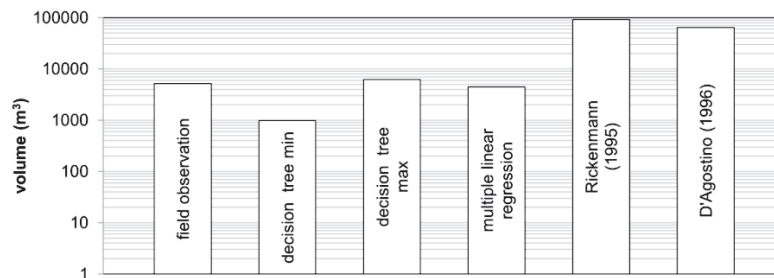
Figure 53: Comparison of the observed total volume of the debris-flow occurred in Schipfenbach with the volumes obtained by the decision tree (minimum and maximum values), multiple linear regression and empirical formulae.

6.7. New general approach to estimate entrainment

We selected the decision tree model to propose a new general approach to estimate the entrainment. Empirical formulae may be adequate for a preliminary estimate without time-consuming field work, but they present several uncertainties, as

mentioned in the review section and as observed in Figure 53. In addition, a comparison between the decision tree (DT) and multiple linear regression (MLR) showed several advantages of the DT: 1) it is simple, intuitive and logical, 2) it can be easily adaptable to other regions, and 3) it showed a better success than the MLR in terms of statistical parameters.

The new approach is based on both the tree obtained from our database and expert criteria. The resulting DT is presented in a qualitative form (Figure 54) and may be adapted by introducing specific values of the different parameters according to the characteristics of the region. Several outputs of the study are included in our general approach. Firstly, sediment availability is the most influencing factor. Second, the reaches with low sediment availability (HL, CL) directly reach the leaf of the corresponding erosion rate, independently of other factors. Thirdly, for the reaches with more sediment available (ML, LL, NL), the key factors are the slope and shape. The upstream contributing area was excluded in this final approach to simplify the decision tree, and because our results pointed out that it is a factor of minimum influence. The erosion classes were simplified into three classes in contrast to the four classes used in the datasets of our study.

Table 16: Values of the F-measure parameter for each class of the two models to predict the entrainment in the training and the validation set.

Model	Class	Training set		Vidation set	
		n (total 93)	F-measure	n (total 10)	F-measure
Multiple linear regression (MLR)	$0 \leq e_i \leq 2.5$ m^3/m	67	0.940	6	0.714
	$2.5 < e_i \leq 5$ m^3/m	17	0.117	3	0
	$5 < e_i \leq 7.5$ m^3/m	8	0	1	0
	$7.5 < e_i \leq 10$ m^3/m	1	0	0	0
	Weighted Average	**0.632**		**0.429**	
Decision tree (DT)	$0 \leq e_i \leq 2.5$ m^3/m	67	0.917	6	0.857
	$2.5 < e_i \leq 5$ m^3/m	17	0.649	3	0.8
	$5 < e_i \leq 7.5$ m^3/m	8	0.4	1	0
	$7.5 < e_i \leq 10$ m^3/m	1	0.5	0	0
	Weighted Average	**0.819**		**0.754**	

It is important to keep in mind that the decision tree was developed on a dataset that includes events volumes from thousands up to a few tens of thousands of cubic meters (see Table 12). Therefore, extreme events (hundreds of thousands or even millions of cubic meters) are not considered. Thus, results of this study are representative for medium and high-frequency debris flows that occur in the Pyrenees and Alps, but not for extreme or low-frequency events with considerably larger volumes. Last but not least, if the method would be applied to other mountainous regions, the values of both the governing factors and the erosion rates should be adapted.
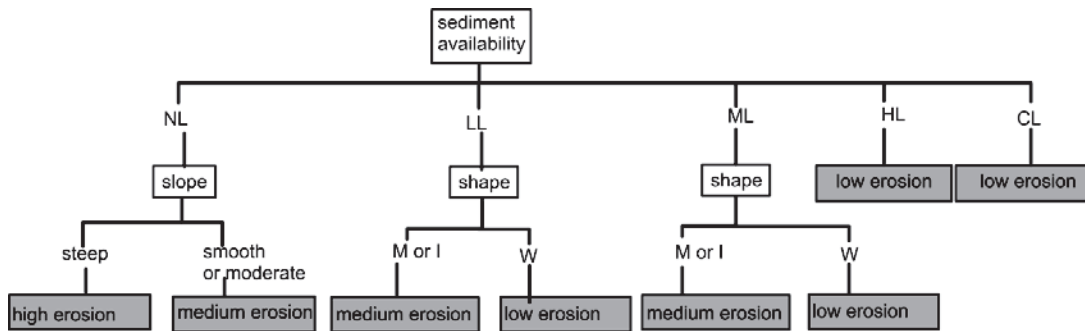
Figure 54: General decision tree proposed as a learning model to estimate the erosion rate in a torrent reach.

6.8.   Conclusions

The entrainment during a debris flow is a complex process. While empirical equations are straightforward and useful to obtain preliminary predicted values of debris-flow volume, detailed information on topographic data and field observations is necessary to determine the erosion rate more precisely.

The preliminary analysis of the field and topographic information collected in 110 channel reaches of 17 debris flows supported the outcomes of previous studies that there is no clear correlation between the erosion rate and pairs of governing factors (Chen et al., 2005; Hungr et al., 2005),

Data mining techniques were applied in order to obtain knowledge to describe a model able to predict the erosion rate in a reach. Data mining revealed that the sediment availability is the most important factor, followed by reach-averaged slope and cross-section shape. The entrainment showed better performance in the decision tree J48 than in multiple linear regression, even if the multiple linear regression revealed good results in the application to the Schipfenbach torrent.

Finally, we proposed a simple general approach to estimate erosion rate in channel reaches. The approach is based on both the decision tree obtained from our database, and expert criteria. We presented the decision tree in a qualitative way in order to make it adaptable to other regions. It has to be stated that this approach only estimates the entrainment directly related to both channel bed erosion and local failures of channel banks neglecting large failures in torrent slopes.

7. Conclusions and future research work

7.1. General conclusions

In this section, general conclusions of the work are presented referring to the three major objectives described in Chapter 1:

- Development and setting up a monitoring system in a selected catchment in the Pyrenees

- Characterization of mass movement processes occurred at the catchment during the last four years and of the corresponding triggering conditions

- Developing a simple methodology to estimate the entrainment involved in a debris-flow event

Detailed conclusions on each of the topics topics have been specified at the end of each chapter. Here, the general conclusions of the thesis are presented.

[139]

This work contributed to the development of tools and techniques used for the debris-flow hazard assessment. In addition, it also permitted to increase the knowledge on debris flows and other torrential processes in the Pyrenees, where data available was scarce.

A sophisticated debris-flow monitoring system was developed and installed, at the Rebaixader torrent (Central Pyrenees). Apart from debris flows, two other torrential processes: debris floods and rockfalls were detected by the monitoring system. The system consists of six stations equipped with ten different types of sensors (and the corresponding synchronization and transmission devices) and collects data on initiation and post-failure behaviour of the torrential processes.

The experiences gathered since the installation of the monitoring system in July 2009 demonstrate that it is a reliable tool for the detection and measuring of torrential processes. Till December 2012: six debris flows, eleven debris floods and four rockfalls have been registered. In the following, the principal outcomes of the data analysis are summarised:

- Firstly, the combination of all the sensors of the monitoring system permitted the characterization of the events. The ground vibration data provided information on several features of the events, such as detection of the flow front arrival or the different phases of the evolution along the torrent. Moreover, flow depth data also provided information on the flow front passing but was not as reliable as ground vibration data for the detection and spatial characterization. The distinction of the different processes is mostly based on the ground vibration data, but differences on the flow depth recordings have also been identified. Three types of torrential processes were distinguished: debris flows, debris floods and rockfalls.

- Secondly, special focus was driven to the analysis of the ground velocity signal and different outcomes were achieved. On one hand, although the ground vibration signal is reliable for the detection of the events and also for their characterization, the ground vibration signal is influenced by on-site factors (distance to the flow path, assembly of the sensor or underground material). These influences are crucial for the tuning of early warning and alarm systems (EWAS). It is worth noting the importance of amplificating the signal, especially if the geophones cannot be placed close to the active channel. On the other hand, the data acquisition system based on the transformation into impulses

presents several advantages among the digital standard recording, emphasized on the power consumption and data processing, but it intrinsically contains a key factor that clearly influences the final signal: the ground velocity threshold to filter the noise.

- Thirdly, it was possible to characterize the rainfalls that triggered events in the catchment. The debris-flow triggering rainfalls in the Rebaixader torrent last around 2 hours and the critical hourly rainfall amounts may be around 15 mm/h. However, it was noticed that during spring season torrential processes associated with the snowmelt can occur, and in this cases the amounts of triggering rainfall can be lower as occurred in March 2010 debris flow when only 9 mm/h were recorded. Unfortunately data available was not sufficient to establish intensity-duration (I-D) thresholds. However, two important outcomes resulted from the I-D analysis: a) the data gathered at the Rebaixader suggests a threshold that could be similar to others established in other monitored torrents, b) a distinction between spring events (affected by snowmelt) and summer events should be done in terms of I-D thresholds (and especially for their application on EWAS).

- A magnitude-cumulative frequency relationship was established for the flow-type events. The volumes were obtained using the data collected from the sensors and observations during the field campaigns. The final volumes of the events range from few hundreds up to tens of thousands of cubic meters. The frequency was established as the number of events per year. The final relationship has a similar slope than the power law described by Corominas and Moya (2010) for another torrent in the Pre-Pyrenees.

Finally, a methodology to estimate the entrainment of single debris-flow events was developed. The methodology is based on a database of geomorphologic parameters, collected on the field and by topographic data and it was obtained from a data mining analysis. The database contains 110 torrent reaches, from which three different sets were separated: a training set, a validation set and a test set. The methodology presents is a decision tree, based on geomorphologic parameters of the torrent reaches and provides an erosion rate class that can take place at each one. The erosion rate classes range from no erosion up to 10 m^3/m. A general decision tree was described, which should be calibrated in order to be adapted to other regions in the world.

[141]

7.1. Future research work

The present study stands for a contribution to the advance on the knowledge of debris-flow phenomenon and its hazard assessment. However, there are still many questions that remain unsolved and that concern future research in the lines that have been followed in this thesis.

First, during the development of this work, many efforts were directed to the technical issues concerning the monitoring system development. Therefore, from the author's point of view, more research should be carried out on the development of efficient techniques to monitor debris flows, especially considering power supply requirements. Moreover, we should put more effort on developing wireless solutions since their advantages in terms of safety of the installation are proved.

Second, considering the ground vibration signal for debris-flow monitoring and alarm purposes, the research should be faced to the definition of some type of guidelines to define thresholds for event detection depending on the on-site factors. Moreover, the detailed analysis of the ground velocity signal is still unfinished in the Rebaixader site.

Third, further research on the triggering conditions of debris flows should be fulfilled. Until now, the widely most studied triggering factor is the rainfall. In the present work, however, an evident influence of the snowmelt was noticed, which should activate the necessity of developing other types of thresholds of triggering conditions.

Forth, the methodology proposed in this work to estimate the entrainment of debris flows should be tested in other regions and some other factors could be added to improve the erosion prediction.

References

Abancó, C. and Hürlimann, M., (in prep). Estimate of debris-flow entrainment by field and topographical data. Natural Hazards.

Abancó, C., Hürlimann, M., Fritschi, B., Graf, C. and Moya, J., (2012). Transformation of Ground Vibration Signal for Debris-Flow Monitoring and Detection in Alarm Systems. Sensors, 12(4): 4870-4891.

Abancó, C., Hürlimann, M. and Moya, J., (in prep). Analysis of the ground vibration produced by debris flows and other torrential processes at the Rebaixader monitoring site (Catalan Pyrenees, Spain). Natural Hazards and Earth System Science: in prep.

Agliardi, F. and Crosta, G.B., (2003). High resolution three-dimensional numerical modelling of rockfalls. International Journal of Rock Mechanics and Mining Sciences, 40(4): 455-471.

Alcoverro, J., Corominas, J. and Gomez, M., (1999). The Barranco de Arás flood of 7 August 1996 (Biescas, Central Pyrenees, Spain). Engineering Geology, 51: 237-255.

Aleotti, P., (2004). A warning system for rainfall-induced shallow failures. Engineering Geology, 73(3-4): 247-265.

Allen, S., Cox, S. and Owens, I., (2011). Rock avalanches and other landslides in the central Southern Alps of New Zealand: a regional study considering possible climate change impacts. Landslides, 8(1): 33-48.

Amitrano, D., Arattano, M., Chiarle, M., Mortara, G., Occhiena, C., Pirulli, M. and Scavia, C., (2010). Microseismic activity analysis for the study of the rupture mechanisms in unstable rock masses. Natural Hazard Earth System Sciences, 10(831-841).

Arattano, M., (2000). On the use of seismic detectors as monitoring and warning systems for debris flows. Natural Hazards, 20: 197-213.

Arattano, M. and Marchi, L., (2005). Measurements of debris flow velocity through cross-correlation of instrumentation data. Natural Hazards and Earth System Sciences, 5(1): 137-142.

Arattano, M. and Marchi, L., (2008). Systems and Sensors for Debris-flow Monitoring and Warning. Sensors, 8(4): 2436-2452.

Arattano, M., Marchi, L. and Cavalli, M., (2012). Analysis of debris-flow recordings in an instrumented basin: Confirmations and new findings. Natural Hazards and Earth System Science, 12(3): 679-686.

Arattano, M. and Moia, F., (1999). Monitoring the propagation of a debris flow along a torrent. Hydrological Sciences Journal, 44(5): 811.

Aulitzky, H., (1982). Preliminary two-fold classification of torrents. Mitteilungen der Forstlichen Bundesversuchsanstalt(144): 243-256.

[143]

Badoux, A., Graf, C., Rhyner, J., Kuntner, R. and McArdell, B., (2009). A debris-flow alarm system for the Alpine Illgraben catchment: design and performance. Natural Hazards: 517-539.

Bardou, E., (2002). Methodologie de Diagnostic des laves torrentielles sur un bassin versant alpin, PhD.

Bartelt, P., Buehler, Y., Christen, M., Deubelbeiss, Y., Graf, C. and McArdell, B., (2012). RAMMS User Manual v1.4 Debris Flow, A modeling system for debris flows in research and practice. WSL Institute for Snow and Avalanche Research SLF, pp. 89.

Baum, R.L. and Godt, J.W., (2010). Early warning of rainfall-induced shallow landslides and debris flows in the USA. Landslides, 7(3): 259-272.

Berger, C., McArdell, B.W. and Schlunegger, F., (2011). Sediment transfer patterns at the Illgraben catchment, Switzerland: Implications for the time scales of debris flow activities. Geomorphology, 125: 421-432.

Berti, M., Genevois, R., La Husen, R., Simoni, A. and Tecca, P.R., (2000). Debris flow monitoring in the Acquabona watershed on the Dolomites (Italian Alps). Physics and Chemistry of the Earth, 25(9): 707-715.

Berti, M., Genevois, R., Simoni, A. and Tecca, P.R., (1999). Field observations of a debris flow event in the Dolomites. Geomorphology, 29(3-4): 265-274.

Bessason, B., Eiriksson, G., Thorarinsson, O., Thorarinsson, A. and Einarsson, S., (2007). Automatic detection of avalanches and debris flows by seismic methods. Journal of Glaciology, 53(182): 461.

Blair, R., (1994). Moraine and valley wall collapse due to rapid deglaciation in Mount Cook National Park, New Zealand. Mountain Research and Development, 14(4): 347-358.

Bordonau, J., (1992). Els complexos glàcio-lacustres relacionats amb el darrer cicle glacial als Pirineus. Geoforma Ediciones, Logroño, 251 pp.

Breien, H., De Blasio, F.V., Elverhoi, A. and Hoeg, K., (2008). Erosion and morphology of a debris flow caused by a glacial lake outburst flood, Western Norway. Landslides, 5(3): 271-280.

Breiman, L., Friedman, J., Olshen, R. and Stone, C., (1984). Classification and regression trees, London.

Brunetti, M.T., Peruccacci, S., Rossi, M., Luciani, S., Valigi, D. and Guzzetti, F., (2010). Rainfall thresholds for the possible occurrence of landslides in Italy. Nat. Hazards Earth Syst. Sci., 10(3): 447-458.

CAC, (2004). Climatic Atlas of Catalonia. http://www.opengis.uab.cat/acdc/. Accessed 22 July 2012.

Caine, N., (1980). The rainfall intensity-duration control of shallow landslides and debris flows. Geografiska Annaler, 62A: 23-27.

Cepeda, J., Höeg, K. and Nadim, F., (2010). Landslide-triggering rainfall thresholds: A conceptual framework. Quarterly Journal of Engineering Geology and Hydrogeology, 43(1): 69-84.

Chang, S.Y. and Lin, C.P., (2007). Debris flow detection using image processing techniques. In: J.J. Major and C. Chen (Editors), 4th Int. Conf. on Debris-Flow Hazards Mitigation. Millpress, Chengdu, China, pp. 549-560.

Chau, K.T. and Lo, K.H., (2004). Hazard assessment of debris flows for Leung King Estate of Hong Kong by incorporating GIS with numerical simulations. Natural Hazards and Earth System Sciences, 4: 103-116.

Chen, J., YP, H. and FQ, W., (2005). Debris flow erosion and deposition in Jiangjia Gully, Yunnan, China. Environ Geol, 48: 771–777.

Chevalier, G., Medina, V., Hürlimann, M. and Bateman, A., (2013). Debris-flow susceptibility analysis using fluvio-morphological parameters: Application to the Central-Eastern Pyrenees. Natural Hazards.

Chiang, S.-H. and Chang, K.-T., (2009). Application of radar data to modeling rainfall-induced landslides. Geomorphology, 103(3): 299-309.

Chou, H.-T., Chang, Y.-L. and Zhang, S.-C., (2010). Acoustic signals and geophone response induced by stony-type debris flows, Interpraevent, Taipei (Taiwan), pp. 712 - 720.

Clague, J.J. and Evans, S.G., (2000). A review of catastrophic drainage of moraine-dammed lakes in British Columbia. Quaternary Science Reviews, 19: 1763-1783.

Coe, J.A., Kinner, D.A. and Godt, J.W., (2008). Initiation conditions for debris flows generated by runoff at Chalk Cliffs, central Colorado. Geomorphology, 96(3-4): 270-297.

Corominas, J., Ayala, F.J., Chacón, J., Díaz de Terán, J.R., González, A., Moya, J. and Vilaplana, J.M., (2005). Impactos sobre los riesgos naturales de origen climático: Riesgo de inestabilidad de laderas de origen climático. In: J.M. Moreno (Editor), Evaluación Preliminar de los Impactos en España por Efecto del Cambio Climático. Ministerio de Medio Ambiente, Madrid, pp. 549-579.

Corominas, J. and Moya, J., (1999). Reconstructing recent landslide activity in relation to rainfall in the Llobregat River basin, Eastern Pyrenees, Spain. Geomorphology, 30: 79-93.

Corominas, J. and Moya, J., (2010). Contribution of dendrochronology to the determination of magnitude-frequency relationships for landslides. Geomorphology, 124(3-4): 137-149.

Corominas, J., Moya, J. and Hürlimann, M., (2002). Landslide rainfall triggers in the Spanish Eastern Pyrenees, 4th EGS Plinius Conference "Mediterranean Storms". Editrice, Mallorca.

Costa, J.E., (1984). Physical geomorphology of debris flows. In: J.E. Costa and P.J. Fleisher (Editors), Developments and applications of geomorphology. Springer-Verlag, Berlin, pp. 268-317.

Coussot, P. and Meunier, M., (1996). Recognition, classification and mechanical description of debris flows. Earth-Science Reviews, 40: 209-227.

Crosta, G.B. and Frattini, P., (2003). Distributed modelling of shallow landslides triggered by intense rainfall. Nat. Hazards Earth Syst. Sci., 3(1/2): 81-93.

Crosta, G.B., Imposimato, S. and Roddeman, D., (2008). Numerical modelling of entrainment/deposition in rock and debris-avalanches. Engineering Geology, Volume 109(Issues 1-2,): Pages 135-145.

Cruden, D. and Varnes, D., (1996). Landslide types and processes. In: A.K. Turner and R.L. Schuster (Editors), Landslides: investigation and mitigation. Transportation Research Board, Washington DC, pp. 36-75.

Curry, A.M., Sands, T.B. and Porter, P.R., (2009). Geotechnical controls on a steep lateral moraine undergoing paraglacial slope adjustment, Geological Society Special Publication, pp. 181-197.

D'Agostino, V., (1996). Analisi quantitativa e qualitativa del transporto solido torrentizio nei bacini montani del Trentino Orientale, 1a Sezione, Volume presentato in occasione del Convegno di Studio: I problemi dei grandi comprensori irrigui, Novara, pp. 111-123.

Davies, T., Phillips, C. and Warburton, J., (2013). Processes, Transport, Deposition and Landforms: Flow. In: J.F. Shroder (Editor), Treatise on Geomorphology

Decaulne, A., Saemundsson, P. and Petursson, O., (2005). Debris flow triggered by rapid snowmelt: A case study in the Gleidarhjalli area, northwestern Iceland. Geografiska Annaler Series a-Physical Geography, 87A(4): 487-500.

Deganutti, A.M., Marchi, L. and Arattano, M., (2000). Rainfall and debris-flow occurrence in the Moscardo basin (Italian Alps). In: G.F. Wieczorek and N.D. Naeser (Editors), 2nd International Conference on Debris-Flow Hazards Mitigation. Balkema, pp. 67-72.

Degetto, M., Crucil, G., Pimazzoni, A., Masetto, C. and Gregoretti, C., (2011). An estimate of the sediments volume entrainable by debris flow along Strobel and South Pezorìes channels at Fiames (Dolomites, Italy). In: R. Genevois, D. Hamilton and A. Prestininzi (Editors), 5th International Conference on Debris Flow Hazards. Mitigation, Mechanics, Prediction and Assessment. Casa Editrice Università La Sapienza, Padua, Italy, pp. 845-855.

Dong, J.J., Lee, C.T., Tung, Y.H., Liu, C.N., Lin, K.P. and Lee, J.F., (2009). The role of the sediment budget in understanding debris flow susceptibility. Earth Surface Processes and Landforms, 34(12): 1612-1624.

Dorren, L., (2003). A review of rockfall mechanics and modelling approaches. Progress in Physical Geography, 27(1): 69-87.

Egashira, S., Honda, N. and Itoh, T., (2001). Experimental study on the entrainment of bed material into debris flow. Physics and Chemistry of the Earth, Part C: Solar, Terrestrial & Planetary Science, 26(9): 645-650.

ESRI, (2005). ArcGIS 9 : what is ArcGIS 9.1? ESRI, Redlands, California, 123 pp.

Evans, S.G. and Hungr, O., (1993). The assessment of rockfall hazard at the base of talus slopes. Canadian Geotechnical Journal, 30: 620-636.

Fang, Y.M., Huang, T.M., Lee, B.J., Chou, H.T. and Yin, H.Y., (2011). Analysis of debris flow underground sound by Wavelet Transform- A case study of events in Aiyuzih River. In: R. Genevois, D.L. Hamilton and A. Prestininzi (Editors), 5th International Conference on Debris-Flow Hazards "Mitigation, Mechanics, Prediction and Assessment". Università La Sapienza, Padua, pp. 545-551.

Fannin, R.J. and Rollerson, T.P., (1993). Debris flows: some physical characteristics and behaviour. Canadian Geotechnical Journal, 30: 71-81.

Fannin, R.J. and Wise, M.P., (2001). An empirical-statistical model for debris flow travel distance. Canadian Geotechnical Journal, 38: 982-994.

Fayyad, U., Piatetsky-Saphiro, G. and Smyth, P., (1996). From Data Mining to Knowledge Discovery in Databases. AI Magazine, 17(3).

Fell, R., Corominas, J., Bonnard, C., Cascini, L., Leroi, E., Savage, W.Z. and and on behalf of the JTC-1 Joint Technical Committee on Landslides and Engineered Slopes, (2008). Guidelines for landslide susceptibility, hazard and risk zoning for land use planning. Engineering Geology, 102: 85-98.

Fiebiger, G., (1997). Hazard mapping in Austria. Wildbach- und Lawinenverbau, 61(134): 121-133.

Flageollet, J.-C., Maquaire, O., Martin, B. and Weber, D., (1999). Landslides and climatic conditions in the Barcelonnette and Vars basins (Southern French Alps, France). Geomorphology, 30(1-2): 65-78.

Fraccarolo, L. and Capart, H., (2002). Riemann wave description of erosional dam-break flows. Journal of Fluid Mechanics, 461: 183-228.

Franzi, L. and Bianco, G., (2001). A Statistical Method to Predict Debris Flow Deposited Volumes on a Debris Fan. Physics and Chemistry of the Earth, 26(9): 683-688.

Fuchs, S., Heiss, K. and Hübl, J., (2007). Towards an empirical vulnerability function for use in debris flow risk assessment. Natural Hazards and Earth System Science, 7(5): 495-506.

Gabet, E.J. and Bookter, A., (2008). A morphometric analysis of gullies scoured by post-fire progressively bulked debris flows in southwest Montana, USA. Geomorphology, 96: 298-309.

Gartner, J.E., Cannon, S.H., Santi, P.M. and DeWolfe, V.G., (2008). Empirical models to predict the volumes of debris flows generated by recently burned basins in the western U.S. Geomorphology, 96: 339-354.

Genevois, R., Berti, M., Ghirotti, M., Simoni, A. and Tecca, P.R., (1999). Debris flow monitoring and analysis in the Dolomitic Region (Upper Boite Valley, Italian Alps).

GEOTEST AG, (2006). ROFMOD 4.1: User Manual, Zollikofen (Switzerland), 25 pp.

Gertsch, E., (2009). Geschiebelieferung alpiner Wildbachsysteme bei Grossereignissen - Ereignisanalysen und Entwicklung eines Abschätzverfahrens Universität Bern, Bern, 204 pp.

Gironès, R., (2003). Estudio hidrológico e hidráulico para la determinación potencial de formación de flujos hiperconcentrados mediante el uso de herramientas gis. Aplicación al evento del 10 de junio del 2000 en la Riera de la Magarola. unpublished tesina, UPC, Barcelona, Barcelona, 136 pp.

Glade, T., (2005). Linking debris-flow hazard assessments with geomorphology. Geomorphology, 66: 189-213.

Godt, J.W., Baum, R.L. and Lu, N., (2009). Landsliding in partially saturated materials. Geophysical Research Letters, 36(2): L02403, doi:10.1029/2008GL035996.

Godt, J.W., Baum, R.L., Savage, W.Z., Salciarini, D., Schulz, W.H. and Harp, E.L., (2008). Transient deterministic shallow landslide modeling: Requirements for susceptibility and hazard assessments in a GIS framework. Engineering Geology, 102(3-4): 214-226.

Gostner, W., Bezzola, G.R., Schatzmann, M. and Minor, H.E., (2003). Integral analysis of debris flow in Alpine torrent- the case study of Tschengls. In: R. Chen (Editor), Debris-Flow Hazards Mitigation: Mechanics, Prediction and Assessment. Millpress, Rotterdam, Davos.

Greco, R., Guida, A., Damiano, E. and Olivares, L., (2010). Soil water content and suction monitoring in model slopes for shallow flowslides early warning applications. Physics and Chemistry of the Earth, 35(3-5): 127-136.

Gregoretti, C., (2012). Monitoring of debris flows in the testbed Fiames Valley, PARAmount Final Conference, Grenoble, pp. http://www.paramount-project.eu.

Gregoretti, C. and Dalla Fontana, G., (2008). The triggering of debris flow due to channel-bed failure in some alpine headwater basins of the Dolomites: analyses of critical runoff. Hydrological Processes, 22(13): 2248-2263.

Gruber, S. and Haeberli, W., (2007). Permafrost in steep bedrock slopes and its temperatures-related destabilization following climate change. Journal of Geophysical Research F: Earth Surface, 112(2).

Guthrie, R.H., Hockin, A., Colquhoun, L., Nagy, T., Evans, S.G. and Ayles, C., (2009). An examination of controls on debris flow mobility: Evidence from coastal British Columbia. Geomorphology, 114(4): 601-613.

Guzzetti, F., Peruccacci, S., Rossi, M. and Stark, C.P., (2007). Rainfall thresholds for the initiation of landslides in central and southern Europe. Meteorology and Atmospheric Physics, 98: 239-267.

Hadley, K.C. and LaHusen, R., (1995). Technical Manual for the Experimental Acoustic Flow Monitor. US Geological Survey; Open-file Reports Section, 24 pp.

Hall, M.A., Frank, E., Holmes, G., Pfahringer, B., Reutmann, P. and Witten, I.H., (2009). The WEKA Data Mining Software: An Update SIGKKD Explorations, 11(1): 10-18.

Harris, C., Arenson, L.U., Christiansen, H.H., Etzelmüller, B., Frauenfelder, R., Gruber, S., Haeberli, W., Hauck, C., Hölzle, M., Humlum, O., Isaksen, K., Kääb, A., Kern-Lütschg, M.A., Lehning, M., Matsuoka, N., Murton, J.B., Nötzli, J., Phillips, M., Ross, N., Seppälä, M., Springman, S.M. and Vonder Mühll, D., (2009). Permafrost and climate in Europe: Monitoring and modelling thermal, geomorphological and geotechnical responses. Earth-Science Reviews, 92(3-4): 117-171.

Havskov, J. and Alguacil, G., (2004). Instrumentation in Earthquake Seismology, Berlin, Germay.

Heinimann, H., Hollenstein, K., Kienholz, H., Krummenacher, B. and Mani, P., (1998). Methoden zur Analyse und Bewertung von Naturgefahren. Bundesamt für Umwelt, Wald und Landschaft (BUWAL), Bern, 248 pp.

Hu, K., Wei, F. and Li, Y., (2011). Real-time measurement and preliminary analysis of debris-flow impact force at Jiangjia Ravine, China. Earth Surface Processes and Landforms, 36(9): 1268-1278.

Huang, C., Yin, H., Chen, C., Yeh, C.H. and Wang, C.L., (2007). Ground vibrations pdoduced by rock motions and debris flows. Journal of Geophysical Research, 112(F2): F02014.

Huang, C.J., Yin, H.Y. and Shieh, C.L., (2003). Experimental study of the underground sound generated by debris flows. In: D. Rickenmann and C. Chen (Editors), Debris-Flow Hazards Mitigation: Mechanics, Prediction and Assessment. Millpress, Davos, pp. 743-753.

Hübl, J., Fuchs, S., Sitter, F. and Totschnig, R., (2011). Towards a frequency-magnitude relationship for torrent events in Austria. In: R. Genevois, D. Hamilton and A. Prestininzi (Editors), 5th International Conference on Debris Flow Hazards Mitigation: Mechanics, Prediction and Assessment, Padua (Italy), pp. 895-902.

Hübl, J. and Kaitna, R., (2010). Sediment delivery from the Lattenbach catchment by debris floods and debris flows, EGU General Assembly, pp. 10585.

Hübl, J., Suda, J., Proske, D., Kaitna, R. and Scheidl, C., (2009). Debris flow impact estimation. In: C. Popovska and M. Jovanovski (Editors), 11th symposium on water management and hydraulic Engineering, Ohrid, Macedonia, pp. 137-148.

Hugenholtz, C., Moorman, B., Barlow, J. and Wainstein, P., (2008). Large-scale moraine deformation at the Athabasca Glacier, Jasper National Park, Alberta, Canada. Landslides, 5(3): 251-260.

Hungr, O., (1997). Some methods of landslide hazard intensity mapping. In: D. Cruden and R. Fell (Editors), Int. Workshop on landslide risk assessment. Balkema, Honolulu, Hawaii, pp. 215-226.

Hungr, O., (2000). Analysis of debris flow surges using the theory of uniformly progressive flow. Earth Surface Processes and Landforms, 25: 483-495.

Hungr, O., Evans, S.G., Bovis, M.J. and Hutchinson, J.N., (2001). A review of the classification of landslides of the flow type. Environmental and Engineering Geoscience, 7(3): 221-238.

Hungr, O., McDougall, S. and Bovis, M., (2005). Entrainment of material by debris flow. In: M. Jakob and O. Hungr (Editors), Debris-flow Hazards and Related Phenomena. Springer, Berlin, pp. 135-158.

Hungr, O., Morgan, G.C. and Kellerhals, R., (1984). Quantitative analysis of debris torrent hazards for design of remedial measures. Canadian Geotechnical Journal, 21: 663-677.

Hürlimann, M., Abancó, C. and Moya, J., (2010). Debris-flow initiation affected by snowmelt. Case study of the Senet monitoring site, Eastern Pyrenees, Mountain Risks: Bringing Science to Society, Florence, Italy, pp. 81-86.

Hürlimann, M., Abancó, C. and Moya, J., (2012). Rockfalls detached from a lateral moraine during spring season. 2010 and 2011 events observed at the Rebaixader debris-flow monitoring site (Central Pyrenees, Spain). Landslides(3): 385-393.

Hürlimann, M., Abancó, C., Moya, J., Raïmat, C. and Luis-Fonseca, R., (2011). Debris-flow monitoring stations in the Eastern Pyrenees. Description of instrumentation, first experiences and preliminary results. In: R. Genevois, D. Hamilton and A. Prestininzi (Editors), 5th Int. Conf. on Debris-Flow Hazards Mitigation, Padua, pp. 553-562.

Hürlimann, M., Abancó, C., Moya, J. and Vilajosana, I., (submitted). Results and experiences gathered at the Rebaixader debris-flow monitoring site, Central Pyrenees, Spain. Landslides.

Hürlimann, M., Copons, R. and Altimir, J., (2006). Detailed debris flow hazard assessment in Andorra: A multidisciplinary approach. Geomorphology, 78: 359-372.

Hürlimann, M., Corominas, J., Moya, J. and Copons, R., (2003a). Debris-flow events in the Eastern Pyrenees. Preliminary study on initiation and propagation. In: D. Rickenmann and C. Chen (Editors), 3rd Int. Conf. on Debris-Flow Hazards Mitigation. Millpress, Davos, pp. 115-126.

Hürlimann, M. and Lantada, N., (2005). Aplicaciones SIG al estudio y la zonificación de la peligrosidad de deslizamientos superficiales y corrientes de derrubios en Cataluña. In: J. Corominas, E. Alonso, M. Romana and M. Hürlimann (Editors), VI Simposio Nacional sobre Taludes y Laderas Inestables, Valencia, pp. 366-377.

Hürlimann, M., Rickenmann, D. and Graf, C., (2003b). Field and monitoring data of debris-flow events in the Swiss Alps. Canadian Geotechnical Journal, 40(1): 161-175.

Hürlimann, M., Rickenmann, D., Medina, V. and Bateman, A., (2008). Evaluation of approaches to calculate debris-flows parameters for hazard assessment. Engineering Geology, 102: 152-163.

Hutchinson, J.N. and Bhandari, R.K., (1971). Undrained loading, a fundamental mechanism of mudflows and other mass movements. Géotechnique, 21(4): 353-358.

Itakura, Y., Fujii, N. and Sawada, T., (2000). Basic characteristics of ground vibration sensors for the detection of debris flow. Physics and Chemistry of the Earth, Part B, 25(9): 717-720.

Itakura, Y., Inaba, H. and Sawada, T., (2005). A debris-flow monitoring devices and methods bibliography. Natural Hazards and Earth System Science, 5(6): 971-977.

Iverson, R.M., (1997). The physics of debris flows. Review of Geophysics, 35(3): 245-296.

Iverson, R.M., Reid, M.E., Logan, M., LaHusen, R.G., Godt, J.W. and Griswold, J.P., (2011). Positive feedback and momentum growth during debris-flow entrainment of wet bed sediment. Nature Geoscience, 4(2): 116-121.

Iverson, R.M., Schilling, S.P. and Vallance, J.W., (1998). Objective delineation of lahar-inundation hazard zones. Geological Society of America Bulletin, 110(8): 972-984.

Jaboyedoff, M., Oppikofer, T., Abellán, A., Derron, M.-H., Loye, A., Metzger, R. and Pedrazzini, A., (2012). Use of LIDAR in landslide investigations: a review. Natural Hazards: 1-24.

Jakob, M., (2005). Debris-flow hazard analysis. In: M. Jakob and O. Hungr (Editors), Debris-flow Hazards and Related Phenomena. Springer, Berlin, pp. 411-443.

Jakob, M. and Friele, P., (2010). Frequency and magnitude of debris flows on Cheekye River, British Columbia. Geomorphology, 114(3): 382-395.

Jakob, M., Holm, K., Lange, O. and Schwab, J.W., (2006). Hydrometeorological thresholds for landslide initiation and forest operation shutdowns on the north coast of British Columbia. Landslides, 3(3): 228-238.

Jakob, M. and Hungr, O., (2005). Debris-flow Hazards and Related Phenomena. Springer, Berlin, 739 pp.

Jakob, M. and Weatherly, H., (2005). Debris flow hazard and risk assessment, Jones Creek, Washington. In: O. Hungr, R. Fell, R. Couture and E. Eberhardt (Editors), Landslide risk management. Taylor & Francis Group, Vancouver, pp. 533-541.

Johnson, A.M. and Rodine, J.R., (1984). Debris flow. In: D. Brunsden and D.B. Prior (Editors), Slope Stability. John Wiley and Sons, New York, pp. 257 - 361.

Julián, A. and Chueca, J., (2007). Permafrost distribution from BTS measurements (Sierra de Telera, Central Pyrenees, Spain): assessing the importance of solar radiation in a mid-elevation shaded mountainous area. Permafrost and Periglacial Processes, 18(2): 137-149.

Kean, J.W., Staley, D.M. and Cannon, S.H., (2011). In situ measurements of post-fire debris flows in southern California: Comparisons of the timing and magnitude of 24 debris-flow events with rainfall and soil moisture conditions. J. Geophys. Res., 116(F4): F04019.

Kienholz, H., (1978). Maps of geomorphology and natural hazard of Grindelwald, Switzerland, scale 1:10.000. Arctic, Antarctic, and Alpine Research, 10: 995-999.

Kogelnig, A., (2012). Development of acoustic monitoring for alpine mass movements. PhD-thesis, University of Natural Resources and Life Sciences, Vienna, 206 pp.

Kogelnig, A., Hübl, J., Suriñach, E., Vilajosana, I. and McArdell, B., (2011a). Infrasound produced by debris flow: propagation and frequency content evolution. Natural Hazards: 1-21.

Kogelnig, A., Hübl, J., Suriñach, E., Vilajosana, I., Zhang, S., Yun, N. and McArdell, B., (2011b). A study of infrasonic signals of debris flow. In: R. Genevois, D. Hamilton and A. Prestininzi (Editors), 5th International Conference on Debris-Flow Hazards "Mitigation, Mechanics, Prediction and Assessment". Università La Sapienza, Padua, pp. 563-572.

Kogelnig, A., Suriñach, E., Vilajosana, I., Hübl, J., Sovilla, B., Hiller, M. and Dufour, F., (2011c). On the complementariness of infrasound and seismic sensors for monitoring snow avalanches. Natural Hazards Earth System Sciences, 11: 2355-2370.

Kronfellner-Kraus, G., (1985). Quantitative estimation of torrent erosion, International Symposium on Erosion and Disaster Prevention, Tsukuba (Japan).

Kung, H.Y., Ku, H.H., Wu, C.I. and Lin, C.Y., (2008). Intelligent and situation-aware pervasive system to support debris-flow disaster prediction and alerting in Taiwan. Journal of Network and Computer Applications, 31(1): 1-18.

LaHusen, R., (1996). Detecting debris flows using ground vibrations.

LaHusen, R., (2005a). Acoustic Flow Monitor System - User Manual. U.S. Geological Survey, Open-File Report 02-429, 16 pp.

LaHusen, R., (2005b). Debris-flow instrumentation. In: M. Jakob and O. Hungr (Editors), Debris-flow Hazards and Related Phenomena. Springer, Berlin, pp. 291-304.

Lavigne, F., Thouret, J.C., Voight, B., Young, K., LaHusen, R., Marso, J., Suwa, H., Sumaryono, A., Sayudi, D.S. and Dejean, M., (2000). Instrumental lahar monitoring at Merapi Volcano, Central Java, Indonesia. Journal Of Volcanology And Geothermal Research. Jul, 100(1-4): 457-478.

Lee, H.C., Banerjee, A., Fang, Y.M., Lee, B.J. and King, C.T., (2010). Design of a multifunctional wireless sensor for in-situ monitoring of debris flows. IEEE Transactions on Instrumentation and Measurement, 59(11): 2958-2967.

Leprettre, B.J.P., Navarre, J.-P. and Taillefer, A., (1996). First results from a pre-operational system for automatic detection and recognition of seismic signals associated with avalanches. Journal of Glaciology 42(141): 352-363.

Liu, X. and Lei, J., (2003). A method for assessing regional debris flow risk: an application in Zhaotong of Yunnan province (SW China). Geomorphology, 52(3-4): 181-191.

Luis-Fonseca, R., Raïmat, C., Hürlimann, M., Abancó, C., Moya, J. and Fernández, J., (2011). Debris-flow protection in recurrent areas of the Pyrenees. Experience of the VX systems after the output results collected in the pioneer monitoring station in Spain. In: R. Genevois, D. Hamilton and A. Prestininzi (Editors), 5th Int. Conf. on Debris-Flow Hazards Mitigation, Padua, pp. 1063-1071.

Mangeney, A., Roche, O., Hungr, O., Mangold, N., Faccanoni, G. and Lucas, A., (2010). Erosion and mobility in granular collapse over sloping beds. Journal of Geophysical Research, 115(F03040).

Marcial, S., Melosantos, A., Hadley, K., La Husen, R. and Marso, J., (1996). Instrumental lahar monitoring at Mount Pinatubo. In: P.I.o.V.a. Seismology (Editor), *Fire and Mud: Eruptions and Lahars of Mt. Pinatubo*, *Philippines*;

Newhall, C.G.,. University of Washington Press: Seattle, WA, USA, Quezon City, Philippines.

Marchi, L., Arattano, M. and Deganutti, A.M., (2002). Ten years of debris-flow monitoring in the Moscardo Torrent (Italian Alps). Geomorphology, 46(1-2): 1-17.

Marchi, L., Cavalli, M., Sangati, M. and Borga, M., (2009). Hydrometeorological controls and erosive response of an extreme alpine debris flow. Hydrological Processes, 23: 2714-2727.

Marchi, L., Comiti, F., Arattano, M., Cavalli, M., Macconi, P. and Penna, D., (2012). A new debris-flow monitoring system in an Alpine catchment. Geophysical Research Abstracts, 14: 6104.

Marchi, L. and D'Agostino, V., (2004). Estimation of debris-flow magnitude in the Eastern Italian Alps. Earth Surface Processes and Landforms, 29(2): 207-220.

Marquis, F.X., (2006). Torrents des Glariers et du Pessot- lave torrentielle et inondation du 22.07.2006: description et analyse de l'événement, Commune de Collombey-Muraz, Monthey.

Marquis, F.X., (2008). Lave torrentielle du 29.06.08- Description et analyse de l'événement (Torrent Sec), Communes de Collonges et de Lavey-Morcles, Monthey.

MATLAB, (2009). The MathWorks Inc., Natick, Massachusetts.

McArdell, B. and Badoux, A., (2007). Influence of rainfall on the initiation of debris flows at the Illgraben catchment, canton of Valais, Switzerland. Geophysical Research Abstracts, 9: 08804.

McArdell, B., Bartelt, P. and Kowalski, J., (2007). Field observations of basal forces and fluid pore pressure in a debris flow. Geophysical Research Letters, 34: doi:10.1029/2006GL029183.

McCoy, S.W., Kean, J.W., Coe, J.A., Staley, D.M., Wasklewicz, T.A. and Tucker, G.E., (2010). Evolution of a natural debris flow: In situ measurements of flow dynamics, video imagery, and terrestrial laser scanning. Geology, 38(8): 735-738.

Medina, V., Hürlimann, M. and Bateman, A., (2008). Application of FLATModel, a 2D finite volume code, to debris flows in the northeastern part of the Iberian Peninsula. Landslides, 5(1): 127-142.

Muñoz, A., (1992). Evolution of a continental collision belt: ECORS-Pyrenees crustal balanced cross-section. In: K.R. McClay (Editor), Thrust Tectonics. Chapman & Hall, pp. 235-246.

Nadim, F. and Lacasse, S., (2008). Strategies for mitigation of risk associated with landslides, First World International Landslide Forum. IPL Global Promotion Comitee, Tokyo, Japan.

Navratil, O., Liébault, F., Bellot, H., Theule, J., Ravanat, X., Ousset, F., Laigle, D., Segel, V. and Fiquet, M., (2011). Installation d'un suivi en continu des crues et laves torrentielles dans les Alpes françaises. In: I.d.G.e.d.A.d.

Risque (Editor), Journée de Rencontre sur les Dangers Naturels, Lausanne, pp. 8pp.

Navratil, O., Liébault, F., Bellot, H., Theule, J., Travaglini, E., Ravanat, X., Ousset, F., Laigle, D., Segel, V. and Fiquet, M., (2012). High-frequency monitoring of debris flows in the French alps. Preliminary results of a starting program, INTERPRAEVENT, Grenoble, pp. 11pp.

Novoa, M., (1984). Precipitaciones y avenidas extraordinarias en Cataluña. In: ETSECCPB (Editor), Inestabilidad de laderas en el Pirineo, Barcelona, pp. I.1.1-I.1.15.

Oller, P. and Pinyol, J., (2009). Nota de la sortida de camp a la barrera flexible d'anells a Erill la Vall i als corrents d'arrossegalls a la vall de Sant Nicolau al Parc Nacional d'Aigüestortes i Estany de Sant Maurici, Institut Geològic de Catalunya.

ONR-24-800, (2007). Schutzbauwerke der Wildbachverbauung –

Begriffsbestimmungen und Klassifizierungen. In: Österreichisches and Normungsinstitut (Editors).

Pack, R.T., (2005). Application of airborne and spaceborne remote sensing methods. In: M. Jakob and O. Hungr (Editors), Debris-flow Hazards and Related Phenomena. Springer, Berlin, pp. 275-289.

Pallas, R., Vilaplana, J.M., Guinau, M., Falgas, E., Alemany, X. and Munoz, A., (2004). A pragmatic approach to debris flow hazard mapping in areas affected by Hurricane Mitch: example from NW Nicaragua. Engineering Geology, 72(1-2): 57-72.

Papa, M., Egashira, S. and Itoh, T., (2004). Critical conditions of bed sediment entrainment due to debris flow. Natural Hazards and Earth System Sciences., 4(3): 469-474.

Pasuto, A. and Soldati, M., (2004). An integrated approach for hazard assessment and mitigation of debris flows in the Italian Dolomites. Geomorphology, 61: 59-70.

Petrascheck, A. and Kienholz, H., (2003). Hazard assessment and mapping of mountain risks in Switzerland. In: D. Rickenmann and C. Chen (Editors), 3rd Int. Conf. on Debris-Flow Hazards Mitigation. Millpress, Davos, pp. 25-39.

Phillips, C.J. and Davies, T.R.H., (1991). Determining rheological parameters of debris flow material. Geomorphology, 4: 101-110.

Pierson, T.C., (1986). Flow behavior of channelized debris flows, Mount St. Helens, Washington. In: A.D. Abraham (Editor), Hillslope Processes, The Binghamton symp. in geomorphology. Allen & Unwin, Boston, pp. 269-296.

Pierson, T.C. and Scott, K.M., (1985). Downstream dilution of a Lahar: Transition from debris flow to hyperconcentrated streamflow. Water resources research, 21(10): 1511-1524.

Pinyol, J., (2008). Nota tècnica sobre la visita al barranc de Portainé i al barranc des Caners els dies 1 i 2 d'octubre 2008 en motiu de la torrentada ocorreguda la matinada del dia 12 de setembre de 2008, Insitut Geològic de Catalunya.

Portilla, M., Chevalier, G. and Hürlimann, M., (2010). Description and analysis of major mass movements occurred during 2008 in the Eastern Pyrenees. Nat. Hazards Earth Syst. Sci., 10: 1635-1645.

Quan Luna, B., Remaître, A., van Asch, T.W.J., Malet, J.P. and van Westen, C.J., (2012). Analysis of debris flow behavior with a one dimensional run-out model incorporating entrainment. Engineering Geology, **in press**.

Reid, M.E., Baum, R.L., LaHusen, R. and Ellis, W.L., (2008). Capturing landslide dynamics and hydrologic triggers using near-real-time monitoring. In: Z. Chen, J. Zhang, Z. Li, F. Wu and K. Ho (Editors), 10th International Symposium On Landslides And Engineered Slopes. Taylor & Francis Group, Xian, pp. 179-191.

Rickenmann, D., (1990). Bedload transport capacity of slurry flows at steep slopes, ETH, Zurich, 249 pp.

Rickenmann, D., (1995). Beurteilung von Murgängen. Schweiz. Ingenieur und Architekt, 113(48): 1104-1108.

Rickenmann, D., (1999). Empirical relationships for debris flows. Natural hazards, 19(1): 47-77.

Rickenmann, D., (2005). Runout prediction methods. In: M. Jakob and O. Hungr (Editors), Debris-flow Hazards and Related Phenomena. Springer, Berlin, pp. 305-324.

Rickenmann, D. and Fritschi, B., (2007). Bedload transport measurements using piezoelectric impact sensors and geophones, International Bedload USGS, Minneapolis, MN, USA.

Rickenmann, D. and McArdell, B.W., (2007). Continuous measurement of sediment transport in the Erlenbach stream using piezoelectric bedload impact sensors. Earth Surface Processes and Landforms, 32(9): 1362-1378.

Rickenmann, D., Weber, D. and Stepanov, B., (2003). Erosion by debris flows in field and laboratory experiments. In: D. Rickenmann and C. Chen (Editors), 3rd Int. Conf. on Debris-Flow Hazards Mitigation. Millpress, Davos, pp. 883-894.

Rickenmann, D. and Zimmermann, M., (1993). The 1987 debris flows in Switzerland: documentation and analysis. Geomorphology, 8: 175-189.

Salameh, T., Zêzere, J. and Trigo, R., (2009). Development of an early warning system for precipitation triggered landslides in Portugal, EGU General Assembly 2009. Geophysical Research Abstracts, Vienna, pp. 2458.

Scheidl, C., Rickenmann, D. and Chiari, M., (2008). The use of airbone LIDAR data for the analysis of debris flow events in Switzerland. Nat. Hazards Earth Syst. Sci., 8: 1113-1127.

Schmitt, O., (1938). A thermionic trigger. J. Sci. Instrum., 15(24).

Smart, G.M. and Jäggi, M.N.R., (1983). Sedimenttransport in steilen Gerinnen. Mitteilung der Versuchsanstalt für Wasserbau, Hydrologie und Glaziologie, 64. ETH Zurich, 191 pp.

Soldati, M., Corsini, A. and Pasuto, A., (2004). Landslides and climate change in the Italian Dolomites since the Late glacial. CATENA, 55(2): 141-161.

Spreafico, M., Lehmann, C. and Naef, O., (1999). Recommandations concernant l'estimation de la charge sédimentaire dans les torrents. Groupe de travail pour l'hydrologie opérationnelle, Berne.

Springman, S.M., Jommi, C. and Teysseire, P., (2003). Instabilities on moraine slopes induced by loss of suction: A case history. Geotechnique, 53(1): 3-10.

Suriñach, E., Vilajosana, I., Khazaradze, G., Biescas, B., Furdada, G. and Vilaplana, J.M., (2005). Seismic detection and characterization of landslides and other mass movements. Nat. Hazards Earth Syst. Sci., 5: 791-798.

Suwa, H., (1989). Field observation of debris flow, Proceedings of the Japan-China (Taipei) Joint Seminar on Natural Hazard Mitigation, Kyoto, Japan, pp. 343-352.

Suwa, H., Okano, K. and Kanno, T., (2009). Behavior of debris flows monitored on test slopes of Kamikamihorizawa Creek, Mount Yakedake, Japan. International Journal of Erosion Control Engineering, 2: 33-45.

Suwa, H. and Okuda, S., (1985). Measurement of debris flows in Japan IV International Conference and Field Workshop on Landslides, Tokyo, pp. 391-400.

Suwa, H., Yamakoshi, T. and Sato, K., (2000). Relationship between debris-flow discharge and ground vibration. In: G. Wieczorek and N. Naeser (Editors), 2nd International Conference on Debris-Flow Hazards Mitigation. Balkema, Taipei, pp. 311-318.

Takahashi, T., (1978). Mechanical characteristics of debris flow. Journal of Hydraulic Division ASCE, 104: 1153-1169.

Takahashi, T., (1981). Debris flow. Annual reviews of fluid mechanics, 13: 57-77.

Takahashi, T., (1991). Debris Flow. IAHR Monograph. Balkema, Rotterdam, 165 pp.

Takahashi, T., (2007). Debris Flow: Mechanics, Prediction and Countermeasures. Taylor & Francis Group, 448 pp.

Takahashi, T., Nakagawa, H., Harada, T. and Yamashiki, V., (1992). Routing debris flows with particle segregation. Journal of Hydraulic Engineering, 118(11): 1490-1507.

Takei, A., (1984). Interdependence of sediment budget between individual torrents and river-system, Interpraevent, Villach, Austria, pp. 35-48.

Theule, J., Liébault, F., Loye, A., Laigle, D. and Jaboyedoff, M., (2012). Sediment budget monitoring of debris-flow and bedload transport in the Manival Torrent, SE France. Natural Hazards and Earth System Sciences, 12: 731-749.

Tiranti, D. and Rabuffetti, D., (2010). Estimation of rainfall thresholds triggering shallow landslides for an operational warning system implementation. Landslides, 7(4): 471-481.

Tuñgol, N. and Regalado, M., (1996). Rainfall, acoustic flow monitor records, and observed lahars of the Sacobia river in 1992. In: P.I.o.V.a. Seismology: and P. Quezon City (Editors), Fire and Mud: Eruptions and Lahars of Mt. Pinatubo, Philippines. University of Washington Press: Seattle, WA, USA, Quezon City, Philippines.

Vallance, J.W., (2000). Lahars. In: H.e.a. Sigurdsson (Editor), Encyclopedia of Volcanoes. Academic Press, San Diego, pp. 601-616.

Vallance, J.W., Cunico, M.L. and Schilling, S.P., (2003). Debris-flow hazards caused by hydrologic events at Mount Rainier, Washington. USGS, Open-file report 03-368.

Van Asch, T.W.J., Buma, J. and Van Beek, L.P.H., (1999). A view on some hydrological triggering systems in landslides. Geomorphology, 30: 25-32.

VanDine, D.F., (1985). Debris flows and debris torrents in the southern Canadian Cordillera. Canadian Geotechnical Journal, 22: 44-68.

Varnes, D.J., (1978). Slope movement types and processes. In: R.L. Schuster (Editor), Landslides: Analysis and control - Special Report 176. National Academy of sciences, Washington DC, pp. 11-33.

Vedie, E., Lagarde, J.L. and Font, M., (2010). Physical modelling of rainfall- and snowmelt-induced erosion of stony slope underlain by permafrost. Earth Surface Processes and Landforms, 36(3): 395-407.

Vilajosana, I., Suriñach, E., Abellán, A., Khazaradze, G., Garcia, D. and Llosa, J., (2008). Rockfall induced seismic signals: case study in Montserrat, Catalonia. Natural Hazards and Earth System Science, 8(4): 805-812.

Vilaplana, J.M., (1983). Quaternary Glacial Geology of Alta Ribagorça Basin (Central Southern Pyrenees). Acta Geológica Hispánica, 18((3/4)): 217-233.

Wan, S. and Chiang Lei, T., (2009). A knowledge-based decision support system to analyze the debris-flow problems at Chen-Yu-Lan River, Taiwan. Knowledge-Based Systems, 22: 580-588.

Wieczorek, G.F. and Glade, T., (2005). Climatic factors influencing occurrence of debris flow. In: M. Jakob and O. Hungr (Editors), Debris-flow Hazards and Related Phenomena. Springer, Berlin, pp. 325-362.

Winter, M.G., Dent, J., Macgregor, F., Dempsey, P., Motion, A. and Shackman, L., (2010). Debris flow, rainfall and climate change in Scotland. Quarterly Journal of Engineering Geology and Hydrogeology, 43(4): 429-446.

Witten, I.H., Frank, E. and Hall, M.A., (2011). Data Mining. Practical Machine Learning Tools and Techniques. Morgan Kaufmann, 629 pp.

Yin, H.Y., Huang, C.J., Fang, Y.M., Lee, B.J. and Chou, T.Y., (2010). The present development of debris flow monitoring technology in Taiwan, INTERPARAEVENT, pp. 992-1000.

Yin, Y.P., Wang, H.D., Gao, Y.L. and Li, X.C., (2009). Real-time monitoring and early warning of landslides at relocated Wushan Town, the Three Gorges Reservoir, China. Landslides, 7(3): 339-349.

Zeller, J., (1985). Feststoffmessung in kleinen Gebirgseinzugsgebieten. Wasser, Energie, Luff, 77(7/8): 246-251.

Zhang, S., (1993). A comprehensive approach to the observation and prevention of debris flows in China. Natural Hazards, 7: 1-23.

Zhang, S., Hong, Y. and Yu, B., (2004). Detecting infrasound emission of debris flow for warning purposes, Interpraevent, Riva/Trient, Italy, pp. 359-364.

Appendix: List of Publications

International Journals Publications

Abancó, C., Hürlimann, M., Fritschi, B., Graf, C., Moya, J., (2012). <u>Transformation of Ground Vibration Signal for Debris-Flow Monitoring and Detection in Alarm Systems.</u> Sensors, 12 (4), 4870-4891.   doi: 10.3390/s120404870

Abancó, C. and Hürlimann, M. (in prep) <u>Estimate of debris-flow entrainment by field and topographical data.</u> Natural Hazards

Abancó C., Hürlimann M and Moya J. (in prep) <u>Analysis of the ground vibration produced by debris flows and other torrential processes at the Rebaixader monitoring site (Catalan Pyrenees, Spain)</u> Natural Hazards and Earth System Sciences

Hürlimann, M., Abancó, C., Moya, J., (2012). <u>Rockfalls detached from a lateral moraine during spring season. 2010 and 2011 events observed at the Rebaixader debris-flow monitoring site (Central Pyrenees, Spain)</u>. Landslides, 3, 385-393, DOI: 10.1007/s10346-011-0314-4.

Hürlimann, M, Abancó, C., Moya, J, Vilajosana, I, (submitted). <u>Results and experiences gathered at the Rebaixader debris-flow monitoring site, Central Pyrenees</u>, Spain. Landslides

Conference Publications

Corominas, J.; Hürlimann, M.; Lantada, N.; Moya, J.; Baeza, C.; Abancó, C.,(2009) <u>The role of landslide inventories and geomorphological observations in landslide susceptibility mapping at local scales.</u> 7th International Conference on Geomorphology : ancient landscapes, modern perspectives.. Melbourne, Australia

Abancó, C.; Lantada, N.; Hürlimann, M.; Corominas, J.; Copons, R., (2009) <u>Validación de mapas de susceptibilidad de deslizamientos elaborados mediante diferentes técnicas. Aplicación a la zona de Sant Salvador de Toló (Cataluña).</u> VII Simposio Nacional sobre Taludes y Laderas Inestables. Barcelona, Spain

[163]

Hürlimann, M.; Moya, J.; Abanco, C.; Portilla, M.; Chevalier, G.; Baeza, C.; Raïmat, C.; Graf, C.; Torrebadella, J.; Oller, P (2009) Peligrosidad de corrientes de derrubios a escala de cuenca vertiente en el Pirineo Oriental: primeros resultados del proyecto "DEBRIS-CATCH". VII Simposio Nacional sobre Taludes y Laderas Inestables. Barcelona, Spain

Hürlimann, M., Abancó, C., Moya, J., Chevalier, G. (2010). Debris-flow monitoring for future set-up of alert and warning systems. Preliminary results from the Eastern Pyrenees. International workshop on EU Flood directive implementation in Mediterranean zone: Tools and challenges for efficient risk management, Barcelona, Spain

Hürlimann, M., Abancó, C., Moya, J., Chevalier, G., Raïmat, C., Luis-Fonseca, R. (2010). Set-up of debris-flow monitoring stations in the Eastern Pyrenees. Preliminary results and first experiences. General Assembly of the European Geosciences Union, Vienna, Geophysical Research Abstract.

Abancó, C. and M. Hürlimann (2010). Preliminary analysis of relevant parameters for debris-flow entrainment using field data and two different numerical codes in the Eastern Pyrenees. General Assembly of the European Geosciences Union, Vienna, Geophysical Research Abstract.

Hürlimann, M., Abancó, C., Moya, J. (2010). Debris-flow initiation affected by snowmelt. Case study of the Senet monitoring site, Eastern Pyrenees. Mountain Risks: Bringing Science to Society, Florence, Italy

Abanco C., Hürlimann, M., Moya, J., Portilla, M, Chevalier G., Baeza C. (2010) Peligrosidad de corrientes de derrubios en el Pirineo Oriental y Central. Metodología y primeros resultados del proyecto "DEBRIS-CATCH". XI Reunión Nacional de Geomorfología. Solsona, Spain

[164]

Abancó, C. and M. Hürlimann (2011). Simple geomorphologic approach to estimate debris-flow entrainment. Applications to the Pyrenees and the Alps. 5th International Conference on Debris Flow Hazards Mitigation: Mechanics, Prediction and Assessment. Padua.

Hürlimann, M., Abancó, C., Moya, J., Chevalier, G., Raïmat, C., Luis-Fonseca, R. (2011). Debris-flow monitoring stations in the Eastern Pyrenees. Description of instrumentation, first experiences and preliminary results. 4th Int. Conf. on Debris-Flow Hazards Mitigation, Padua.

Hürlimann, M., Chevalier G., Moya, J., Abancó C., Llorens, M. (2012) Elaboration of a magnitude-frequency relationship for debris flows by aerial photographs. Case study from a national park in the Spanish Pyrenees. XI Int. Symposium on Landslides and Engineered Slopes, Banff, Canada. 717-722.

Abancó C., Hürlimann, M., Sempere, D. Berenguer, M. (2012) Benefits and limitations of using the weather radar for the definition of rainfall thresholds for debris flows. Case study from Catalonia (Spain). Geophysical Research Abstracts. Vol. 14, EGU2012-2683.

Abancó C., Hürlimann, M., Moya, J., (2012) Auscultación de corrientes de derrubios en el barranco El Rebaixader, Pirineo Central. Primeras experiencias para un sistema de alerta temprana y alarma. XII Reunión Nacional de Geomorfología, Santander, p. 57-60.

Hürlimann, M, Abancó, C, Moya, J, Vilajosana, I, Llosa, J. (2013) Monitoring of debris flows and landslides by wired and wireless systems. Experiences from the Catalan Pyrenees. Geophysical Research Abstracts. Vol. 15, EGU2013-7285